Medizinische Fakultät Charité – Universitätsmedizin Berlin
Campus Benjamin Franklin
aus dem Max-Delbrück Centrum für molekulare Medizin
Direktor: Univ. Prof. Dr. med. Walter Rosenthal

Suppression of pain by nociceptor-specific expression of tethered toxins *in vivo*

Inaugural-Dissertation
zur Erlangung des Grades
Doctor rerum medicarum
Charité – Universitätsmedizin Berlin
Campus Benjamin Franklin

vorgelegt von
Annika Stürzebecher
aus Berlin

Referent: Prof. Dr. G. Lewin

Koreferent: Prof. Dr. med. Chr. Stein

Gedruckt mit Genehmigung der Charité - Universitätsmedizin Berlin

Campus Benjamin Franklin

Promoviert am: 16.05.2010

Contents

Abbreviations

BAC	Bacterial artificial chromosome
BCIP	5-Bromo-4-Chloro-Chlor-3-indolylphosphate
BSA	Bovine serum albumin
cDNA	Complementary DNA
CNS	Central nervous system
DIG	dioxygenin
DMEM	Dulbecco's modified Eagle's medium
DMSO	Dimethyl sulfoxide
DNA	Deoxyribonucleic acid
dNTP	Deoxynucleotidetriphosphate
DRG	Dorsal root ganglion
DTT	Dithiothreitol
EDTA	Ethylenediaminetetraacetic acid
EGFP	Enhanced green fluorescent protein
FCS	Fetal calf serum
Gensat	Gene expression atlas of the central nervous system
GPI	Glycosylphosphatidylinositol
HCl	Hydrochloric acid
IB4	Isolectin B4
MiliQ	Ultrafiltrated water (from MiliQ-Plus water system, Millipore)
mRNA	Messenger ribonucleic acid
NaCl	Sodium chloride
NaOH	Sodium hydroxide
Na_v	Voltage-gated sodium channel α-subunit
NBT	Nitro blue tetrazolium chloride
OD	Optical density
o/n	Over night
pBS	pBluescript SK II (+)
PBS	Phosphate buffered saline
PBT	PBS-Tween-20
PCR	Polymerase chain reaction
PFA	Paraformaldehyde
pH	potentium hydrogenii
PI-PLC	Phosphatidylinositol-specific phospholipase C

PNS	Peripheral nervous system
RNase	Ribonuclease
rpm	Revolutions per minute
RT	Room temperature
SDS	Sodium dodecyl sulphate
TTX	Tetrodotoxin
SSC	Sodiumchloride-sodiumcitrate
STX	Saxitoxin
TAE	Tris-acetate EDTA
TE	Tris-EDTA
t-MrVIa	Membrane tethered conotoxin MrVIa
Tris	Tris-(hydroxymethyl-) aminoethane
t-RNA	Transfer ribonucleic acid
VGSC	Voltage-gated sodium channel

Units

bp	base pairs
^{0}C	degrees Celsius
d	days
g	gram
h	hour
kb	kilobase
kDa	kilodalton
l	liter
M	molar
min	minute
ml	milliliter
mM	millimolar
nA	nanoampere
ng	nanogram
µg	microgram
s	second
U	unit (unit for enzyme activity)

1 Introduction

1.1 Nociception and Pain

The International Association for the Study of Pain (IASP) defines pain as “an unpleasant sensory and emotional experience associated with actual or potential tissue damage, or described in terms of such damage”. Thus, pain serves an important physiological function which prevents the organism from severe tissue damage. Whereas acute pain serves as a warning mechanism, chronic pain is beyond the point of tissue healing. Two types of chronic pain exist: inflammatory and neuropathic pain resulting from either a chronic inflammation or severe damage of the peripheral nervous system. Chronic pain states are accompanied by hyperalgesia (lowered threshold to painful stimuli) or allodynia (responses to usually non-painful stimuli) (Holden and Pizzi, 2003; Lewin et al., 2004). Each mammalian organism possesses a specialized nociceptive system which senses and transmits sensory information from free nerve endings to higher brain centres. The triggering, sensing, transmitting and central perception of such nerve impulses is referred to as nociception.

Specialized sensory neurons (called nociceptors), receive a broad range of painful (noxious) input such as extreme heat, cold, mechanical and chemical stimuli like protons and bradykinin which get released after tissue damage (Julius and Basbaum, 2001; Scholz and Woolf, 2002; Snider and McMahon, 1998; Wood, 2004). Nociceptors innervate skin, muscle and viscera. Their somata are located in the dorsal root ganglia (DRG) which project to the spinal cord. The peripheral endings receive environmental information which is conveyed centrally to the dorsal horn via neurotransmitter release at the presynaptic terminal. All nociceptive information targets within the laminae I, II and V of the dorsal horn (Braz et al., 2005). From there on the signals get processed (either directly or indirectly via interneurons) to wide dynamic range neurons which transmit them to afferent tracts (spinothalamic tract, spinoreticular tract and spinomesencephalic tract) that project to the thalamus and the somatosensory cortex (Figure 1). Whereas the emotional and cognitive perception of pain requires the involvement of the limbic system, vegetative pain reactions are controlled via the hypothalamus (Hunt and Mantyh, 2001; Price, 2000).

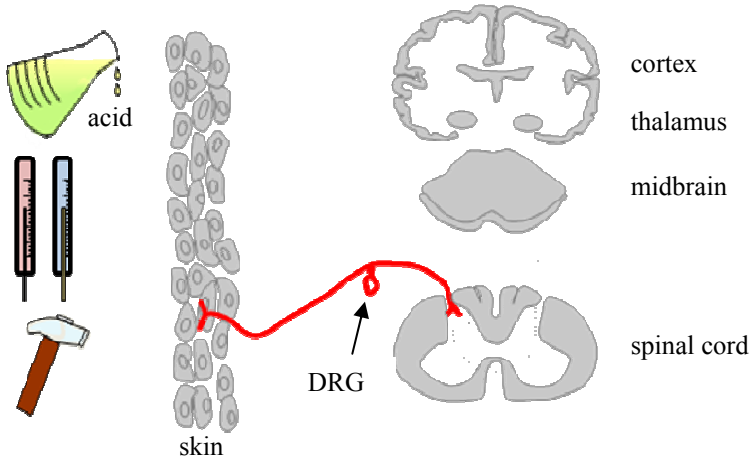

Figure 1: Overview of the nociceptive pain pathway.

The pain pathway initiates at the peripheral terminals of nociceptors which are activated by noxious stimuli such as temperature, mechanical force or chemical stimuli. These stimuli are conducted along the nociceptor axons to their cell bodies, located in the DRG, and then to their central terminals located in the dorsal horn. Here, the action potentials initiate neurotransmitter release from nociceptor central terminals which relay the signal across synapses to the dorsal horn neurons. The signal is then relayed via ascending nociceptive pathways to higher centers in the brain where it is perceived as pain (modified from Scholz 2002).

1.1.1 Myelination and conduction velocity

DRG neurons constitute a heterogenous population of primary afferent neurons which can broadly be subdivided into Aα-, Aβ-, Aδ- and C-fibers based on their grade of myelination, conduction velocity and sensory modality (Lumpkin and Caterina, 2007; Millan, 1999). For instance, Aα-fibers serve as proprioreceptors giving information about limb positions whereas Aβ-fibers (mechanoreceptors) transmit innocuous stimuli like light touch and pressure. Based on their high degree of myelination both fiber types conduct stimuli with >10 m/s in mice (Koltzenburg and Lewin, 1997). In contrast to proprioreceptors and mechanoreceptors, thinly myelinated Aδ- and unmyelinated C-fibers receive and transduce mainly nociceptive information (Millan, 1999; Sherrington, 1906) and have a significantly lower conduction velocity (Harper and Lawson, 1985). Importantly, C-fiber neurons constitute about 70% of cutaneous primary afferent neurons (Millan, 1999). Whereas Aδ-fibers elicit a first phase of pain which is usually sharp in nature, C-fibers evoke a second wave of dull pain (Belmonte and Cervero, 1996; Raja et al., 1999). A strong correlation exists between the grade of myelination and the cell soma size (Harper and Lawson, 1985; Lawson and Waddell, 1991). For instance, in mice, fast-conducting Aα- and Aβ-fibers have a large soma diameter (30-50 µm) whereas nociceptors are rather small (15-30 µm). Since it has been shown difficult to gain access to the nociceptor terminal, neuronal cultures serve as an *in vitro* model to sudy the function of A- und C-fiber neurons at the cell body. Despite some minor differences in protein expression levels depending on culture

conditions the different morphology and electrical characteristics of A- and C-fibers makes them easily distinguishable and accessible for functional studies *in vitro* (Gold et al., 1996).

1.1.2 Neurochemical composition of nociceptors

Nociceptors display an array of unique functions and morphological features which make them distinguishable from mechanosensitive neurons. They express a variety of different molecular markers, ion channels and receptors and can be subdivided into two molecularly and anatomically distinct groups: peptidergic and non-peptidergic nociceptors. Those groups are classified based on the absence or presence of the receptor for the plant isolectin B4 (IB4) receptor and are thus referred to as IB4- (peptidergic) and IB4+ (non-peptidergic) (Stucky and Lewin, 1999) (Figure 2). During embryonic development only IB4- nociceptors are present in mice (Molliver et al., 1997). They contain the peptide neurotransmitter substance P (subP) and calcitonin gene-related peptide (CGRP) and express the kinase receptor trkA, which binds the nerve growth factor NGF and is required for nociceptor survival (Silos-Santiago et al., 1995; Thoenen and Barde, 1980; Zylka, 2005). This cell-population is suggested to play a main role in the transduction of noxious heat stimuli and inflammation (Marmigere and Ernfors, 2007; Stucky and Lewin, 1999). IB4+ nociceptors arise much later from lineage (Chen et al., 2006; Zhang and Bao, 2006). At around P0 40-50 % of IB4- nociceptors undergo a Runx1-mediated transition and become IB4+ (Chen et al., 2006; Kramer et al., 2006). IB4+ nociceptors are mainly characterized by the expression of the GDNF receptor Ret and the receptor for IB4 (Bennett et al., 1998; Zylka, 2005). Importantly, both populations show differences in their central innervation pattern (Figure 2) and recent evidence indicates that these two nociceptive subpopulations also process noxious stimuli through parallel pathways which might even be independent from each other (Braz et al., 2005; Chen et al., 2006; Zylka et al., 2005). Whereas IB4- nociceptors directly contact lamina I projection neurons that transmit nociceptive information to the brain stem and the thalamus, IB4+ nociceptors engage limbic regions of the brain via projection neurons from the deep dorsal horn (Braz et al., 2005). Thus, it is speculated that IB4- nociceptors are important for sensory-discriminative aspects of pain (e.g. where is the pain stimulus located) and IB4+ nociceptors convey information which upon integrative modulation at the somatosensory cortex form the motivational and affective dimensions of pain (e.g. how unpleasant is the pain). These results together with the distinct expression of various ion channels and receptors suggest a different role of IB4- and IB4+ neurons in pain transmission and perception.

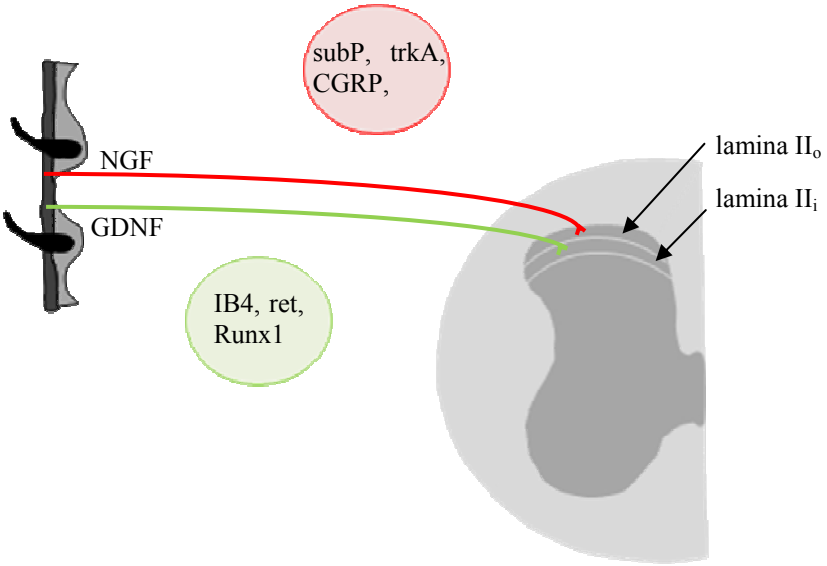

Figure 2: Schematic drawing of nociceptive afferents and their peripheral and central targeting pattern.

The two major subclasses of cutaneous nociceptors have distinct central targeting pattern and trophic factor dependence. NGF depending primary afferents represent roughly 40 % of DRG neurons in rodents, whereas the GDNF depending primary afferents (IB4+) population represents roughly 30 %.

1.1.3 Stimulation of primary afferent neurons

Nociceptive neurons detect heat, cold, mechanical and chemical stimuli and can be functionally classified based on their adequate stimuli. Nociceptive Aδ-fibers are mainly A-mechanonociceptors (A-M) whereas the majority of C-fibers are polymodal and respond to heat and mechanical stimuli (C-MH). However, C-fibers which exclusively respond to heat (C-H) or mechanical stimuli (C-M), also exist (Lewin and Moshourab, 2004). Many polymodal C-fibers additionally respond to protons or chemicals like capsaicin (compound derived from chili pepper) and 5-10% are activated by noxious cold (C-MHC) (Lewin and Moshourab, 2004). Whereas temperature perception is extensively studied, many cold-sensing ion channels have only recently been described (Noel et al., 2009; Zimmermann et al., 2007). For instance, mouse knockout studies of the transient receptor potential M8 (TRPM8) ion channel have demonstrated its clear role in perceiving environmental cold (Bautista et al., 2007). Recently, the voltage-gated sodium channel (VGSC), $Na_v1.8$, has been suggested to play a role in the transduction of noxious cold pain (Zimmermann et al., 2007). However, further studies need to be done to elucidate the mechanism of perception and transmission of cold stimuli. Interestingly, previous studies have identified another class of nociceptive C-fibers which are mechano- and heat insensitive under physiological conditions (Meyer et al., 1991). In accordance with the

nomenclature they are referred to as C-MiHi. In higher mammals they constitute around 15-25 % of C-fibers but they are less abundant in mice (~10%) (Handwerker et al., 1991; Kress et al., 1992; Lewin and Mendell, 1994). While C-MiHi fibers do not get activated by acute noxious stimuli they gain responsiveness upon sensitization with algogens (e.g. capsaicin) or in chronic pain conditions (Lewin and Moshourab, 2004).

1.2 Ion channels that mediate nociception

Nociceptors transduce noxious stimuli into depolarization that trigger action potentials, conduct them along the axon and convert them into neurotransmitter release at the peripheral synapse (McCleskey and Gold, 1999). All these actions depend on ion channel function. The expression of ion channels is dynamic and allows cells to undergo fundamental changes in their excitability in response to altered environmental conditions (Waxman, 2000). This neuronal plasticity provides a powerful adaptive mechanism. However, inappropriate changes of the cell excitability triggered by ion channel malfunctioning can lead to a variety of neurological disorders and severe pain (Cox et al., 2006; Kearney et al., 2001; Yang et al., 2004). Thus, recent ion channel research has been primarily dedicated to identifying unknown structures and binding sites for the modulation of ion channel function and for the development of new potential drugs for clinical interventions. Nociceptors express a wide variety of ion channels ranging from heat- to cold-activated channels, ligand-gated channels like ATP-and proton-gated channels and voltage-gated channels (McCleskey and Gold, 1999). The coexistence of these ion channels together with a distinct set of molecular markers contributes to the unique features of nociceptors as initial sensors of noxious stimuli.

1.2.1 Voltage-gated sodium channels

The detection of painful stimuli relies on the intrinsic property of sensory neurons to generate action potentials by activation of voltage-gated sodium channels (VGSC). VGSC comprise a pore-forming α-subunit, which is approximately 260 kDa, associated with one or two auxiliary β-subunits (Goldin et al., 2000). Whereas the α-subunit is sufficient for mediating ionic currents, β-subunits play a fundamental role in the modification of kinetics, channel gating, channel localization and expression at the plasma membrane (Isom, 2001). Nine α-subunits have been functionally characterized ($Na_v1.1$ – $Na_v1.9$) (Goldin et al., 2000). Each of them is organized in four homologous domains containing six transmembrane segments with defined amino acid

sequences for the voltage sensor and the ion selectivity filter (Figure 3) (Catterall et al., 2005; Chahine et al., 2005; Yu and Catterall, 2003). A tenth sodium channel Na_x also exists diverging from Na_v1 (Goldin et al., 2000). Key differences in functionally important regions of the voltage sensor and the inactivation gate suggest that Na_x may not function as a VGSC but is involved in salt homeostasis (Wood et al., 2004; Yu and Catterall, 2003). VGSC are classified into two main groups based on their sensitivity to the puffer-fish-derived compound tetrodotoxin (TTX). While $Na_v1.5$, $Na_v1.8$ and $Na_v1.9$ are resistant to nanomolar concentrations of TTX, all other VGSC are blocked (Rogers et al., 2006). The expression pattern of VGSC in mammals is highly diverse. Many VGSC are expressed within the central nervous system (CNS), the peripheral nervous system (PNS) and even in skeletal muscle and heart (Table 1) (Yu and Catterall, 2003).

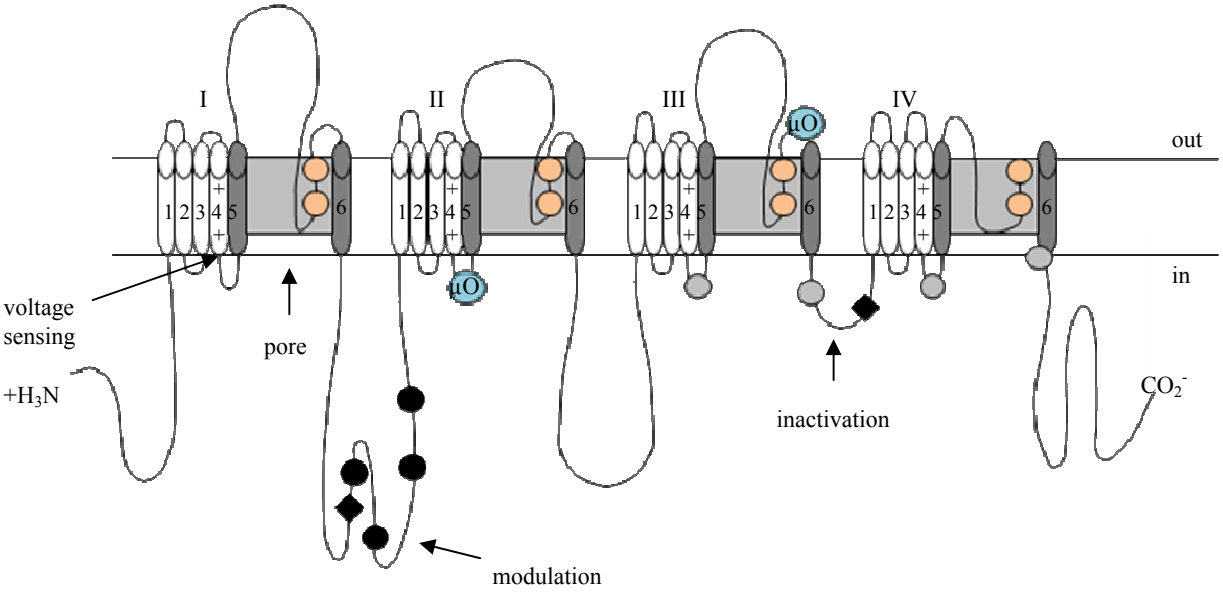

Figure 3: Transmembrane organization of VGSC α-subunits.

Cylinders represent α-helical segments whereas bold lines represent the polypeptide chains with length approximately proportional to the number of amino acids of $Na_v1.2$. P: site of possible protein phosphorylation by proteinase K (circles) and protein kinase C (diamonds). shaded boxes: pore-lining S5 and S6-segments, ++: voltage sensors, orange circles: TTX-binding site, μO: interaction site for μO-conotoxins (modified from Catterall et al., 2005)

$Na_v1.8$ and $Na_v1.9$ expression is restricted to sensory neurons with high amounts of transcript expression in nociceptors (Table 1) (Agarwal et al., 2004; Akopian et al., 1996). Together they account for up to 80% of the voltage-gated sodium currents in these cells (Akopian et al., 1996; Dib-Hajj et al., 1998). Due to their restricted expression pattern they have been implicated to play a role in pain. Importantly, nociceptors are the sole neurons in mammals in which the

tetrodotoxin resistant (TTX-R) channels $Na_v1.8$ and $Na_v1.9$ and the TTX-sensitive (TTX-S) channel $Na_v1.7$ coexist. Gene deletions in mice have demonstrated an important role in the transmission of noxious stimuli for each nociceptive VGSC (Akopian et al., 1999; Nassar et al., 2004; Priest et al., 2005). Importantly, mutations in the SCN9A gene encoding for $Na_v1.7$ have been recently linked to pain states in humans. Loss-of-function mutations of $Na_v1.7$ result in insensitivity to pain (Cox et al., 2006), while gain-of-function mutations in the same gene lead to severe pain like erythromelalgia or "Burning Feet Syndrome" (Fertleman et al., 2006; Yang et al., 2004). No linkage to pain syndromes in humans has yet been found for the SCN10a gene encoding $Na_v1.8$ (Drenth et al., 2008). However, null mutation of $Na_v1.8$ in mice implicates this channel in the establishment of visceral pain, inflammatory hyperalgesia and the transduction of noxious cold stimuli (Akopian et al., 1999; Laird et al., 2002; Yoshimura et al., 2001; Zimmermann et al., 2007). Thus, the coexpression of $Na_v1.8$ and $Na_v1.9$ together with $Na_v1.7$ gives rise to the unique function of nociceptive neurons to sense and transmit environmental stimuli. Dissecting the role of each VGSC in nociceptors will give insight into the mechanisms of different types of pain.

Table 1: Classification of sodium channel α-subunits (modified from Chahine et al., 2005)

Name	TTX-sensitivity	Expression	Expression level in DRGs
$Na_v1.1$	yes	CNS, DRG	+++ (mechanoreceptors)
$Na_v1.2$	yes	CNS, DRG	+ (mechanoreceptors)
$Na_v1.3$	yes	Embryonic CNS, injured DRG	-
$Na_v1.4$	yes	Skeletal muscle	-
$Na_v1.5$	no	Heart, embryonic CNS	-
$Na_v1.6$	yes	DRG, motor neurons	+++ (mechanoreceptors)
$Na_v1.7$	yes	DRG, low levels in CNS	+++ (nociceptors)
$Na_v1.8$	no	DRG	+++ (nociceptors)
$Na_v1.9$	no	DRG	+++ (nociceptors)

1.3 Conotoxins: Peptide toxins derived from conesnails

Venomous animals like spiders, snakes, snails, sea anemones and scorpions produce a wide range of peptide toxins which they use to capture prey, for defense and for competitor deterrence (Lewis and Garcia, 2003; Terlau and Olivera, 2004). These toxins act specifically on certain ion channels and are able to discriminate between closely related subtypes (Terlau and Olivera, 2004). This specificity as well as their high affinity makes them useful tools for ion channel research. Conotoxins originate from the venom of fish-hunting cone snails. They are very small (~10–50 amino acids) disulfide rich and compact molecules (Bulaj and Olivera, 2008). After secretion into the cone snail duct, conotoxin precursors are cleaved by proteases generating active toxins which are often subject to posttranslational modifications (Ekberg et al., 2008). These modifications together with the complex disulfide backbone allow these peptides to fold into stabilized structures. It has been shown that distinct classes of conotoxins are able to target acetylcholine receptors (α-conotoxins), noradrenaline transporters (κ-conotoxins), sodium channels (μ-, μO- and δ-conotoxins), calcium channels (ω-conotoxins), the N-methyl-D-aspartate (NMDA) receptor (conantokins) and neurotensin receptors (contulakins) (Lewis and Garcia, 2003). It is assumed that more than 50,000 conopeptides exist in nature but less than 0.1% has been characterized so far (Lewis and Garcia, 2003). Given their impressive number and specificity for very diverse ion channels and receptors, conotoxins are suitable tools to discriminate between closely related ion channels, which was so far limited to the use of "conventional" blockers like TTX or saxitoxin (STX).

Conotoxins acting on VGSC have been divided into three groups (μ-, δ- and μO-conotoxins) based on their mode of action and structural framework. Whereas δ-conotoxins delay the fast inactivation from VGSC resulting in a prolongation of the action potential, μ- and μO-conotoxins inhibit ion conductance and thus "block" the channel (Ekberg et al., 2008). Importantly, μO-conotoxins block sodium conductance independent of the TTX-binding site (Figure 3) (Heinemann and Leipold, 2007). Previous studies suggested that they act on the voltage sensor in domain-2 and the pore loop of domain-3 (Leipold et al., 2007; Zorn et al., 2006). However, the detailed mechanism of toxin action is so far unknown. Only two μO-conotoxins have been identified from the venom of *Conus marmoreus*: MrVIa and MrVIb (Figure 4). They are the first known peptide blockers of TTX-R VGSC and thus have a substantial therapeutic potential to treat pain. Studies on rat DRG neurons clearly demonstrated

that MrVIa strongly affects TTX-R currents (IC_{50} = 82.5 nM) but has little effect on TTX-S VGSC current (Daly et al., 2004). Furthermore, intrathecal administration of the closely related μO-conotoxin MrVIb in rats resulted in a significant reduction in chronic pain behavior without motor deficits (Ekberg et al., 2006). Thus, MrVIa and MrVIb are the first analgesic conotoxins reported to act by blocking VGSC. Importantly, both μO-conotoxins only affect $Na_v1.8$ but not $Na_v1.7$ or $Na_v1.9$ in mammalian DRGs and thus serve as important tools to dissect the function of VGSC in nociceptive neurons.

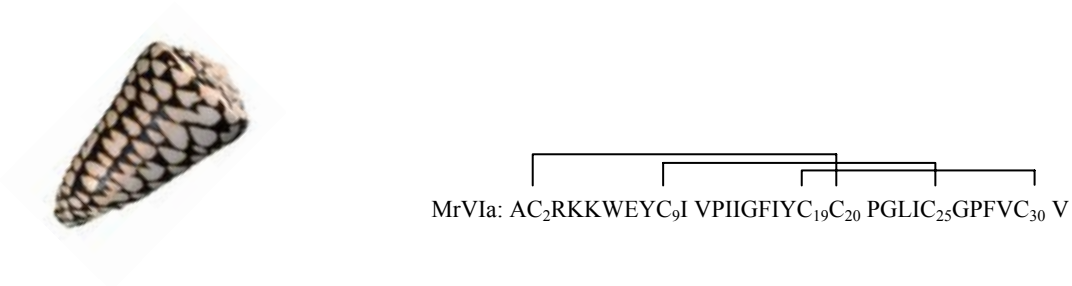

Figure 4: Structural framework of MrVIa derived from Conus marmoreus.

Shell from Conus marmoreus (left, adapted from Terlau and Olivera, 2004) and peptide sequence of the μO-conotoxin MrVIa with indicated disulfide bridges (right).

1.4 Cell-autonomous inactivation of ion channels using tethered toxins

Conotoxins are potent modulators of ion channels and receptors and are able to discriminate between closely related subtypes. It has been demonstrated that these toxins retain their activity and specificity when tethered to the plasma membrane via a glycosylphosphatidylinositol (GPI) anchor (Ibanez-Tallon et al., 2004). This idea was prompted by studies on the protoxin lynx1 which shares structural similarity with the snake α-bungarotoxin. Lynx1 is a GPI tethered molecule which is highly expressed in the mammalian CNS and physically interacts with nicotinic acetylcholine receptors (nAChR) (Ibanez-Tallon et al., 2002; Miwa et al., 1999). Similarly, naturally occurring peptide neurotoxins can be genetically expressed on the cell surface where they remain anchored via the GPI anchor (Figure 5) (Ibanez-Tallon et al., 2004). The efficiency of this strategy has been shown in zebrafish and in chick to block nAChRs (Hruska and Nishi, 2007; Ibanez-Tallon et al., 2004) and in Drosophila to modulate VGSCs (Wu et al., 2008). Previous studies on X. laevis oocytes furthermore demonstrated the efficiency of tethered MrVIa (t-MrVIa) to specifically block the $Na_v1.2$ VGSC without affecting the $Ca_v2.2$

voltage-gated calcium channel (VGCC) or the potassium shaker channel. Thus, tethered toxins provide a powerful tool to block or modulate ion channels cell-autonomously.

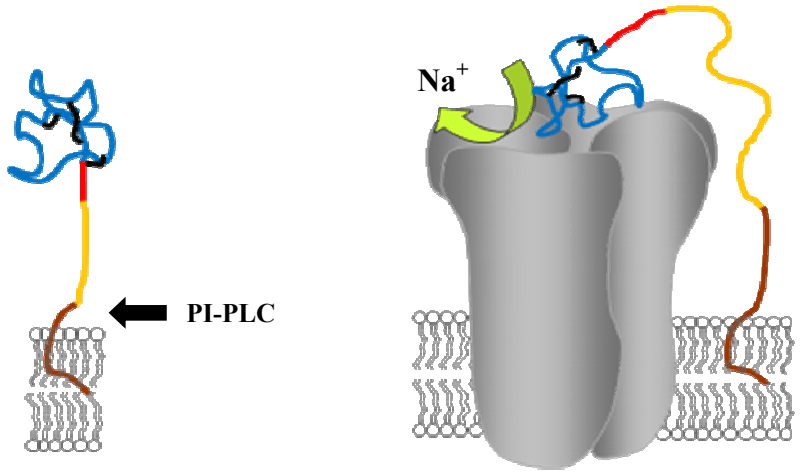

Figure 5: Construction of tethered toxins for cell-autonomous inactivation of VGSC.

Model representing the binding of tethered MrVIa to a VGSC. Tethered toxins are anchored to the plasma membrane via a GPI anchor (brown). The long linker (yellow) ensures rotational freedom whereas the flag sequence (red) allows the construct to be detected. The toxin is shown in blue. The arrow indicates a cleavage site for the enzyme phosphatidylinositol-specific phospholipase C (PI-PLC) (modified from Ibañez-Tallon et al., 2004).

1.5 Genetic approaches to study ion channel function in mice

Ion channels and receptors are the fundamental framework for neuronal circuit function. Detailed knowledge of these elements is essential for understanding how the nervous system works under physiological and pathophysiological conditions. Conventional methods to study ion channel function include pharmacological manipulations and the generation of genetically engineered knock-out (ko) mice with specific gene deletions. Ko mice provide a powerful opportunity to study native ion channel/receptor complexes but also to study the role of certain ion channel subunits. However, the interpretation of results obtained from ko mice are often hampered by compensatory upregulation of related ion channels (Akopian et al., 1999; Inchauspe et al., 2004). Other methods have been developed to silence neuronal circuits *in vivo* by delivering exogenous ion channels which upon activation by specific ligands shift the membrane potential to more hyperpolarized states. However, these approaches are often hampered by the inaccessibility of the ligands (chemicals or light) to certain tissues (Lechner et al., 2002; Lerchner et al., 2007) and may result in alteration of the physiology of the neuron due to the hyperpolarization of the plasma membrane. Recently, gene delivery based on viral vectors such as lentivirus or adeno-

associated virus (AAV) has become a desirable tool to target and modify the expression of a gene of interest. Viruses are naturally evolved vehicles which efficiently transfer their genes into host cells. This ability has made them desirable for engineering vector systems for the delivery of therapeutic genes. However, viruses harbour disadvantages such as small packaging capacities, toxicities, and immunoresponses towards viral antigens.

1.5.1 Genetically targeting the pain pathway using BAC transgenesis

Bacterial Artificial Chromosome (BAC) transgenesis is an alternative approach to interfere with neuronal circuitry. BACs are large genomic DNA fragments able to carry inserts up to 350 kb. Despite their random integration into the genome BAC transgenesis provides a powerful tool for *in vivo* studies. A comprehensive array of BAC transgenic mice with cell-specific expression in different neuronal population demonstrates the utility of this approach for mapping genes in the CNS (Gong et al., 2003). Furthermore the use of homologous recombination enables the expression of large transgenes avoiding the introduction of point-mutations by PCR. This precise and efficient engineering of BACs facilitates a variety of studies which could not be accomplished by conventional approaches. In this study BAC transgenesis was combined with the tethered toxin approach to block $Na_v1.8$ VGSC cell-autonomously in nociceptive neurons. The large genomic inserts of BACs contain whole transcription units including promoter and regulatory elements that allow gene expression in a cell-specific manner. Besides, the two homologous recombination method developed by Gong (Gong et al., 2002) enables precise targeting of the expression cassette into the BAC together with the complete removal of any unwanted bacterial vector sequences (Gong et al., 2002; Heintz, 2001). These features make BAC transgenesis a powerful tool to study ion channel function in certain neuronal circuits when combined with the tethered toxin approach.

2 Aims

This thesis aims to establish a novel genetic strategy using conotoxins to block the $Na_v1.8$ VGSC in mice and reduce pain. Although analgesic drugs blocking VGSCs have been evaluated, much of the clinical current treatment is only partially effective and leads to severe side-effects. Therefore novel therapeutic tools need to be developed.

Based on the genetic elements of the $Na_v1.8$ BAC it was possible to drive the t-MrVIa expression exclusively to nociceptors. T-MrVIa mice were characterized at a transcriptional and functional level. As it was aimed to reduce the pain responses of these mice to acute and chronic pain a battery of behavior assays was carried out. Furthermore the cell survival of DRG neurons, their central innervation pattern and the distribution of DRG subpopulations were analyzed.

In summary, the specific aims of this project, in detail, are

- Optimization of t-MrVIa constructs to obtain functional block of VGSC and adequate expression *in vitro*
- Generation of BAC transgenic mice expressing t-MrVIa in nociceptors
- Determination of t-MrVIa expression in various tissues of the pain pathway
- Determination of the transcription level of all VGSC expressed in DRGs
- Determination of possible t-MrVIa-mediated changes in nerve morphology or the composition of neurochemical markers
- Functional characterization of t-MrVIa action on $Na_v1.8$ and related VGSC
- Behavioral analyses to assess the role of $Na_v1.8$ in acute nociception and inflammation
- Performance of skin nerve assays to evaluate the firing frequency of cutaneous receptive fibers

3 Materials and Methods

Chemicals, enzymes, oligonucleotides, molecular weight markers and antibiotics were ordered from the following companies: Ambion, Biorad, Biotez, Calbiochem, Fluka, GE Healthcare, Gibco, Invitek, Invitrogen, Merck, New England Biolabs, PAN Biotech GmbH, Peqlab, Promega, Prozyme, Roche, Roth, Sakura, Serva, Sigma and USB corporation.

3.1 Buffers and solutions

All buffers and solutions were set up in MiliQ water which was previously purified to the grade "aqua bidest"

Name	**Composition**
20x SSC	3 M NaCl, 300 mM Sodium citrate, adjusted to pH 7.0 (with citric acid)
4% paraformaldehyde	4% paraformaldehyde in PBS pH7.4
50x TAE	242 g/l Tris base, 5.71 % (v/v) Glacial acetic acid, 0.05 M EDTA pH 8.0
6x loading dye	0.2 % Xylene cyanol, 0.2 % Bromphenolblue, 30 % Glycerol
Acetylation buffer	1.34 % Triethanolamin, 0.053 % HCl
Denaturation buffer	0.5 M NaOH, 1.5 M NaCl
Denhardt's solution	1 % Ficoll, 1 % Polyvinylpyrolidone, 1 % BSA V
Extracellular patch clamp solution	140 mM NaCl, 4 mM KCl, 1 mM $MgCl_2$, 1 mM $CaCl_2$, 4 mM Glucose, 10 mM HEPES, adjusted to pH 7.4
High salt buffer (Southern Blot)	0.1x SSC, 0.1 %SDS
Hybridization buffer (*in situ*)	3.3 % SSC, 33 % Formamide, 3.3 % Boehr. Block, 6.7 % Dextrane sulfate, 3.3 mM EDTA, 0.07 % Tween-20, 67 µg/ml Heparine, 100 µg/ml Yeast t-RNA, 100 µg/ml ssDNA
Hybridization buffer (Southern Blot)	6x SSC, 0.5 % SDS, 10 % Denhardt's solution, 100 µg Salmon sperm (denaturated)
Injection buffer	10 mM Tris-HCl, pH 7.5, 0.1 mM EDTA, 100 mM NaCl
Intracellular patch clamp solution	122 mM KCl, 10 mM NaCl, 1 mM $MgCl_2$, 1 mM EGTA, 10 mM HEPES, adjusted to pH 7.3
L15/OR2	50 % OR2, 50 % L15 media, 1x Penicillin/Streptomycin
LB medium (Luria-Bertoni medium)	10 % (w/v) Tryptone, 5 % (w/v) Yeast extract, 10 % (w/v) NaCl, adjusted to pH 7.0

Name	Composition
LB agar	LB-medium + 15 % (w/v) agar,
Low salt buffer (Southern Blot)	2x SSC, % SDS
Lysis buffer (In vitro transcription)	20 mM tris-HCl, pH 7.5, 1 % SDS, 100 mM NaCl, 10 mM EDTA, 5µl of 20µg/µl Proteinase K
Lysis buffer (Western Blot)	150 mM NaCl, 50 mM HEPES, 10 % Gylcerol, 1 % Triton-100
MAST	100 mM maleic acid, 150 mM NaCl, 0.3 % Tween-20, adjusted to pH 7.5
MAST++	MAST +10 % normal goat serum,
NTMT	100 mM NaCl, 100 mM Tris-HCl (pH9.5), 50 mM $MgCl_2$, 0.1 % Tween-20
OR2	82.5 mM NaCl, 2.5 mM KCl, 1 mM $MgCl_2$, 1 mM $CaCl_2$, 1 mM Na_2HPO_4, 5 mM HEPES, adjust to pH 7.8
PBS (10x)	80 g NaCl, 2.4 g KH_2PO_4, 2 g KCl, 14.4 g Na_2HPO_4
PBT	1x PBS, 0.15 % Tween-20
Phosphate buffer (for Electron microscopy)	0.1 M KH_2PO_4, 0.1 M Na_2HPO_4 x $2H_2O$
Prehybridization buffer	50 ml Formamide, 25 ml 20 x SSC, 40 µl Heparine (100 mg/ml), 1 ml salom sperm DNA (10 mg/ml), 100 µl t-RNA (50 mg/ml), 150 µl Tween-20, 6 ml 1M citric acid, ad 100 ml H_20
Ringer solution	82.5 mM NaCl, 2 mM KCl, 1 mM $MgCl_2$, 1 mM $CaCl_2$, 10 mM HEPES, adjust to pH 7.4
SOC medium	2 % Tryptone, 0.5 % Yeast extract, 10 mM NaCl, 10 mM $MgCl_2$, 10 mM $MgSO_4$, 20 mM Glucose
Solution I	125 ml formamide, 62.5 ml 20x SSC, 375 µl Tween-20, ad 250 ml H_20
Solution II	2.5 ml 1M Tris-HCl, pH 7.5, 25 ml 5M NaCl, 375 µl Tween-20, ad 250 ml H_20
SIF (Synthetic Interstitial Fluid)	2 mM $CaCl_2$, 5.5 mM glucose, 10 mM HEPES, 3.5 mM KCl, 0.7 mM $MgSO_4$, 123 mM NaCl, 1.5 mM NaH_2PO_4, 9.5 mM Na-gluconate, 7.4 mM saccharose, adjusted to pH 8.4, carbogene used for oxygenation during the experiment will bring it to pH 7.4
Tail buffer 1	200 mM NaCl, 100 mM Tris-HCl pH 8.5, 5 mM EDTA, 0.2 % SDS
Tail buffer 2	50 mM Tris (pH 8.0), 100 mM EDTA, 0.5 % SDS, 50 µg/ml Proteinase K
TBS (10x)	0.5 M Tris/HCl pH 7.9, 1.5 M NaCl, 0.2 g KCl
TBS-T	TBS+0.05 % Tween-20,
TE buffer	10 mM Tris pH 8.0, 1 mM EDTA

3.2 Plasmids

Name	Supplier
pCS2	Roche
pLD53	GE Healthcare
pNa200-rNa_v1.2	Kindly supplied by Alan Goldin
RP23-H214 (Na_v1.8-BAC)	Qiagen

3.3 Primers

Name	Sequence (5' → 3')
BAC-F	CCCTTTCCATTCTTTCAACCCCTAAC
MrVIa-RT-F	TGGGAGTACTGCATAGTGCCGAT
polyA-RT-R	CCCGTAGTTCCATCCTTCCTTCAA
Genotyping-F	TCCTAGCTCTTGTTGGAGCTG
Genotyping-R	GGGTAGCAAAGCCAGCAC
Hypoxanthin-F	TCCTCCTCAGACCGCTTTT
Hypoxanthin-R	CCTGGTTCATCATCGCTAATC
Na_v1.1-F	TGTCCCTGTTTCGACTGATG
Na_v1.1-R	AGTGTGGCCTGATTCTGCTC
Na_v1.2-F	ACAGAAAGAGCAGGCTGGAG
Na_v1.2-R	TGCTGTCGTTGTCCTCAAAC
Na_v1.3-F	TGGTTTGAGACGTTCATTGTG
Na_v1.3-R	AGAAGTCCAACCAGCACCAG
Na_v1.6-F	TCCACTCCTTCCTCATCGTC
Na_v1.6-R	GGGTCTGACTCGCTGCTAAC
Na_v1.7-F	AGCCAAGGGACACAAAGATG
Na_v1.7-R	GGTCCAATCTGGAGGGTTG
Na_v1.8-F	CCCAAGAAGAATGAGAAGATGG
Na_v1.8-R	GGGACTGAAGAGCCACAGAG
Na_v1.9-F	CAGAGGCCAAGGAGAAGATG
Na_v1.9-R	GAGGCATCGTCCTCTGAATC
β1-F	GTGTATCTCCTGTAAGCGTCGTAG
β1-R	ATTCTCATAGCGTAGGATCTTGACAA
β2-F	GGCCACGGCAAGATTTACCT
β2-R	CACCAAGATGACCACAGCCA
β3-F	ACTGAAGAGGCGGGAGAAGAC
β3-R	GGTGAGGAAGACCAGGAGGAT
β4-F	CCCTTGGTGTAGAAACTAAGCAGAG
β4-R	CAGAAGCGAGTCAGTCAGATACG

3.4 Bacteria strains

Name	Genotype
E.coli DH5α	fhuA2 Δ(argF-lacZ)U169 phoA glnV44 Φ80Δ (lacZ)M15 gyrA96 recA1 relA1 endA1 thi-1 hsdR17
E.coli DH10B	F- mcrA Δ(mrr-hsdRMS-mcrBC) ϕ80lacZΔM15 ΔlacX74 recA1 endA1 araΔ139 Δ(ara, leu)7697 galU galK λ-rpsL (StrR) nupG
Pir2	F- Δlac169 rpoS(Am) robA1 creC510 hsdR514 endA recA1 uidA(ΔMluI)::pir

3.5 Kits

Name	Supplier
DIG RNA labeling mix	Roche
ECL plus western blotting detection system	GE Healthcare
Gel purification kit	Qiagen
mMESSAGE mMACHINE Sp6 /T7 (for in vitro transcription)	Ambion
One step RT-PCR	Invitrogen
Plasmid Miniprep Kit	Qiagen
Plasmid Maxiprep Kit	Qiagen
Prime-ItRmT Random primer Labelling kit	Stratagene
Random Primer labeling kit	Stratagene
RNeasy micro kit	Qiagen
TOPO cloning kit	Invitrogen

3.6 Culture media

Name	Composition / Supplier
HEK 293-T medium	10 % FCS (Gibco), in DMEM (Gibco)
DRG medium	10 % horse serum (Gibco), 2 mM glutamine (Gibco), 100 U penicillin/streptomycin (Gibco), 50 µg/ml NGF in DMEM/F12 (Gibco)
RPMI 1640 medium	supplied by Gibco

3.7 Antibodies and markers

Name	Supplier
1 kb ladder plus	Invitrogen
Goat anti-mouse Alexa 633	Molecular probes
Goat anti-mouse-HRP	Jackson Immunoresearch
Isolectin B4-Alexa480	Vector laboratories
Mouse anti-flag	Sigma
Rabbit anti-substanceP	Zymed laboratories
RNA ladder (high range)	Fermentas
Sheep anti-Digoxigenin-POD	Roche
Wheat germ agglutinin	Molecular probes

3.8 Ion channel blockers

Name	Supplier
Tetrodotoxin	Alomone labs

3.9 Animals

Mice were housed with ad libitum access to food and water in room air conditioned at 22-23 ^{0}C with a standard 12 h light/dark cycle. All procedures were in accordance with ethical guidelines laid down by the local governing body.

3.10 Molecular cloning

3.10.1 Restriction digest

DNA was digested using specific endonucleases (New England Biolabs). 0.5 µl of the restriction enzyme and 2 µl of the required restriction buffer were added to an appropriate amount of DNA (~0.5 µg). The final volume was adjusted to 20µl with DNase-free water. Afterwards the digest was incubated for 1.5–2 h at the temperature required for the restriction enzyme. Preparative digestions were set up in 50 µl to cut constructs which were further used for molecular cloning. Depending on the expected fragment sizes 5-15 µg of DNA was digested.

3.10.2 Vector dephosphorylation

Vector dephosphorylation was used to decrease vector background after transformation. It was carried out in a total volume of 25 µl using 10 x buffer and 1 µl of the shrimp alkaline phosphatase. The samples were incubated at 37 ^{0}C for 1 h.

3.10.3 Ligation

DNA fragments can be rejoined by ligation. All ligations were carried out as sticky end ligations. In terms of molar ratios 3-6 times more inserts than vectors were used. Each ligation was set up in 10 µl containing 1 µl of T4 DNA ligase and 1 x ligation buffer. The ligations were incubated at 12 ^{0}C o/n.

3.10.4 Transformation

Transformation was done using the heat shock method. For this purpose the cells were thawed on ice and mixed with 5 µl of the ligation. After 20 min incubation on ice the suspension was heat shocked at 42 ^{0}C for 45 s. Afterwards the cells were washed out with 1mL of LB medium and incubated at 37 ^{0}C for 1-2 h with shaking at 200 rpm to allow the expression of the marker gene. Finally, several dilutions were spread on agar plates containing the appropriate antibiotic. Incubation took place in a 37 ^{0}C incubator (Heraeus) o/n.

3.10.5 Extraction of genomic DNA from mice tails

For standard genotyping the tissue was digested in tail buffer 1 at 55 ^{0}C for 2 h. Following heat inactivation for 10 min at 90 ^{0}C, 300 µl of MiliQ water was added to the sample. 1 µl of this sample was used in a PCR reaction (3.10.10). For Southern Blot analysis the tails were digested in tail buffer 2 and the genomic DNA was extracted with phenol/chloroform. After precipitation and two washing steps in 70 % ethanol the DNA was dissolved in 100 µl of TE.

3.10.6 Plasmid DNA extraction

Plasmid DNA extraction was carried out using the Miniprep kit. All steps were done according to the manual. For isolating larger amounts of plasmid DNA from overnight cultures the Plasmid Maxiprep Kit was used. The isolation was performed according to the manual.

3.10.7 DNA extraction from agarose gel

The Qiagen gel purification kit was used to isolate and purify digested plasmid DNA which will be further used for cloning. The extraction was performed according to the manual but 30 µl of EB elution buffer was used.

3.10.8 Determination of nucleic acid concentration

Quantification of DNA and RNA was performed using a spectrophotometer (Eppendorf). The nucleic acid concentration was calculated as follows:

DNA OD_{260} x 50 µM/ml
RNA OD_{260} x 40 µM/ml

3.10.9 Sequencing

DNA sequencing was carried out by InViTek, Berlin Buch. For double-stranded plasmid-DNA 1.25 µg of DNA was mixed with 10 pmol of sequencing-primer.

3.10.10 Amplification of DNA fragments

PCRs were carried out for genotyping (analytical PCRs), to analyze colonies after transformation (colony PCRs) and to prepare DNA fragments for cloning (preparative PCR). For analytical PCRs genomic DNA was extracted from mouse tails as described in 3.10.5. The PCR reaction contained 1 µ of heat inactivated lysate, 2.5 µl 10x PCR buffer, 0.75 µl $MgCl_2$, 1 µl of 80mM dNTPs (Invitek), 1 µl F-primer (10 µM), 1 µl R-primer (10 µM) and 0.1 µl of Taq DNA polymerase in a volume of 25 µl. For colony PCRs the DNA template was substituted by a bacterial colony. All PCRs were carried out in the PCR cycler PT200 (MJ Research). The cycler program was chosen as follows: 2 min at 94 ^{0}C, 35 cycles of 30 s at 94 ^{0}C, 30 s at 55–60 ^{0}C, 1 min at 72 ^{0}C followed by a final elongation time of 10 min at 72 ^{0}C. PCR products were analyzed on an agarose gel.

3.10.11 TOPO cloning

The TOPO cloning kit from Invitrogen was used to subclone PCR fragments for molecular cloning. Every step was done according to the manual. Clones were selected on kanamycin (50 µg/ml) containing agar plates.

3.11 Generation of BAC transgenic mice

A mouse BAC clone (RP23-214H2) encompassing the $Na_v1.8$ gene was modified by two steps of homologous recombination in DH10B bacteria as described (Gong et al., 2002). Therefore the t-MrVIa expression cassette (containing a secretion signal, the mature MrVIa toxin sequence, the flag sequence, a hydrophobic linker sequence, a GPI sequence and a polyA) was cloned between two recombination boxes upstream and downstream of the ATG of the $Na_v1.8$ gene into the pLD53 shuttle vector (Figure 6). All steps were performed as indicated in the gensat protocol (www.gensat.org). Electroporation (V = 1.8 kV, R = 200 Ω, C = 25 µF) of the pLD53 plasmid encoding t-MrVIa into the $Na_v1.8$ containing BAC led to full insertion of the modified shuttle vector (Figure 6). Incubation of co-integrates in selective LB-chloramphenicol media removed the selective pressure of the shuttle vector leading to the resolved modified BAC clone and the free shuttle vector via a second homologous recombination event (Figure 6). Resolved clones were screened by PCR and Southern Blotting as described in 3.10.10 and 3.15. One modified clone was purified by ultracentrifugation as described in 3.11.1.

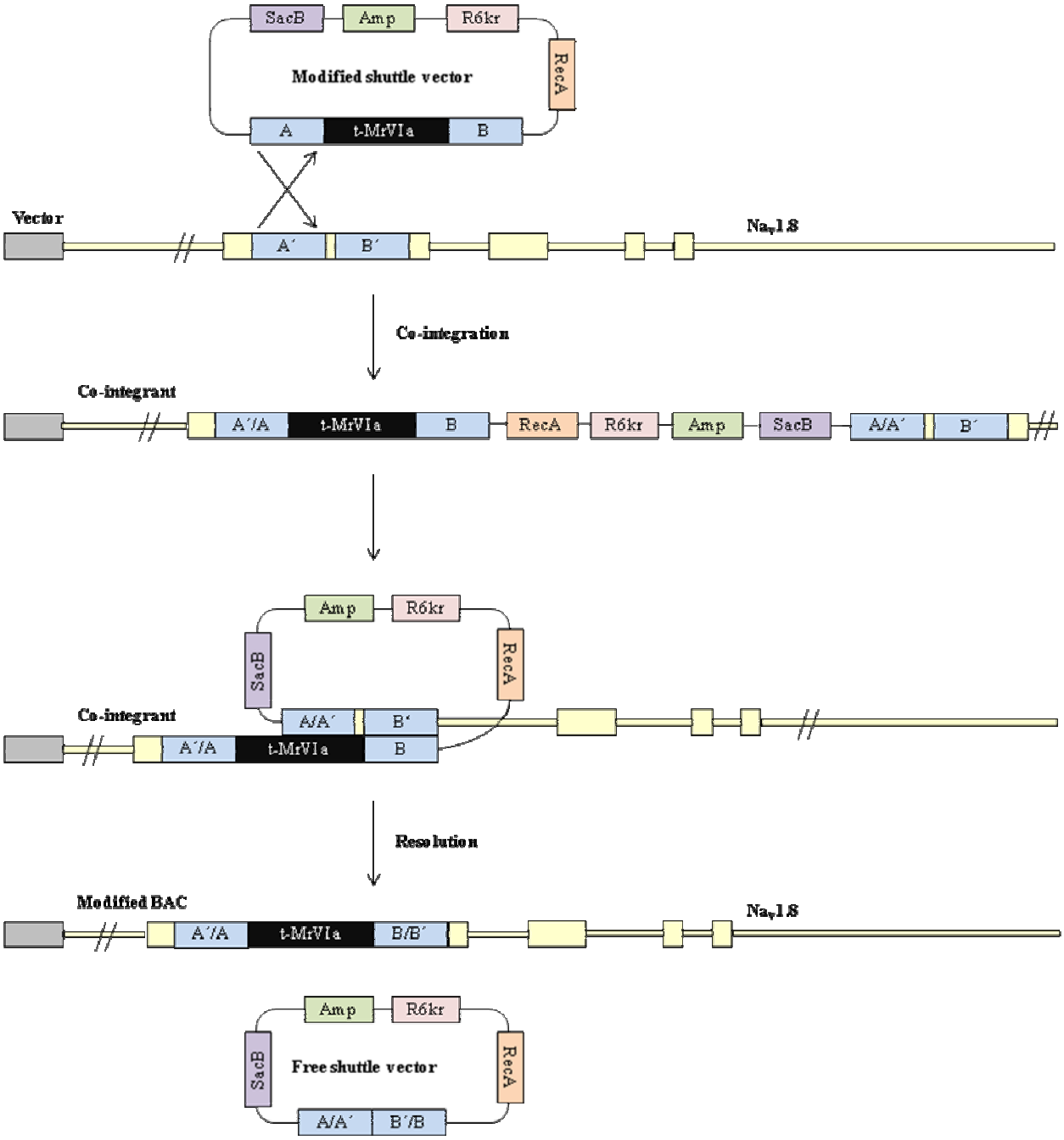

Figure 6: Schematic overview of the BAC manipulation

SacB: levansucrase, AmpR: ampicillin resistance gene, R6kr: origin of replication, RecA: enzyme mediating homologous recombination (modified from Heintz 2001 et al.).

3.11.1 BAC DNA purification for transgenesis

All steps of BAC DNA isolation and ultracentrifugation were performed according to the gensat protocol (www.gensat.org). The extracted BAC DNA was purified by ultracentrifugation in a CsCl gradient. Ultracentrifugation was performed for 20 h at 18 ^{0}C at 360000 x g using a Ti90 rotor (Beckmann). The bottom band was pulled with a needle, five times extracted with NaCl saturated butanol, precipitated and dissolved in 30 µl TE. The BAC DNA was then linearized with 4 µl of PI-SceI in a final volume of 100 µl and dialyzed for at least four hours against the injection buffer. BAC DNA (3 ng/µl) was injected into the fertilized oocytes of BDF/BL6 mice.

3.12 Synthesis of cDNA and RT-PCR

Mouse tissues were rapidly dissected and stored in trizol. The tissue was disrupted mechanically and incubated at RT for 5 min to allow the dissociation of nucleic acids. The following steps were carried out at 4 ^{0}C. 200 µl chloroform was added to the sample which was mixed and centrifuged for 5 min at 16000 x g. The upper RNA containing phase was transferred to a new tube where 500 µl isopropanol was added. The sample was incubated on ice for 10 min to allow precipitation of nucleic acids. After a 10 min centrifugation at 16000 x g the pellet was washed twice with 70 % ethanol and was finally resuspended in 20 µl of RNase-free water. The following DNaseI reaction contained 2.5 µl 10x DNase buffer, 1.25 µl 20mM DTT, 0.2 µl RNase-free DNaseI and 10 µg RNA in a total volume of 25 µl. After 1.5 h incubation at 37 ^{0}C another 0.5 µl of DNaseI was added to the sample which was incubated for at least 1 h. 75 µl of RNase-free water was added to the sample followed by a phenol/chloroform (24:1) extraction and precipitation. After two washes in 70 % ethanol the RNA was finally dissolved in 22 µl of RNase-free water and the concentration was determined spectrophotometrically. Using the one step PCR kit, the purified RNA was used to set up the RT-reaction as follows: 12.5 µl RT buffer, 5 mM $MgCl_2$, 5 µmol F-primer, 5 µmol R-primer and 20 ng RNA template in a final volume of 25 µl.

3.13 Quantitative real-time PCR

4.5 µg of RNA was reversed transcribed following the manufacturer's instructions (Promega). Hypoxanthine primer pairs were chosen as an endogenous control to normalize expression levels of the different Na_v α- and β-subunits. Real-time PCRs were performed in a total volume of 20

µl containing 250 nM of each primer, 10 µl of 2 x IQ SYBR Green (Abgene) mix containing nucleotides, iTaq DNA polymerase, SYBR GreenI dye, fluorescein and template using the iCycler IQ TM 5 multicolor real-time detection system (BioRad). The amplification protocol was as follows: 15 min at 95 ^{0}C, 50 cycles of 20 s at 94 ^{0}C, 45 s at 60 ^{0}C and 45 s at 72 ^{0}C. The PCRs were performed in duplicate. The primer specificity was assessed by the analysis of the melting curves obtained by measuring fluorescence during gradual temperature increments from 55 ^{0}C to 95 ^{0}C.

3.14 In vitro Transcription

50 µg of plasmid DNA was linearized in a total volume of 300 µl with 100 U of the appropriate enzyme at 37 ^{0}C for 4 h. Afterwards 300 µl lysis buffer was added to the mix which incubated at 37 ^{0}C for 30 min. Phenol/chloroform extraction was followed by a precipitation and incubation at -20 ^{0}C for 2 h. Afterwards the pellet was washed with 70 % ethanol and dried. 3 µg of plasmid DNA was used as starting material for in vitro transcription. The following steps were done according to the manual (Ambion). After resuspension in 50 µl nuclease-free water, RNA quality was assessed by agarose gel electrophoresis using an RNA ladder (Fermentas). The RNA quantity was measured spectrophotometrically. Purified RNA was used for oocyte injections and two-electrode voltage clamp (3.21.2).

3.15 Southern Blot

Southern Blot was used to screen for modified BAC clones and to determine the copy number of each transgenic founder line. Therefore 5 µl of BAC DNA and 5 µg of genomic DNA were digested in 20 µl and 300 µl, respectively. For larger volumes the digests were precipitated. The digests were then run on a 1 % agarose gel for 20 mV o/n.

The gel was washed in 0.2 M HCl for 15 min to depurinate the DNA. Afterwards the gel was washed twice in denaturation buffer for 25 min each followed by a quick wash in 10x SSC. The gel was placed upside-down on top of a glass plate and moistened with 10x SSC. The nylonmembrane Hybond N+ (Amersham) was placed on top of the gel avoiding the inclusion of air bubbles. Three whatman papers were soaked in 10x SSC and placed on top of the pile. A 10 cm pile of paper was placed on top of the blotting sandwich which was weighted with two heavy glass plates. A sufficient amount of 10x SSC was put at the bottom of the blotting sandwich

which was left o/n to ensure the DNA transfer from the gel to the membrane. The next day the blotting sandwich was removed, the membrane was quickly neutralized in 2x SSC dried for 2 h and crosslinked with UV light (Hoefer). In the meantime radioactive labeled probes were generated. DNA probes for southern blotting were digested as required, gel-purified and radioactively labeled with α-^{32p}-dCTP (NEN) using the Prime-ItRmT Random primer Labelling kit (Stratagene). The samples were purified via Probe-Quant G50 microcolumns (Amersham) and denatured at 95^0C for 5min before hybridization.

The crosslinked membrane was transferred to a glass tube which was preheated to 65 ^{0}C. 20 ml of hybridization buffer was added to equilibrate the membrane for 30 min at 65 ^{0}C. Afterwards 25-30 µg of radioactively labeled probe was denatured for 5 min at 90 ^{0}C and added to the hybridization buffer. Incubation took place at 65 ^{0}C o/n. On the next day the solution was disposed of and substituted by 10 ml of high salt solution. The membrane was washed three times with this solution for 15 min each before the radioactivity was measured. If the radioactivity was near background levels autoradiography was processed, otherwise the membrane was washed in more stringent low salt buffer until the radioactivity reached innocuous levels. Finally, the washed membrane was covered in cling foil and exposed to a film for at least two hours up to one week at -80 ^{0}C under light protection until it was developed in a film processor (Fuji).

3.16 Cell culture methods

Mammalian cells were handled in a hood under sterile conditions. UV light, 70 % ethanol, autoclaving and ultrafiltration were used for sterilization. The cells were grown at 37 ^{o}C in 5 % CO_2 atmosphere (Hera).

3.16.1 Transfection

Transfection of HEK-293 T cells was done using lipofectamine 2000 (Invitrogen), a cationic lipid which forms a complex with the plasmid DNA and enables its uptake into the cells. 2 µg of plasmid DNA was mixed with the appropriate amount of lipofectamine. EGFP was used as a control to enable the determination of transfection efficiency. Optimem (Gibco) was used as a minimal media. Transfections were performed according to the manual.

3.16.2 Primary DRG culture

Coverslips were coated with 100 µg/ml PLL for 1 h at 37 ^{0}C. After several washes with PBS 120 µl of 20 µg/ml laminin was added to the coverslips which were incubated at 37 ^{0}C for at least 1 h. In the meantime mice were anesthetized in a CO_2 atmosphere and afterwards decapitated. The DRGs were removed and collected in ice-cold PBS. The DRGs were incubated in 1 mg/ml Collagenase IV (Gibco) at 37 ^{0}C for 30 min to dissociate the tissue. After removal of the supernatant the DRGs were incubated in 0.05 % trypsin (Gibco) in PBS at 37 ^{0}C for 20 min. The trypsin was removed and the cells were gently resuspended in 1 ml of DRG medium. For neonatal cultures 100 ng/µl NGF was added to the medium. The cells were spun down at 170 x g for 4 min and the cell pellet was resuspended in another 1 ml of DRG medium to ensure complete removal of trypsin residues. 120 µl of cell suspension was plated on each coated coverslip. The cells were flooded with medium 4 h after plating. If required, neurons were incubated for 1 h in 10 µg/ml PI-PLC in extracellular patch clamp solution. For IB4 live labeling experiments 200 µg/ml of biotinylated IB4 Alexa-488 (Vector laboratories) in extracellular patch clamp solution was added to the culture for 15 min. The cells were further used for electrophysiological recordings, electroporation or immunostainings.

3.17 Western Blotting

HEK 293T cells were lysed in 500 µl of lysis buffer. All subsequent steps were carried out at 4 ^{0}C. The cells were spun down at 16000 x g for 10 min. The pellet containing the membrane fraction was resuspended in 500 µl lysis buffer containing 1 % triton-100, 1 % NP40, 0.05 % deoxycholate and protease inhibitor (Roche). The detergents allowed the extraction of membrane proteins during a 2-3 h incubation time with gentle shaking at 4 ^{0}C. The membrane fraction was then spun down at 16000 x g. The supernatant contained the membrane proteins. The cytosolic fraction was directly used for immunoprecipitation.

Immunoprecipitation makes it possible to detect even low amounts of flag-tagged proteins. 5 µl of flag labelled agarose beads (Sigma) was mixed with 20 µl of sepharose beads (Roth) for each sample and 500 µl of lysis buffer was added. The beads were spun down at 4 ^{0}C for 1 min at 2300 x g. After the removal of the supernatant another 500 µl of lysis buffer was added to the beads which were then incubated at 4 ^{0}C with gentle rocking for 1 h to equilibrate. After another 1 min centrifugation at 4 ^{0}C for 1 min the supernatant was removed and the protein sample was

added to the beads. The immunoprecipitation took place at 4 ^{0}C with gentle rocking o/n. On the next day 500 µl lysis buffer was added to the beads which were again spun down carefully before the supernatant was carefully removed. The last steps were repeated four times. Finally 10 µl of 3x lysis buffer and the appropriate amount of loading buffer and reducing agent (Invitrogen) were added to the beads according to the manufacturer's instructions. The samples were boiled at 92 ^{0}C for 5 min to denature the protein. Finally the sample was spun down at 16000 x g at 4 ^{0}C to obtain the bead-containing pellet and the protein in the supernatant. The samples were then loaded directly onto a polyacrylamide gel.

Proteins can be separated in a polyacrylamide gel according to their molecular weight and the pore size of the gel. 12 % gels (Invitrogen) were used to separate molecules smaller than 20 kDa. 1x running buffer (Invitrogen) was used for the gel electrophoresis. Before starting the electrophoresis 500 µl of antioxidant (Invitrogen) was added to the upper chamber. The gel was run at 180 V until the desired proteins were clearly separated. Afterwards the gel was removed from the chamber and used for blotting.

Blotting is the process of transferring proteins from a polyacrylamide gel to a membrane where they are fixed and can be detected by specific antibodies. PVDF membranes (Immobilon) were used for blotting. According to the manufacturer's instructions, the membrane was quickly soaked in methanol before it was washed in water for 5 min. The membrane was then incubated in 1x blotting buffer (Invitrogen) together with the gel, blotting and filter papers for 10 min. The blotting sandwich was set up according to the manual. The blotting took place in semi-wet conditions for 1 h at 30 V in a blotting apparatus (Biorad). Afterwards the membrane was quickly washed in 1x TBS-T.

Before immunolabelling, the membrane was blocked in 5 % milk powder in TBS-T for 1 h at RT. Afterwards the mouse anti flag antibody was diluted 1:1000 in blocking solution and incubated with the membrane at 4 ^{0}C o/n. This step was followed by four 10 min washing steps with TBS-T to ensure complete removal of unbound antibody. Afterwards the membrane was incubated with the secondary antibody goat anti mouse-HRP (diluted 1:10000 in blocking solution) for 1.5 h. The washing steps were performed as described above.

The signal of bound antibody was detected using the ECL plus western blotting detection system (GE Healthcare). 1 ml of solution A was mixed with 25 µl solution B and incubated with the membrane for 30 s. The membrane was then wrapped in clingfoil put into a cassette and was

exposed to a film for 1 min to 30 min to detect the chemiluminescence. The films were developed in film processor apparatus (Fuji).

3.18 Electroporation of DRGs

For immunostainings the dissected DRGs were dissociated as described (3.16.2) and transiently transfected with the use of the commercially available Nucleofector system (Amaxa Biosystems). In brief, neurons were suspended in 100 ml of Mouse Neuron Nucleofector Solution and 5 µg of plasmid DNA (pCS2-t-MrVIa) at 22–25 ^{0}C. The mixture was transferred to a cuvette for electroporation with the program C-13. After electroporation the cell suspension was transferred to 500 µl of RPMI 1640 medium (Gibco) for 10 min at 37 ^{0}C. This suspension, supplemented with 10% horse serum, was used to plate the cells onto glass coverslips for immunostaining. The RPMI medium was replaced with the standard DRG medium 3-4 h later. One day later cells were treated with 10 µg/ml PI-PLC in extracellular patch clamp solution for 1 h at 37 ^{0}C, fixed and stained as described in 3.19.

3.19 Immunocytochemistry

Animals were anaesthetized with Ketamin (10 mg/ml) and Rompun (0.04 %) in PBS and perfused with 4 % PFA in 0.1 M PBS, pH 7.4 and 4 ^{0}C. Immediately after perfusion the spinal cord was removed and post-fixed in the perfusion fixative at 4 ^{0}C for 2 h. The tissue was immersed in 25 % sucrose in PBS o/n. Spinal cord sections were cut on a cryostat (14 µm). Neuronal DRG cultures were post-fixed in PFA. All tissues were blocked for 1 h in 3 % goat serum (Gibco) in PBS. The following antibodies and markers were used o/n in blocking solution: mouse anti-flag (Sigma): 1:1000, wheat germ agglutinin (Molecular probes): 1:200 (5 µg/ml), rabbit-anti-subP (1:1000), isolectinB4-Alexa-488 (1:500). At the next day the cells were washed with PBS and incubated with a secondary antibody goat-anti-mouse-Alexa633 (1:4000), horse-anti rabbit-Alexa594 (1:1000) for 1.5 h at RT. The samples were washed three times in PBS for 10 min each and mounted with immunomount (Thermo). Pictures were taken on a Zeiss LSM 510 confocal microscope.

3.20 *In situ* Hybridization

3.20.1 DIG labeling of RNA probes

40 U of the required restriction enzyme (New England Biolabs) was used to linearize the plasmid construct at 37 ^{0}C o/n. 1 µg of the linearized plasmid was used for the labeling reaction which furthermore contained the following components: 2 µl DIG labeling mix (Roche), 2 µl transcription buffer, 20 U RNase inhibitor, 1 µl T7 RNA polymerase in a final volume of 20 µl. This reaction was incubated at 37 ^{0}C for 2 h and was purified via columns using the RNeasy kit according to the manual. After elution with 50 µl of RNase-free water, 50 µl formamide was added and the probe was analyzed on agarose gel and stored at -80 ^{0}C.

3.20.2 Whole mount *in situ* hybridization

DRGs from neonatal mice were removed, collected in PBS and postfixed with 4 % PFA in PBS o/n. After two washes in PBT for 15 min the DRGs were progressively dehydrated for storage through a series of 25 %, 50 %, 75 % and 100 % methanol dilutions in PBT. At that stage DRGs could be stored in methanol for several weeks at -20 ^{0}C. For hybridization DRGs were progressively rehydrated by washing with 75 %, 50 %, 25 % methanol in PBT and three times with PBT successively. DRGs incubated in 20 µg/ml proteinase K in PBT at RT with gentle rocking for 20 min. After washing in PBT postfixation in 0.2 % glutaraldehyde / 4 % PFA in PBS was carried out at RT for 20 min. After three 15 min washes with PBT at RT to remove fixatives the DRGs incubated in the prehybridization buffer for 15 min. After 15 min the solution was changed and prehybridization took place at 65 ^{0}C with vigorous shaking for 2 h. For hybridization the probe was denatured at 80 ^{0}C for 10 min and diluted 1:3000 into the hybridization solution. Hybridization took place at 65 ^{0}C o/n. On the next day unbound probe was removed by washing in prewarmed solution I and 3h in solution II. DRGs were washed three times in TBST for 15 min and 1 h with TBST / 20 % goat serum at RT. Afterwards they were incubated overnight at 4 ^{0}C with anti-DIG antibody coupled with alkaline phosphatase (1:3000). At the next day the DRGs were intensively washed with TBST for 7 h at RT with rocking and incubated at 4 ^{0}C o/n in TBST. At day 4 the DRGs were washed 2 times for 45 min in AP buffer at RT with shaking. Afterwards they were incubated with BCIP/NBT (Roche) in AP buffer in the dark until the staining was obtained. The reaction was stopped by three washes with PBT. The tissue was postfixed in 4 % PFA washed in PBS and stored.

3.20.3 *In situ* hybridization on cryosections

DRGs from neonatal mice were collected in ice-cold PBS and frozen in OCT (Sakura). Cryosections of 12 µm thickness were cut. At the first day the cryosections were defrozen for 30 min, fixed in 4 % paraformaldehyde (PFA) at 4 ^{0}C for 20 min and washed 3 times in PBS. Afterwards the sections were bleached in 3 % H_2O_2 in methanol for 15 min at RT and washed three times in PBS. The endogenous alkaline phosphatase activity was quenched by incubation in 0.2 M HCl for 8 min at RT. Following another three washes in PBS the sections were acetylated in acetylation buffer for 10 min at RT. In the meantime the coverslips were silanized and the DIG-RNA probes were diluted in hybridization buffer (1:100), denatured for 5 min at 80 ^{0}C and immediately cooled on ice. The probe was transferred to the section which was covered by a silanized cover slip and incubated at 70 ^{0}C o/n in a humid chamber. At the next day sections were washed in 2x SSC at 45 ^{0}C for 10 min to remove the cover slips and excess probe. The sections were washed stringently for 1.5 h in 50 % formamide/1x SSC at 60 ^{0}C. The slides were then rinsed in MAST at RT, washed in PBS and blocked in freshly prepared MAST++ to remove excess detergent. After removal of this blocking solution the sections were incubated with the anti-DIG antibody which is bound to an alkaline phosphatase (1:2000) in MAST++ at 4 ^{0}C o/n. At the third day the sections were washed four hours in MAST while the solution was frequently changed. Sections were equilibrated in NTMT for 10 min and then stained with BCIP/NBT (Roche) in NTMT under light protection at RT until the staining showed the desired intensity. The sections were finally washed in PBS three times and mounted with immunomount (Thermo).

3.21 Electrophysiology

3.21.1 Whole cell patch clamp recordings

Recordings were performed on DRG primary cultures 4-24 h after plating using polished glass pipettes with a resistance of 5-7 MΩ. The recording chamber was perfused with extracellular solution and electrodes were filled with intracellular solution. In some experiments cells were incubated with 10µg/ml PI-PLC in extracellular patch clamp solution for 1 h at 37 ^{0}C. All cells were recorded with the EPC10 amplifier (HEKA), sampled at 50 kHz and analyzed using the fitmaster software. The holding potential was set to -60 mV. In voltage clamp conditions the DRGs were hyperpolarized at -120 mV for 150 ms to remove inactivation of VGSC followed by 50 ms step depolarizations from -50 to +40 mV in 10 mV increments. For current clamp analyses

the neurons were kept at their resting membrane potential. Current injection was increased from 80 pA in 80 pA increments until an action potential was evoked. To separate the TTX-R voltage-gated sodium currents from the TTX-S, recordings were done in the presence of 0.5 µM TTX. The series resistance was compensated for 40–60 %.

3.21.2 Two-electrode voltage clamp

Female adult Xenopus laevis frogs were anesthetized in 0.35 % ethyl 3-aminobenzoate methane sulfate salt (tricain, Roth). Afterwards they were placed on ice and the oocytes were removed and collected in OR2 media. The oocytes were digested with 2 mg/ml collagenase I in calcium-free Ringer solution for 3 h at RT to remove connected tissue. Then they were quickly washed in OR2 and transferred into L15/OR2 media were they incubated at 18 ^{0}C o/n. At the next day the stage V and VI oocytes were collected and the RNAs were diluted in DNase-free water to a final concentration of 50 ng/µl (for ion channels) and 225 ng/µl (for t-toxins). 20 µl of each mix was injected per oocyte (Harvard apparatus, PLI-100) which was returned into the 18^{0}C incubator (Binder). The medium was changed every two days. 5 days after injection the oocytes were placed in the recording chamber. Borosilicate glass capillaries (WPI) were pulled with a resistance of 0.7-1.5 MΩ. The oocytes were clamped by two electrodes (Axon Instruments) at -90 mV. Recordings were performed using the gene clamp 500 amplifier (Axon Instruments) and data was digitized using the 1322A 18 bit data acquisition system (Axon Instruments). The protocol was applied as follows: Oocytes were clamped at -90 mV and depolarized for 600 ms in steps of 10 mV increment ranging from -70 to +40 mV. The data were analyzed using the clampex and clampfit software (Axon).

3.21.3 Skin-nerve preparation

Skin nerve preparation allows to quantitatively measure changes in the physiological properties of functionally defined afferent neurons. For this purpose adult mice were sacrificed by CO_2 inhalation and the hair of the hindlimb was removed. The saphenous nerve up to the lumbosacral plexus and a piece of the innervated skin reaching from the toes up to halfway between the ankle and the knee was excised and transferred to an organ bath where it was perfused with oxygen-saturated synthetic interstitial fluid (SIF) at a flowrate of 10ml/min. The nerve was pulled through a gap and the fluid in this chamber to the recording chamber and laid on top of a small mirror that served as the dissecting plate. The aqueous solution in the recording chamber was

overlaid by mineral oil. The nerve was desheathed, carefully removing its surrounding epineurium, and to tease small filaments from the nerve so that the activity from single units could be recorded by placing the individual strands of the nerve onto the silver recording electrode installed in the chamber's wall. Recordings were performed using the NeuroLog^{TM} system (Digitimer Ltd.) which included a low-noise amplifier. The recordings were visualized by on a Tektronix TDS 220 two-channel digital real-time oscilloscope and acquired on a PC by a PowerLab/4s converter (AD Instruments). Single afferent units of the saphenous nerve were identified by their action potential shape, conduction velocity and their mechanical threshold upon mechanical stimulation. C-fibers were subsequently examined for responsiveness to a cold ramp in which the temperature decreased from 30 to 0 ^{0}C. The experiments were carried out with individual littermates while blind to genotype.

3.22 Behavior experiments

Mice were backcrossed to C57/BL6/J for at least five generations. For all behavior experiments the genotypes of the mice were not made known to the experimenter.

3.22.1 Locomotion

Motor coordination was assessed by placing the mice on a rotarod apparatus (Ugo Basile, Italy) accelerating from 4 rpm to 40 rpm within 9 min. The experiment was done on three following days. Animals were scored for time to fall. The first run was used to acclimatize the animals to the apparatus and was not considered for analysis.

3.22.2 Thermal nociception

Thermal latency was determined using the plantar test (Ugo Basile) based on the method described by Hargreaves (Hargreaves et al., 1988). Animals were trained once to adjust to the experimental situation. 15 min after placing the mice in the plexiglas chamber (15 cm diameter, 22.5 cm in height) a high intensity light beam was directed at the plantar surface of the hindpaw. Movement of the paw stopped the light beam and the latency was indicated on a digital screen. Measurements were done five times on each paw and mean values were used for statistical analysis. Criteria for inclusion were calm behavior of the mouse prior to testing and a clear paw withdrawal.

3.22.3 Mechanical nociception

Mechanical sensitivity was determined using a dynamic plantar aesthesiometer (Ugo Basile, Milan, Italy). Animals were trained once to adjust to the experimental situation. Mice were acclimatized to the behavioral testing apparatus for 15 min. A mechanical force was applied to the plantar surface of the mouse hindpaw. The force was increased with a ramp by 1 g/s with a maximum of 20 g. Each paw was measured five times and mean values of the applied forces were determined and used for statistical analysis. Criteria for inclusion were calm behavior of the mouse prior to testing and a clear paw withdrawal.

3.22.4 Cold nociception

Mice were placed on top of a peltier-cooled plate (MDC) which was kept at 0 ^{0}C ± 1 ^{0}C. The number of lickings and jumps were determined during 90 s.

3.22.5 Preferential heat test

Two teflon isolated plates were kept at 10 ^{0}C and 30 ^{0}C, respectively. Mice had free access to both plates. The animals were tracked by an automatic monitoring system (Actimot, TSE Systems, Germany) and the time they spent on each plate was measured and used for analysis.

3.22.6 Inflammatory pain

30 µl of 2 % carrageenan in saline (Fluka) was injected into the plantar surface of the mouse right hindpaw to induce inflammatory hyperalgesia. On the following 3 days mice were tested for responses to heat and mechanical stimuli as described in 3.22.2 and 3.22.3.

3.23 Electron microscopy

Mice were perfused with 4 % PFA in 0.1 M phosphate buffer. The saphenus nerves were dissected and post-fixed in 4 % PFA/2.5% glutaraldehyde in 0.1 M phosphate buffer o/n. Following treatment with 1 % OsO_4 in 0.1 M phosphate buffer for 2 h for osmication, they were dehydrated in a graded ethanol series (30-100 %) and propylene oxide and embedded in Poly/BedR 812 (Polysciences, Inc.). Semithin sections (1 µm) were stained with toluidine blue. Ultrathin sections (70 nm) were contrasted with uranyl acetate and lead citrate and examined

with a Zeiss 910 electron microscope. Digital images were taken with a 1kx1k high speed slow scan CCD camera (Proscan) at an original magnification of 1600x. Three ultrathin sections per nerve were analyzed. On each section, four images were taken each representing an area of 18.3 µm x 18.3 µm. Axons were counted on these areas using the analySIS 3.2 software (Soft Imaging System), and calculated for the whole nerve with the aid of the area of the semithin section.

3.24 Statistical analysis

Results are presented as means ± SEM. Data were checked for normal, (parametric) distribution. Unpaired two-tailed t-tests or two-way ANOVAs were used as appropriate. $P < 0.05$ was considered statistically significant.

4 Results

This study establishes a novel genetic approach to analysing the contribution of VGSC to pain states in mice. Although VGSC are already the focus of pain research, much of the current treatment is only partially effective and leads to severe side effects possibly due to cross-reactions of drugs with related channel subtypes or insufficient delivery. This thesis demonstrates a clear dissection of related VGSC subtypes using tethered toxins for the first time in mice. Based on the genetic elements of the BAC, t-MrVIa expression was directed to nociceptive neurons. T-MrVIa mice were analyzed on transcriptional and functional levels. Since t-MrVIa-mediated manipulation of $Na_v1.8$ *in vivo* was aimed to reduce pain responses in transgenic mice, a battery of pain assays was carried out. Furthermore the question of the role of $Na_v1.8$ in cold detection was pursued in detail.

4.1 Toxin selection

Animal models and knockdown strategies have revealed an important role for $Na_v1.8$ in transmission of noxious stimuli and action potential generation (Akopian et al., 1999; Lai et al., 2002; Mikami and Yang, 2005). In this study the μO-conotoxin MrVIa was used to block $Na_v1.8$. MrVIa shows very high affinity (IC_{50} = 82.5 nM) for the TTX-R $Na_v1.8$ VGSC without interfering with $Na_v1.9$. Furthermore MrVIa is 10 times less potent for TTX-S channels. It interacts with the voltage sensor of sodium channels to inhibit their ion conductance without competing with TTX. To achieve a stable and long-lasting block of $Na_v1.8$, MrVIa was tethered to the membrane via a GPI anchor as described (Ibanez-Tallon et al., 2004) (Figure 7).

Figure 7: Schematic drawing of the t-MrVIa expression cassette.

The μO-conotoxin MrVIa is tethered to the plasma membrane via a GPI anchor. The long hydrophobic linker sequence ensures rotational freedom whereas the flag sequence is used to detect this construct in cells. The secretion signal transports the mRNA out of the nucleus.

4.2 Optimization of tethered MrVIa constructs

Previous studies have shown the potential of GPI-tethered toxins to functionally block ion channels *in vitro* (Ibanez-Tallon et al., 2004). However, distinct membrane domains integrate into different parts of the plasma membrane and transmembrane fusion proteins might lose their potential to be stably expressed. To optimize the membrane expression of MrVIa, several constructs with different tethers were generated and functionally tested in X. laevis oocytes using two-electrode voltage clamp. T-MrVIa containing the GPI sequence to tether it to the plasma membrane is shown in chapter 4.1. The second construct contains the transmembrane domain derived from the human protein NYD-SP16 (TM-MrVIa) (Cheng et al., 2003). The next construct was generated using a part of the plasma membrane domain derived from the VGSC $Na_v1.2$ which was combined with the axonal initial segment (AIS) known to target to the site of axon potential generation (Garrido et al., 2003). Additionally, the transmembrane domain of the β1 VGSC subunit was used to ensure coexpression with α-subunits at the plasma membrane. Two constructs varying in their linker lengths were generated (β1-MrVIa and Lβ1-MrVIa). As $Na_v1.8$ cDNA was not available recordings were done using the $Na_v1.2$ VGSC coexpressed with each tethered MrVIa construct. It is known that MrVIa has a lower affinity for $Na_v1.2$ than for $Na_v1.8$, however, t-toxins get highly overexpressed in this system. Thus, this model was used to optimize the "tether" for MrVIa. The functional assays of these constructs indicates that t-MrVIa was the most efficient blocker of $Na_v1.2$ sodium currents, whereas β1-MrVIa and Lβ1-MrVIa coexpression with $Na_v1.2$ even increased sodium current (Figure 8). TM-MrVIa and TM-AIS-MrVIa also reduced sodium peak current but to a lesser extent than t-MrVIa did (Figure 8). Thus, all further studies were carried out using t-MrVIa.

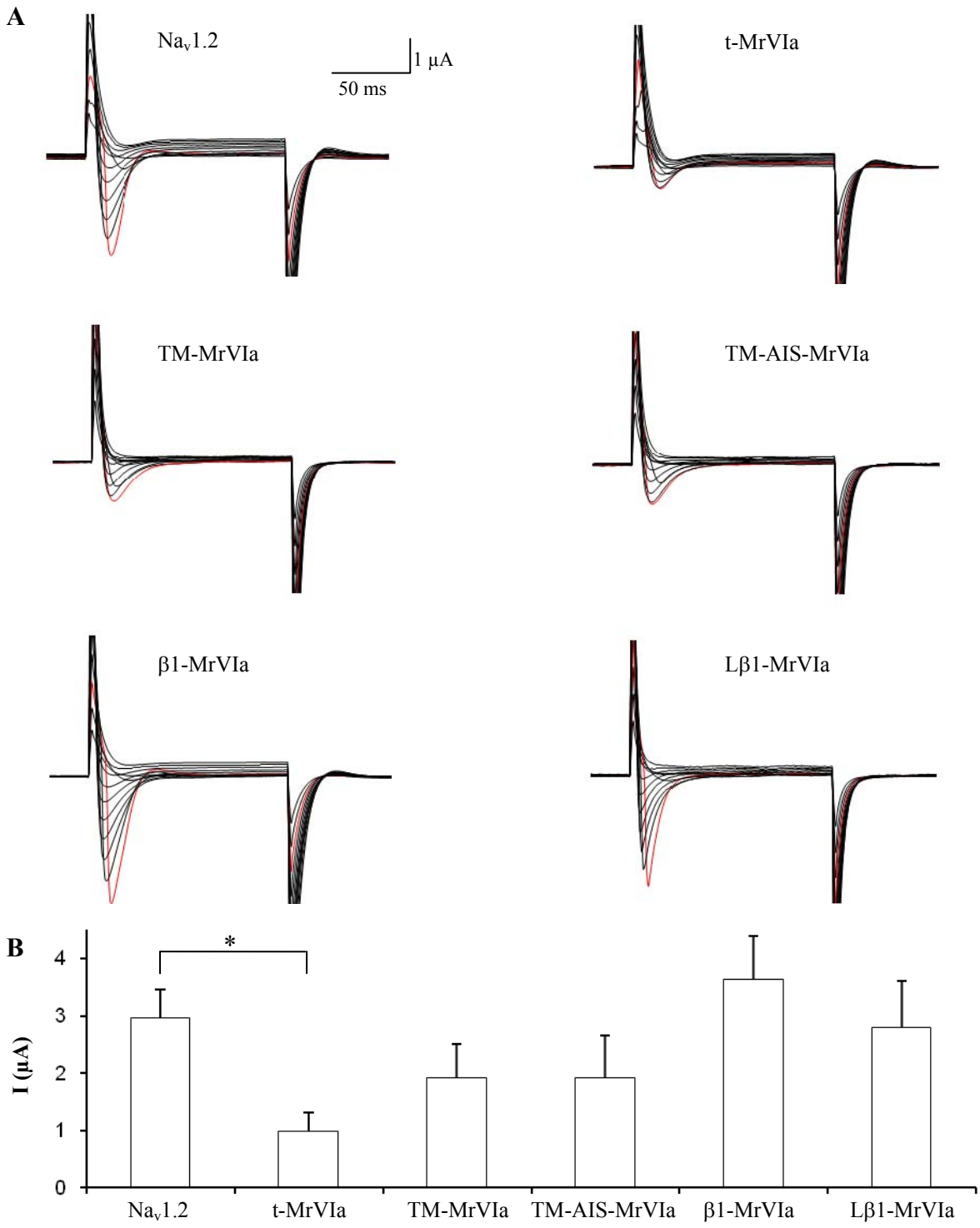

Figure 8: Differentially tethered MrVIa constructs were functionally tested on the $Na_v1.2$ VGSC using two-electrode voltage clamp in X. laevis oocytes.

A) Five MrVIa constructs with different membrane tethers were tested on the $Na_v1.2$ VGSC. Representative currents traces from X. laevis oocytes coinjected with $Na_v1.2$ and a membrane tethered form of MrVIa. Oocytes were kept at -90 mV and were depolarized by -10mV steps from -70 to +40 mV.

B) Bar graph indicating the quantification of VGSC currents from X. laevis oocytes coinjected with $Na_v1.2$ and a membrane tethered form of MrVIa. Only t-MrVIa significantly reduced VGSC current (control: 3.0 ± 0.5 µA, +t-MrVIa: 1.0 ± 0.3 µA) whereas the other constructs did not significantly change the peak current amplitude ($Na_v1.2$: n= 13, t-MrVIa: n= 12, TM-MrVIa: n = 12, TM-AIS-MrVIa: n = 11, β1-MrVIa: n = 10, Lβ1-MrVIa n = 8).

4.3 T-MrVIa is expressed at the plasma membrane in mammalian cells

Transfection and immunoprecipitation assay in HEK 293-T cells were carried out to ensure membrane expression of the tethered toxin. Mammalian HEK 293-T cells were transfected with the plasmid encoding t-MrVIa. Untransfected cells served as a control. Immunoprecipitation with the flag antibody and Western Blot analysis revealed that the tethered toxin had the correct molecular weight, was enriched in membrane fractions and was not released into the culture medium (Figure 9).

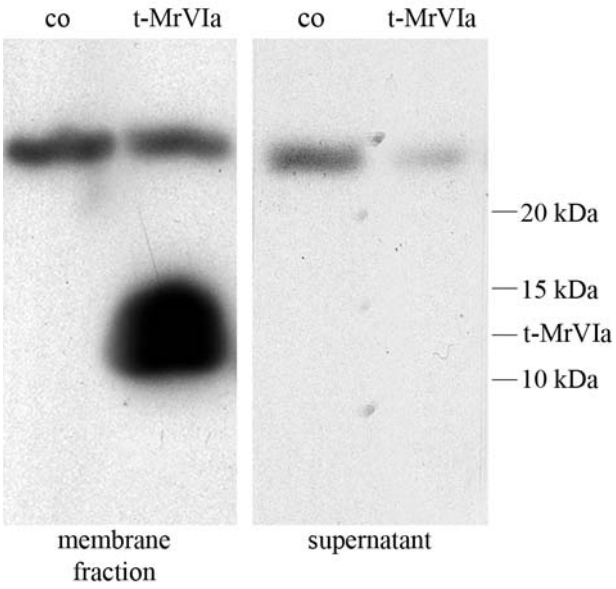

Figure 9: Western Blot analysis of t-MrVIa expression in HEK 293-T cells

Transfection of a plasmid encoding t-MrVIa into HEK 293-T cells and immunoprecipitation analysis using an anti-flag antibody. The construct had correct molecular weight (13 kDa) was exclusively detected in the membrane fraction and was not released into the supernatant. Untransfected cells did not show any band.

4.4 Membrane targeting of tethered constructs in DRG neurons of mice

Next, the t-MrVIa containing plasmid construct was delivered to sensory neurons prepared from C57/BL6 mice using the nucleofection based method (Wetzel et al., 2007). Flag staining revealed coexpression of the t-MrVIa construct with the plasma membrane marker wheat germ agglutinin (WGA) in cells cotransfected with cytoplasmatic EGFP (Figure 10, upper panel), indicating proper insertion into the plasma membrane. After treatment of the cells with phosphatidylinositol-specific phospholipase C (PI-PLC) which cleaves GPI-anchored proteins from the surface (Theveniau et al., 1992), antibody staining directed against the Flag epitope of t-MrVIa was reduced to background levels (Figure 10, lower panel).

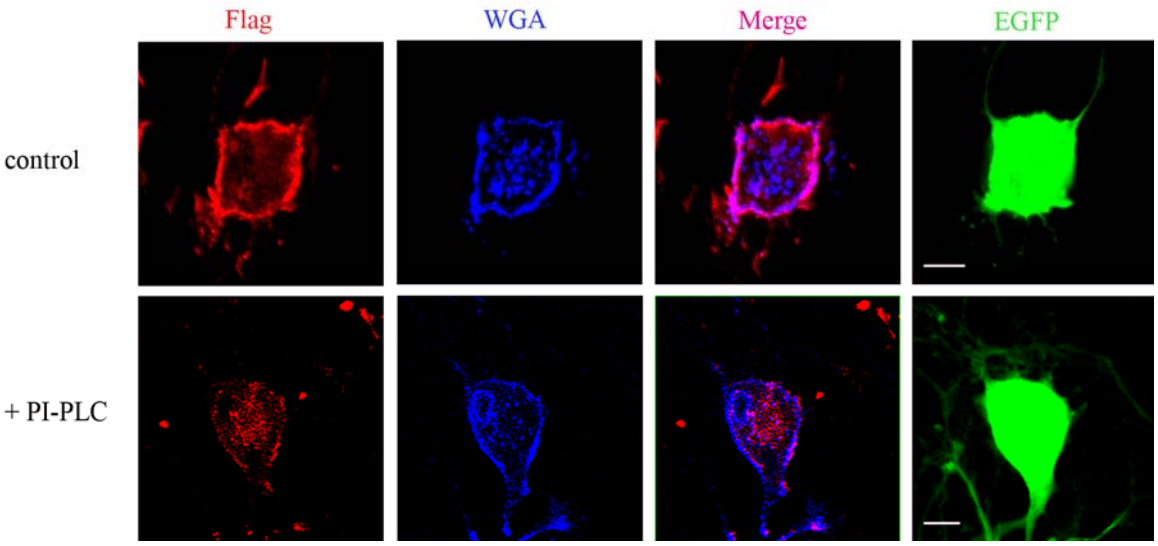

Figure 10: Immunohistochemical expression analysis of t-MrVIa in DRG neurons of c57/bl6J mice

Immunostaining using an anti-flag antibody revealed colocalization of t-MrVIa (red) with the plasma membrane marker wheat germ agglutinin (WGA) (blue) in DRGs cotransfected with cytoplasmatic EGFP (green) (upper panel). PI-PLC treatment of electroporated DRGs shows specific cleavage of the GPI-anchored toxin (lower panel). Scalebars: 5 µm (experiment carried out by Dr. Jing Hu).

Altogether, these protein expression analyses demonstrate that t-MrVIa gets delivered and correctly inserted into the plasma membrane of mammalian cells where it is stably expressed. Moreover the tethered toxin can be cleaved from the membrane upon PI-PLC treatment, providing reversibility to the t-toxin approach.

4.5 Generation of BAC transgenic t-MrVIa mice

Transgenic mice are important tools for *in vivo* genetic studies of the nervous system. In this study BAC transgenic mice were generated to express t-MrVIa in nociceptors using the two-step modification system described by Gong (Gong et al., 2002). This approach allows the precise targeting of the transgene into the genomic locus of the BAC via homologous recombination. Figure 11 shows the diagram of the BAC containing the $Na_v1.8$ locus and the integration site of the t-MrVIa construct.

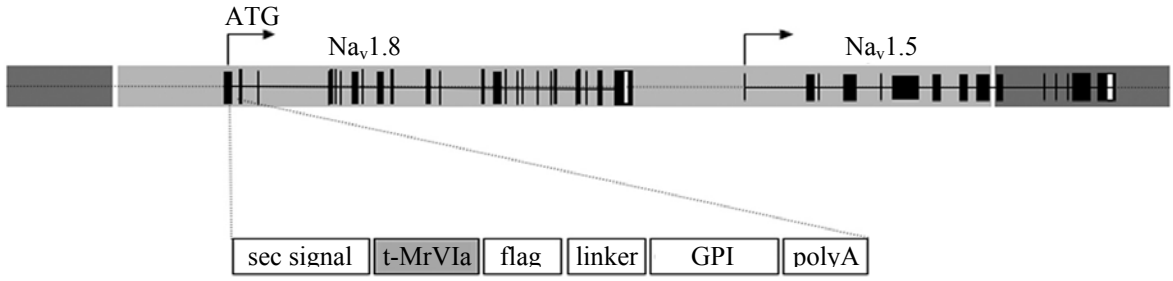

Figure 11: Generation of the modified BAC construct

Diagram of a BAC containing the $Na_v1.8$ locus. The t-MrVIa expression cassette was inserted within the first $Na_v1.8$ exon disrupting the initiator methionine. The expression cassette also contained a polyadenylation signal ensuring cessation of transcription. Sec signal: secretion signal.

4.5.1 Generation of co-integrates

The t-MrVIa expression cassette flanked by homology boxes A and B was inserted into the shuttle vector pLD53. This construct was then electroporated into E.coli DH10B encompassing the $Na_v1.8$ BAC. After homologous recombination co-integrates were screened by PCR using two primers flanking the boxA homology regions. The primer regions are indicated in Figure 12A. The PCR result is shown in Figure 12B.

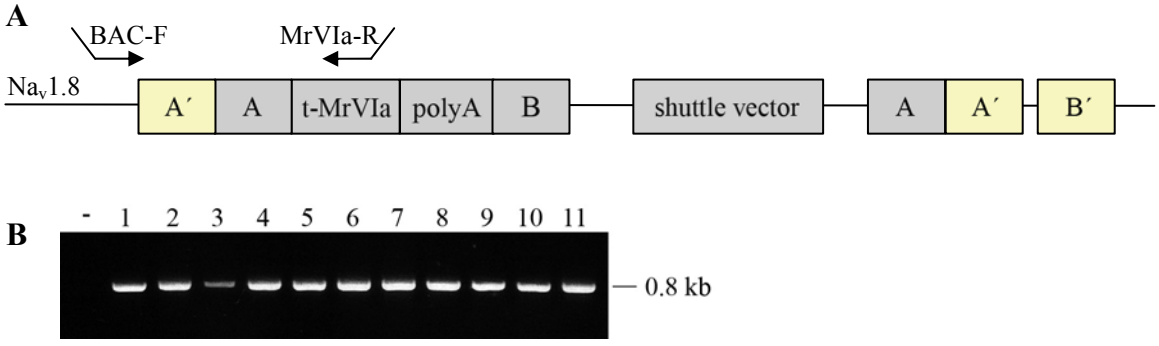

Figure 12: Screening for cointegrates

A) Schematic representation of cointegrates with indicated primer sequences used for PCR.
B) PCR analysis of cointegrative clones. Cointegrates showed a 0.8 kb band. All clones were positive.

4.5.2 Generation of resolved modified BAC clones

A second homologous recombination was induced by selective incubation of co-integrates in chloramphenicol-containing media lacking ampicillin to obtain the modified BAC clone. After selection for sucrose tolerance and UV sensitivity the remaining positive clones were further analyzed by Southern Blot using the boxA as a probe to ensure exclusion of unwanted bacterial vector sequence (Figure 13). Resolved clones showed a 1.4 kb band, whereas co-integrates showed a double band. To ensure that the positive clones contained the t-MrVIa expression cassette, a second Southern Blot was carried out using the toxin sequence as a probe. All clones were positive (Figure 14).

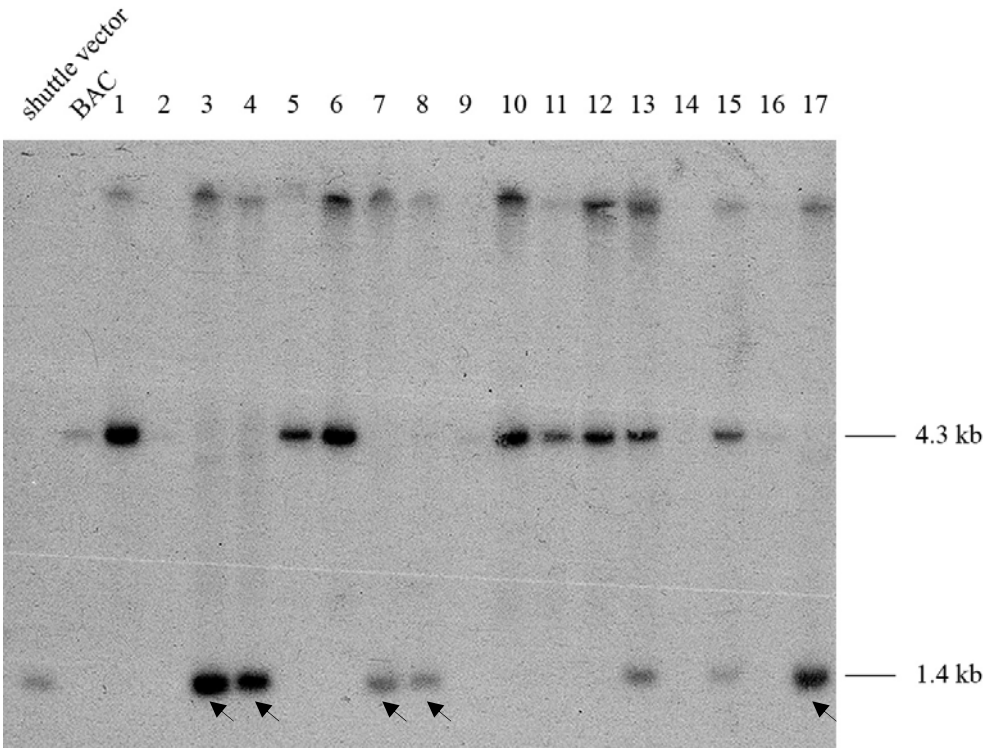

Figure 13: Screening for modified BAC clones by Southern Blot

Southern Blot of the BAC clones after the second recombination event. The BAC DNA was digested with EcoRI and the boxA sequence was used as a probe. Whereas unmodified clones showed a 4.3 kb band, resolved clones (arrows) showed a 1.4 kb band. Cointegrates showed a double band. The unmodified BAC and the modified shuttle vector served as a control.

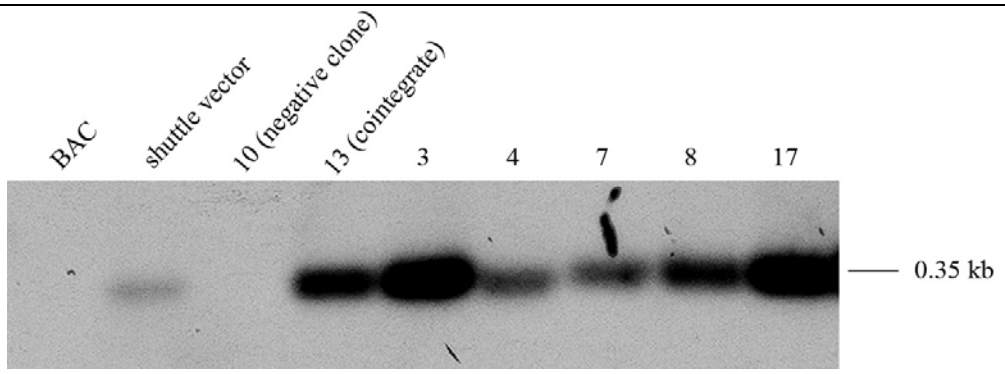

Figure 14: Confirmation of modified BAC clones by Southern Blot

Southern Blot using the t-MrVIa expression cassette as a probe. The BAC DNA was previously digested with EcoRI. All clones contained the t-MrVIa expression cassette (0.35 kb) and were proven positive.

Clone 8 was selected and the DNA was purified via ultracentrifugation in a CsCl gradient. After linearization and dialysis it was injected into the fertilized oocytes of BDF/BL6 mice.

4.6 Screening of BAC transgenic founder lines

Following BAC injection into fertilized oocytes of BDF/BL6J mice, six transgenic founders were obtained. Two lines were discarded due to breeding problems and mosaic expression. The remaining four founder lines were analyzed by Southern Blot analysis using the boxA sequence as a probe. In every line two bands were obtained, the smaller one (1.5 kb) represents the endogenous band whereas the bigger one (2.3 kb) corresponds to the number of BAC copies integrated into the genome. The results are shown in Figure 15. Lines 2 and 27 contained the highest BAC copy number in the genome but due to breeding problems of line 27, line 2 was used for further characterization.

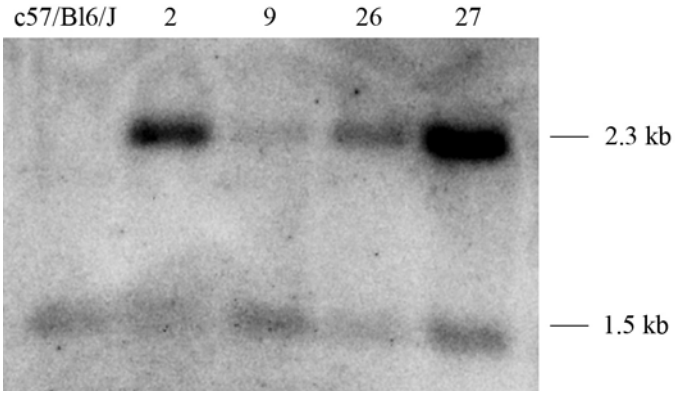

Figure 15: Determination of the BAC copy number by Southern Blot

Southern Blot using the boxA as a probe. The lower band (1.5 kb) represents the endogenous $Na_v1.8$ DNA, whereas the of the upper band (2.3 kb) represents the exogenous band derived from the modified BAC. The intensity ratio of those two bands correspond to the numbers of BAC integration into the mouse genome. Line No. 2 showed the highest copy number.

4.7 Analyses of gene expression in t-MrVIa mice

4.7.1 Expression studies by RT-PCR

Primary sensory afferents whose somata are located in the DRG innervate the skin and the dorsal horn of the spinal cord from where the signals are processed centrally to the thalamus and the somatosensory cortex. To confirm that transgenesis using the $Na_v1.8$ BAC correctly targeted the expression of t-MrVIa to DRG neurons, RT-PCR was performed. As shown in Figure 16 t-MrVIa parallels the expression of $Na_v1.8$ in the DRGs and spinal cord of transgenic mice but not in any other tissue involved in pain signaling. Wt littermates showed comparable levels of $Na_v1.8$ but lacked t-MrVIa expression.

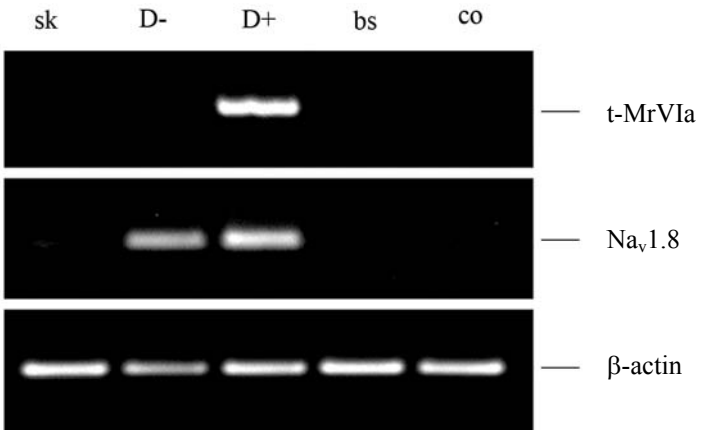

Figure 16: RT-PCR expression studies of $Na_v1.8$ and t-MrVIa in DRG neurons

RT-PCR analysis showed coincident expression of $Na_v1.8$ and t-MrVIa transcripts in the DRGs of t-MrVIa mice but not in any other tissues in the pain pathway. Wt littermates showed comparable levels of $Na_v1.8$ but lacked the t-MrVIa expression in DRGs. Sk: skin, D-: DRG (wt), D+: DRG (t-MrVIa), bs: brain stem, co: cortex.

4.7.2 T-MrVIa expression studies by *in situ* hybridization

To assess the cell-specific targeting and temporal expression of t-MrVIa in t-MrVIa mice, whole mount *in situ* hybridization was performed using t-MrVIa antisense RNA as a probe. Figure 17A shows strong t-MrVIa expression in the DRG of t-MrVIa mice whereas the toxin was not expressed in DRGs of wt mice. However, DRG neurons are a heterologous cell population. To gain further insights into the toxin expression in DRG subpopulations, *in situ* hybridization on cryosections was performed. T-MrVIa antisense strand was used as a probe on DRG sections of wt and t-MrVIa mice. Very large amounts of t-MrVIa mRNA were detected in nociceptors

(small diameter cells, <30 µm) but not in mechanoreceptors (large diameter cells, >30µm) of t-MrVIa mice demonstrating the cell autonomy of this approach, while wt mice did not show any toxin expression (Figure 17B). Thus a stable and cell-specific expression of the t-MrVIa was achieved in the nociceptor population that also expresses $Na_v1.8$ mRNA.

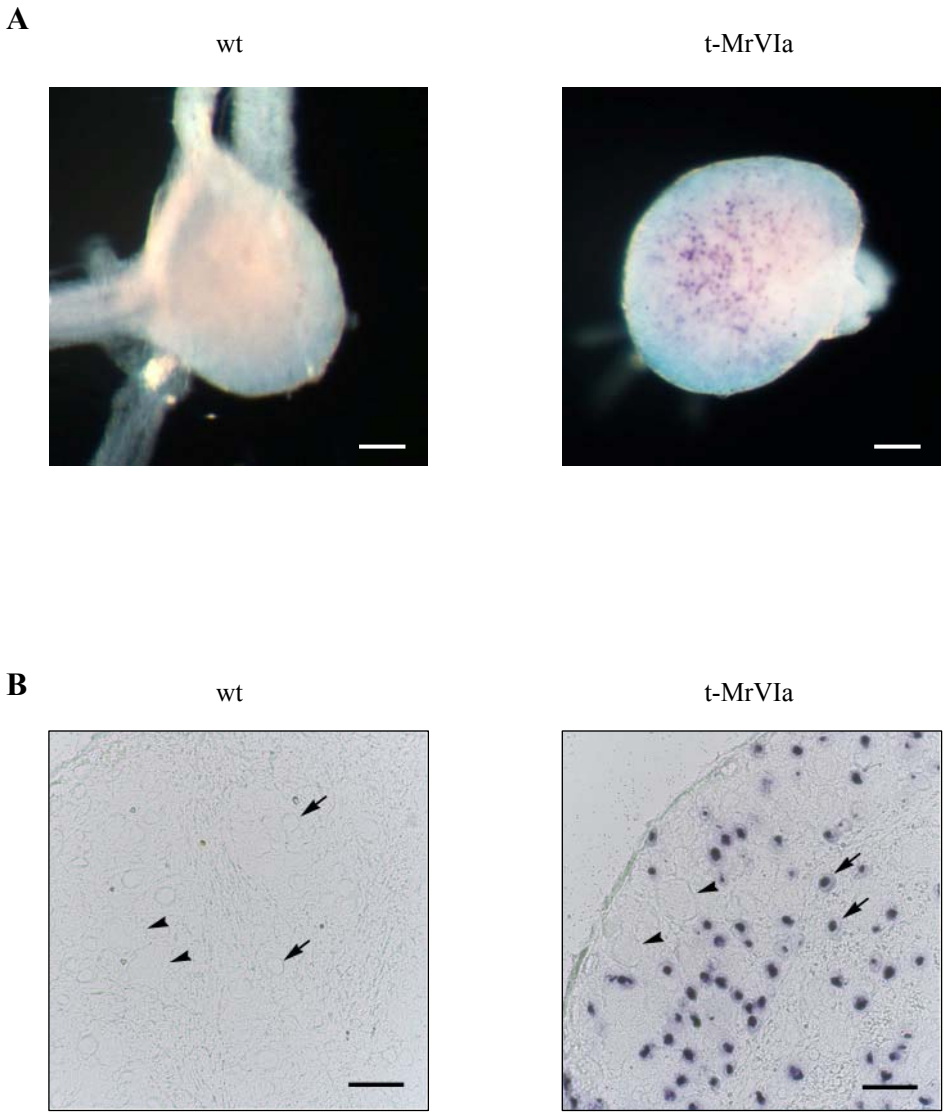

Figure 17: *In situ* hybridization on DRGs using an antisense t-MrVIa probe

A) Whole mount *in situ* hybridization showed strong t-MrVIa expression in the whole DRG of t-MrVIa mice (right panel) but not in wt mice (left panel). Scalebars: 180 µm.
B) *In situ* hybridization on DRG sections showed a strong t-MrVIa signal in nociceptors (arrow) of t-MrVIa mice (right panel) but not in mechanoreceptors (arrowhead) or in wt mice (left panel). Scalebars: 50 µm (experiment carried out by Dr. Silke Frahm-Barske).

It could be shown that t-MrVIa expression in DRG neurons of transgenic mice is restricted to nociceptors. However, it did not indicate how strongly the toxin is expressed during development. Previous studies indicated that $Na_v1.8$ expression initiates from embryonic day E13 and steadily increases until it reaches a stable and strong expression at postnatal day P7 which then remains constant into adulthood (Benn et al., 2001). To investigate the level of toxin expression during embryogenesis, *in situ* hybridization on transversal embryo sections was performed using t-MrVIa antisense RNA as a probe. Figure 18 shows strong t-MrVIa expression in the DRG of t-MrVIa mice and no signal in the spinal cord and in DRGs of wt mice. Thus, these analyses indicate that t-MrVIa is expressed only in nociceptors in t-MrVIa mice from E14 on and is maintained until adulthood.

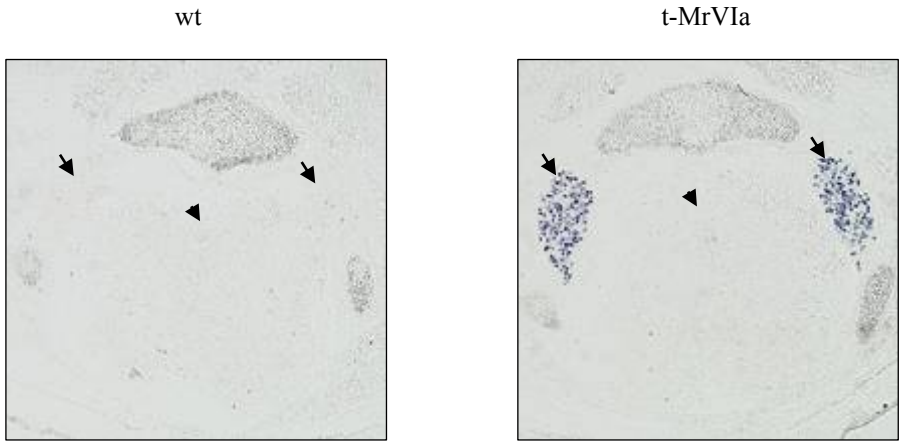

Figure 18: *In situ* hybridization on transversal embryo sections using an antisense t-MrVIa probe

In situ hybridization on transversal embryo sections showed a strong t-MrVIa signal in DRGs (arrow) of t-MrVIa mice at E14 (right panel) but not in SC (arrowhead) or wt mice (left panel) (experiment carried out by Dr. Silke Frahm-Barske).

4.8 Functional characterization of t-MrVIa mice

In contrast to conventional superfusion systems, the tethered toxin approach could allow permanent blocking of ion channels in a subset of certain neurons. As RNA expression studies showed high and restricted toxin expression in nociceptive neurons, these studies were followed by functional ion channel analysis. For this purpose, whole cell patch clamp recordings were performed on DRG cultures from wt and t-MrVIa mice. Mechanoreceptors and nociceptors can be distinguished based on their distinct soma size and action potential shape. Whereas mechanoreceptors have big soma diameters and narrow action potentials, nociceptors are small diameter neurons and show a characteristic hump in the falling phase of the action potential (Figure 19). For this study nociceptors < 25 µm were used for analysis.

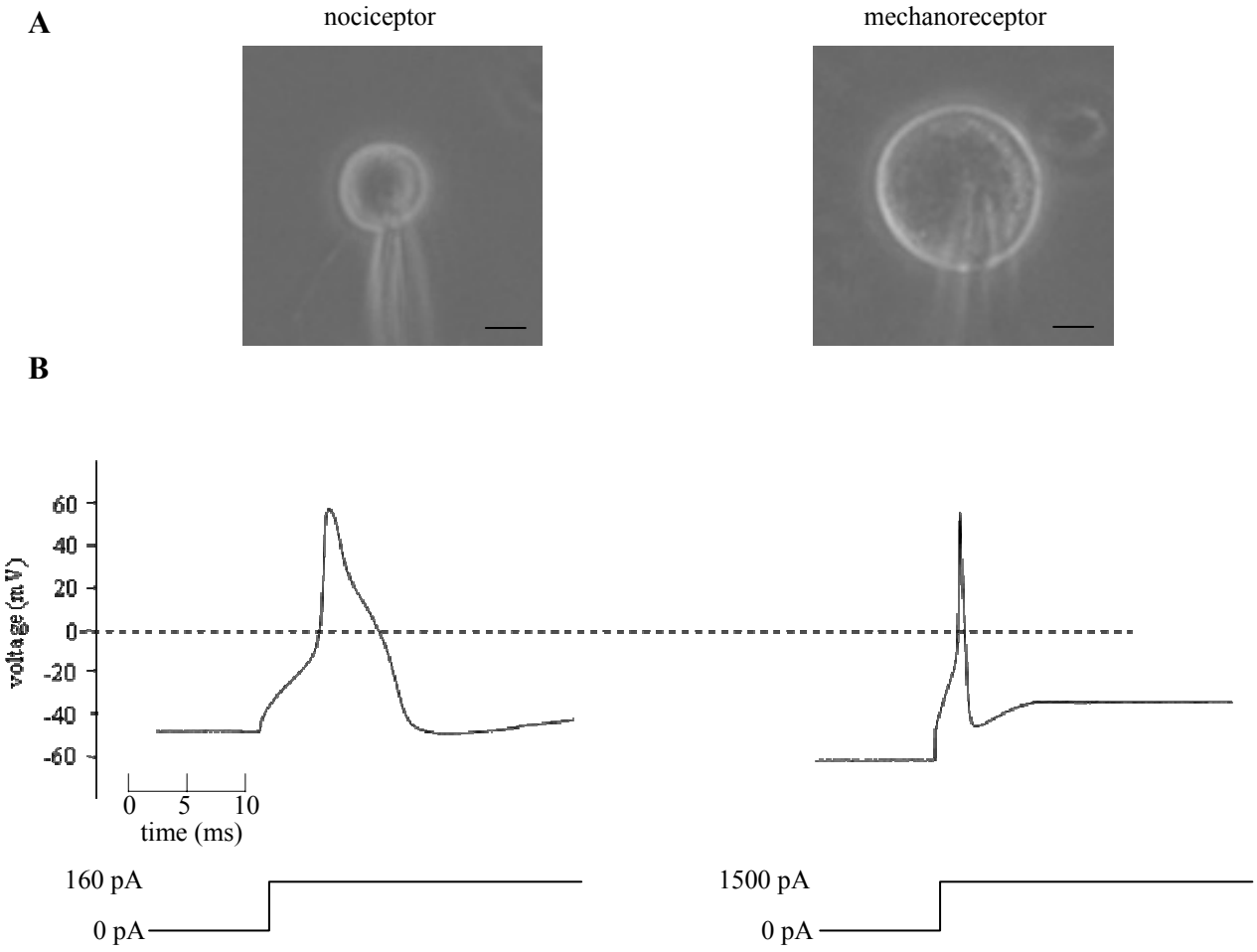

Figure 19: Basic characteristics of nociceptors and mechanoreceptors

A) Phase contrast images of a nociceptor (left panel) and a mechanoreceptor (right panel) in culture. Scalebars: 10 µm.
B) Representative action potential traces of a nociceptor (left panel) showing the characteristic hump on the falling phase and a narrow action potential from a mechanoreceptor (right panel). The bottom traces represent the stimuli.

4.8.1 Whole cell inward currents are reduced in t-MrVIa mice

Whole cell inward currents were measured in nociceptors and mechanoreceptors of wt and t-MrVIa littermates. The sensory neurons were held at -60mV and hyperpolarized to -120 mV to prevent inactivation of sodium channels followed by step depolarizations of 10 mV increment from -50 mV up to +40 mV. This protocol allows to record $Na_v1.8$-mediated sodium currents without detecting the persistant TTX-R sodium current $Na_v1.9$ (Cummins et al., 1999). The current amplitudes obtained were normalized to the cell capacitance. Whereas nociceptors of t-MrVIa mice showed a two-fold decrease of whole cell inward current compared to wt mice, mechanoreceptive currents were not altered (Figure 20B), demonstrating the cell autonomy of this approach. Importantly, voltage-gated potassium currents were not significantly changed, reflecting the specificity of the t-MrVIa toxin to VGSC. Representative traces of nociceptors of wt and t-MrVIa mice are shown in Figure 20A. Figure 20C shows the current voltage relationship (IV curve) of whole cell inward current recorded from nociceptors (left panel) and mechanoreceptors (right panel). The amplitude of the IV curve recorded from nociceptors is reduced in t-MrVIa mice (as quantified in Figure 20B), whereas mechanoreceptive currents were not affected (Figure 20C). In agreement with studies using the soluble toxin, t-MrVIa-mediated block did not shift the IV curve but remained the threshold of activation at -30mV for nociceptors and -40mV for mechanoreceptors (Daly et al., 2004). The difference in this threshold between nociceptors and mechanoreceptors is known and results from their different composition of VGSC with distinct kinetics.

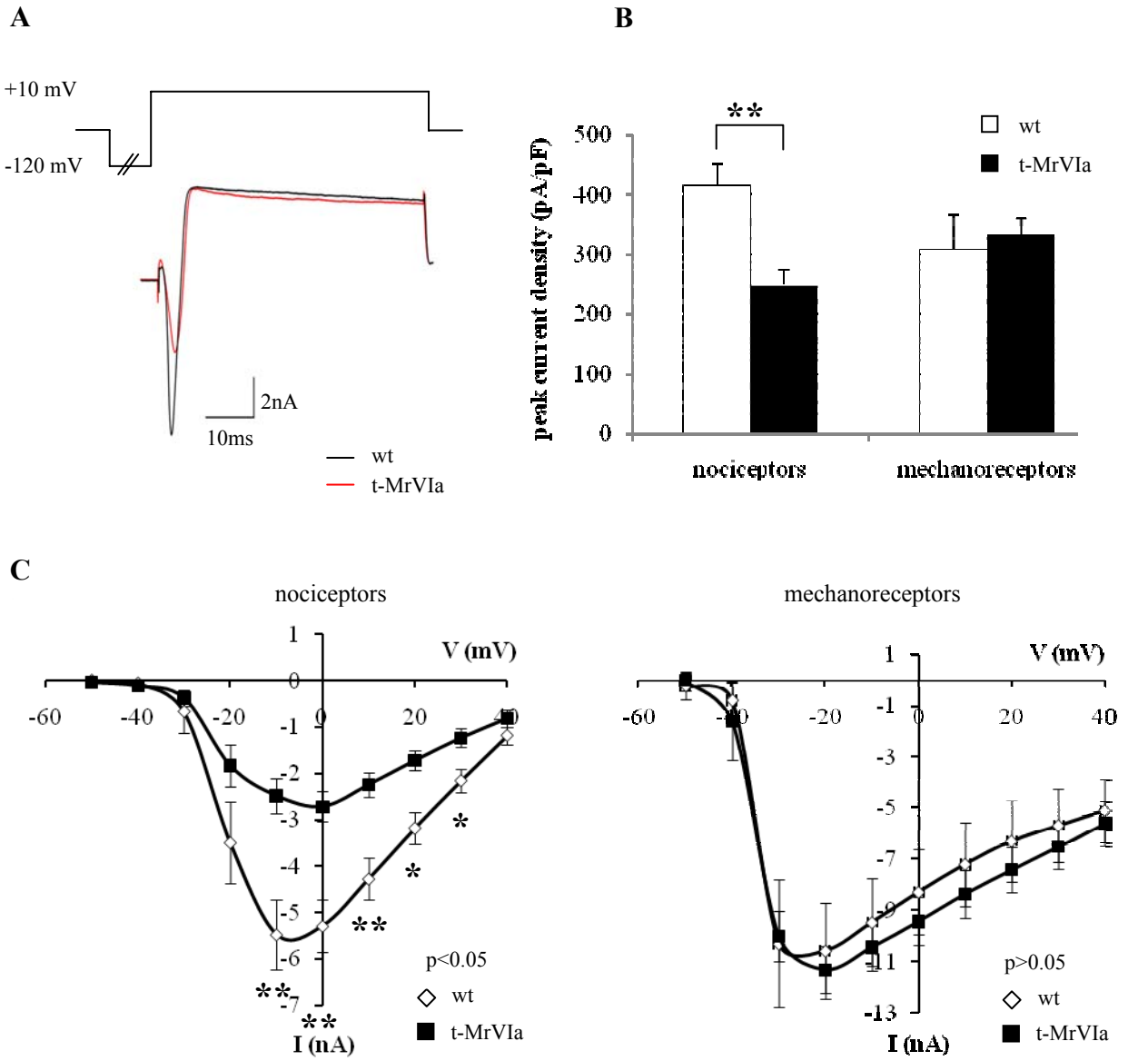

Figure 20: Voltage clamp analyses on nociceptors and mechanoreceptors of wt and t-MrVIa mice

A) Representative traces of peak inward currents in nociceptors of t-MrVIa mice (red trace) and wt littermates (black trace). Neurons were kept at -60 mV and hyperpolarized to -120 mV to remove inactivation of VGSCs. Depolarization took place in -10 mV steps from -50 to +40 mV.

B) Bar graph indicating the quantification of whole cell VGSC currents from nociceptors of wt (n = 32 cells) and t-MrVIa mice (n = 31 cells), and mechanoreceptors of wt (n = 9 cells) and t-MrVIa mice (n = 9 cells) (right panel). Peak currents were normalized with respect to the capacitance of the individual cells. In nociceptors the density of total VGSC currents was significantly reduced in t-MrVIa mice (243.5 ± 37.2 pA/pF) with respect to wt mice (413.7 ± 37.2 pA/pF), whereas mechanoreceptors did not reveal any differences in the peak current density (wt: 306.9 ± 57.4 pA/pF, t-MrVIA: 343.1 ± 18.1 pA/pF) ($p>0.05$ t-test).

C) IV-curves showing whole cell inward current recorded in nociceptors (left panel) (wt: n = 32 cells, t-MrVIa: 30 cells) ($p<0.05$, two-way-Anova) and mechanoreceptors (right panel) (n = 9 cells each) ($p>0.05$, two-way-Anova) (t-test for single voltage steps).

Furthermore, other basic electrophysiological parameters were unaltered in t-MrVIa mice. Results are summarized in table 2.

Table2: Basic electrophysiological parameters of wt and t-MrVIa DRG neurons

Cell type	Soma diameter (µm)	Cell capacitance (pF)	Resting membrane potential (mV)
wt nociceptor	22.0 ± 0.6	16.8 ± 1.3	-52.2 ± 1.1
t-MrVIa nociceptor	22.0 ± 0.6	15.5 ± 1.1	-52.5 ± 1.0
wt mechanoreceptor	42.8. ± 1.5	42.2 ± 2.2	-59.2 ± 1.0
t-MrVIa mechanoreceptor	39.3 ± 1.1	42.0 ± 2.0	-57.3 ± 0.8

4.8.2 Genetic t-MrVIa expression results in a VGSC subtype-specific block

The conotoxin MrVIa has been described to be a potent blocker of the TTX-R VGSC $Na_v1.8$ at nanomolar range (IC_{50} = 83nM) (Daly et al., 2004). In contrast MrVIa affinity for TTX-S VGSC is more than 10 times lower and it is not able to block the other sensory neuron specific VGSC $Na_v1.9$. Additionally, previous tethered toxin studies have implied that toxins remain their specificity when tethered to the membrane (Ibanez-Tallon et al., 2004). Thus, subdivisions into VGSC currents were done by recording in the presence of 0.5 µM TTX. Figure 21 shows that TTX-R currents are significantly reduced in nociceptors of t-MrVIa mice. Importantly, this block did not result in upregulation of related TTX-S channels. We even observed a very slight reduction in TTX-S currents probably reflecting the toxin affinity to VGSCs, however, it was never proven significant. This is in clear contrast to studies from $Na_v1.8$ null-mutant mice where marked upregulation of $Na_v1.7$, the main TTX-S current in nociceptors, occurred.

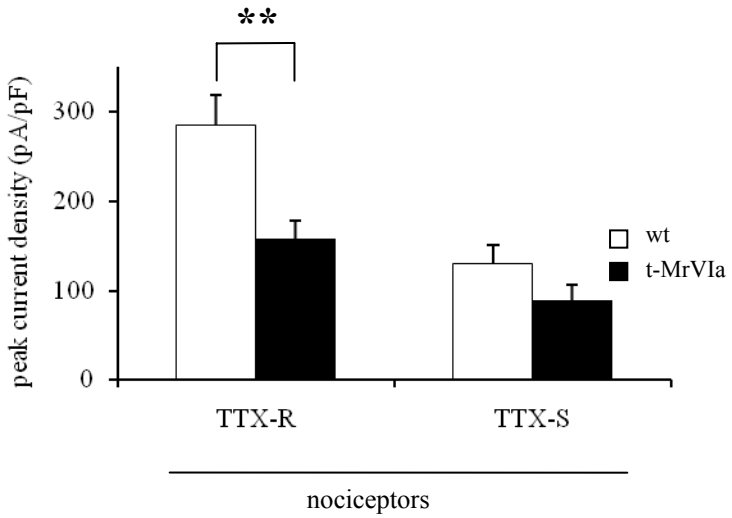

Figure 21: Quantification of TTX-R and TTX-S VGSC currents from nociceptors of wt and t-MrVIa mice

The peak currents were normalized with respect to the capacitance of the individual cells. The density of TTX-R VGSC currents was significantly reduced in t-MrVIa mice (TTX-R: wt: 284.3 ± 34.1 pA/pF, t-MrVIa: 158.6 ± 20.4 pA/pF) ($p<0.05$, t-test), whereas TTX-S currents were not altered (TTX-S: wt: 129.6 ± 20.1 pA/pF, t-MrVIa: 89.3 ± 16.6 pA/pF) ($p>0.05$, t-test)

4.8.3 T-MrVIa preferentially blocks TTX-R currents in IB4+ nociceptor subpopulation

All nociceptors transduce noxious stimuli but they can be further divided into certain subpopulations due to the expression of cell-type-specific markers. Such subdivision is made based on the presence or absence of binding sites for isolectin B4, thus nociceptors are referred to as IB4+ and IB4-, respectively. Their afferents target into different laminae of the dorsal horn and also process signals centrally via distinct second order neurons. Importantly, it is known that IB4+ nociceptors are particularly rich in TTX-R VGSC including $Na_v1.8$. To evaluate whether these molecular differences could be reflected in the genetic expression and specificity of t-MrVIa, *in vitro* labeling experiments with fluorescently tagged IB4 were performed and either fluorescent or non-fluorescent nociceptors subpopulations were recorded in the presence of TTX. As shown in Figure 22 both subpopulations are markedly blocked by the toxin. However, the block was more pronounced in the IB4+ subpopulation probably based on higher t-MrVIa expression levels mediated by the $Na_v1.8$ BAC.

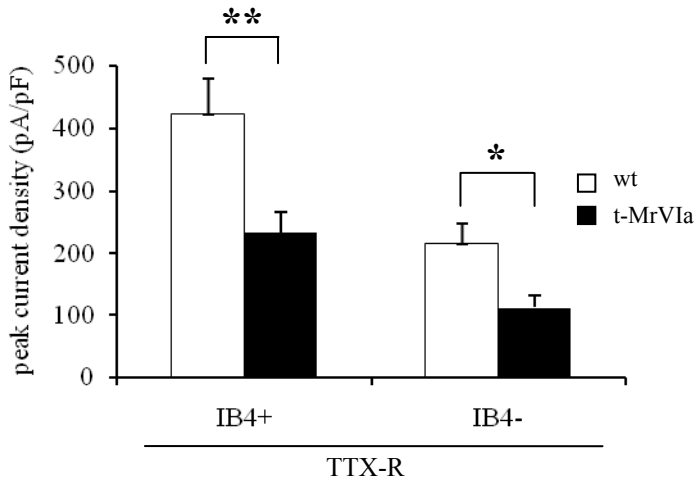

Figure 22: T-MrVIa action on TTX-R currents in the IB4+ and IB4- nociceptive subpopulation

Whole cell patch clamp recordings were done in the presence of 0.5 µM TTX. Bar graph indicating the quantification of TTX-R VGSC currents from nociceptors of wt and t-MrVIa mice in the IB4+ and IB4- subpopulation. Peak currents were normalized with respect to the capacitance of the individual cells. The density of TTX-R VGSC currents was significantly reduced in both subpopulations in t-MrVIa mice (wt: IB4+: 422.7 ± 57.0 pA/pF, t-MrVIa: IB4+: 232.9 ± 34.0 pA/pF, wt: IB4-: 215.1 ± 33.6 pA/pF, t-MrVIa IB4-: 111.6 ± 19.2 pA/pF) (IB4+: $p<0,005$, t-test, IB4-: $p<0.05$).

4.8.4 Action potential amplitude is reduced in IB4+ nociceptors of t-MrVIa mice

To further evaluate the effect of $Na_v1.8$-mediated current reduction in t-MrVIa mice, current clamp analyses were performed to gain insights into the generation and propagation of action potentials using IB4 live labeling of DRG cultures. No significant changes were observed in the half peak duration of action potentials and in the threshold of activation (Figure 23A,B, bargraphs show mean value of IB4+ and IB4- subpopulation). However, reduced action potential amplitudes were detected in nociceptors of t-MrVIa mice (Figure 24). This effect was restricted to the IB4+ subpopulation and did not occur in IB4- nociceptors or mechanoreceptors.

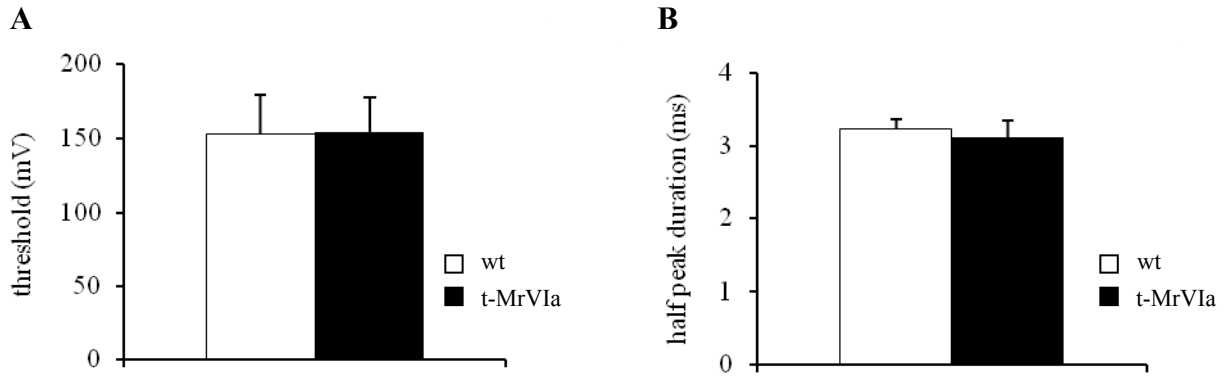

Figure 23: Action potential threshold and half peak duration are not changed in nociceptors of t-MrVIa mice.

A) Patch clamp recordings revealed no differences in the threshold for action potential generation in t-MrVIa mice (154.3 ± 22.5 mV, n= 28) compared to wt (152.7 ± 26.4 mV, n = 33) ($p>0.05$, t-test).

B) The action potential half peak duration is unchanged in t-MrVIa mice (3.4 ± 0.2 ms, n = 31) compared to wt (3.4 ± 0.2 ms, n = 31) ($p>0.05$, t-test).

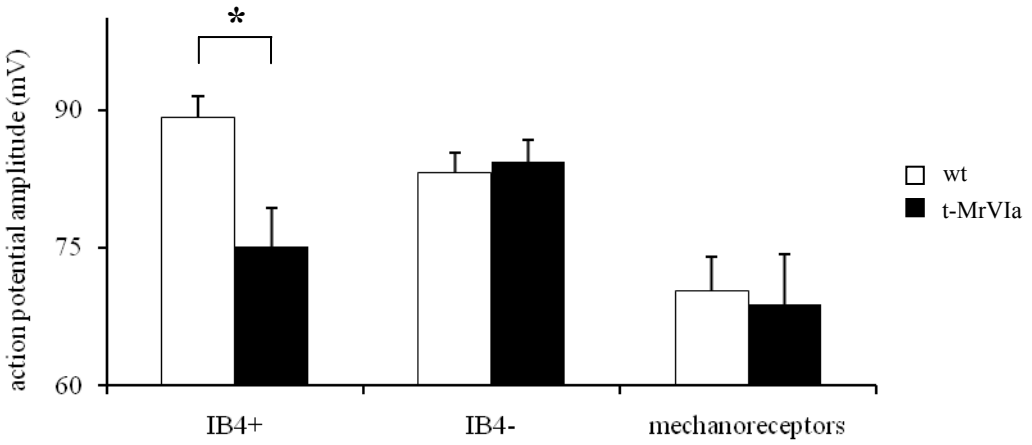

Figure 24: Action potential amplitude is reduced in IB4+ nociceptors of t-MrVIa mice.

Quantification of action potential amplitudes in sensory neuron subpopulations revealed a significant reduction in IB4+ nociceptors (wt: n = 11 cells, t-MrVIA: n = 14 cells) of t-MrVIa ice (wt: 89.2 ± 2.3 mV, t-MrVIa: 74.3 ± 3.9 mV), whereas the action potential amplitude in IB4- nociceptors (wt: n = 20 cells, t-MrVIa: n = 18 cells) and mechanoreceptors (wt: n = 9 cells, t-MrVIa n = 9 cells) is not affected compared to wt mice (t-test).

4.8.5 T-MrVIa action on nociceptors is reversible

Immunostaining of DRG neurons transfected with a t-MrVIa expressing plasmid already indicated strong toxin expression at the plasma membrane which can be reversed by PI-PLC treatment (see Figure 10). To ensure that the reduction in TTX-R peak current density in transgenic mice is due to the activity of the toxin at the cell membrane, DRG cultures from t-MrVIa mice were treated with PI-PLC for 1 h. Whole cell patch clamp recordings revealed an increase of the TTX-R peak current density which also resulted in a larger density of total VGSC currents (Figure 25). The values did not reach the wt level, however, no significant differences between wt mice and PI-PLC-treated nociceptors from t-MrVIa mice were detected. The TTX-S current also slightly increased, which reflects the affinity of MrVIa to act on TTX-S VGSC when it is overexpressed (Figure 25). However, no significant changes in the TTX-S peak current density were obtained. Thus, this result proves that the block of TTX-R channel obtained is mediated by the tethered toxin which can be reversed up to 80 % upon PI-PLC treatment.

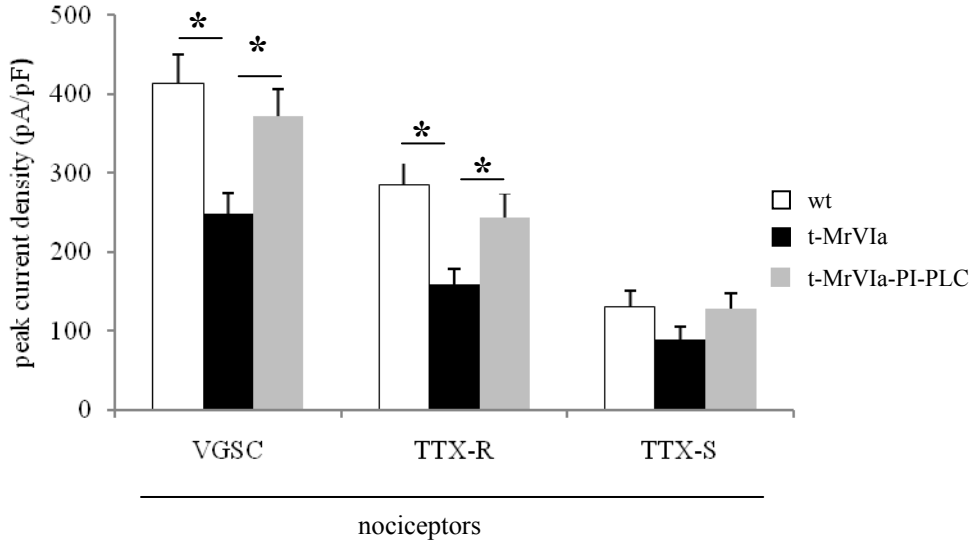

Figure 25: PI-PLC treatment increases peak current density in t-MrVIa mice.

Bar graph indicating the quantification of VGSC currents from nociceptors of wt and t-MrVIa mice before and after PI-PLC treatment. Peak currents were normalized with respect to the capacitance of the individual cells. The current density of TTX-R and total VGSC currents was significantly reduced in t-MrVIa mice compared to wt and PI-PLC-treated t-MrVIa cultures (wt: VGSC: 413.7 ± 37.2 pA/pF, t-MrVIa VGSC: 247.9 ± 16.1 pA/pF, t-MrVIa-PI-PLC: VGSC: 371.6 ± 34.2 pA/pF, wt: TTX-R: 284.3 ± 34.1 pA/pF, t-MrVIa: TTX-R: 158.6 ± 20.4 pA/pF, t-MrVIa-PI-PLC: TTX-R: 243.6 ± 31.5 pA/pF, wt: TTX-S: 129.6 ± 22.1 pA/pF, t-MrVIa: TTX-S: 89.3 ± 16.6 pA/pF, t-MrVIa: TTX-S: 128.0 ± 20.1) (t-test).

Summary

Whole cell patch clamp recordings showed that t-MrVIa expression resulted in a cell-autonomous block of VGSC in nociceptors which could be reversed by PI-PLC treatment while adjacent mechanoreceptors were not affected. Furthermore, the block was restricted to TTX-R $Na_v1.8$ VGSC consistent with the affinity of the toxin for this channel subtype. Importantly, no upregulation of TTX-S channels was observed. The block was more pronounced in the IB4+ subpopulation which also resulted in a reduction of action potential amplitude. Voltage-gated potassium channels and all basic electrophysiological parameters like resting membrane potential were not changed.

4.9 T-MrVIa mice do not show compensatory upregulation of related VGSC subunits

Gene deletion of ion channel subunits very often leads to compensatory upregulation of associated genes as a result of current loss. The electrophysiological data already indicated no dysregulation of TTX-S VGSC. However, to rule out that the toxin block does not affect the expression of $Na_v1.8$ or other VGSC in the DRG, detailed analysis was done by real-time PCR. Primers for all VGSC α- and β-subunits expressed in DRG neurons were used. No significant changes of any VGSC subunit were detected at the RNA level in DRGs of t-MrVIa mice compared to wt (Figure 26).

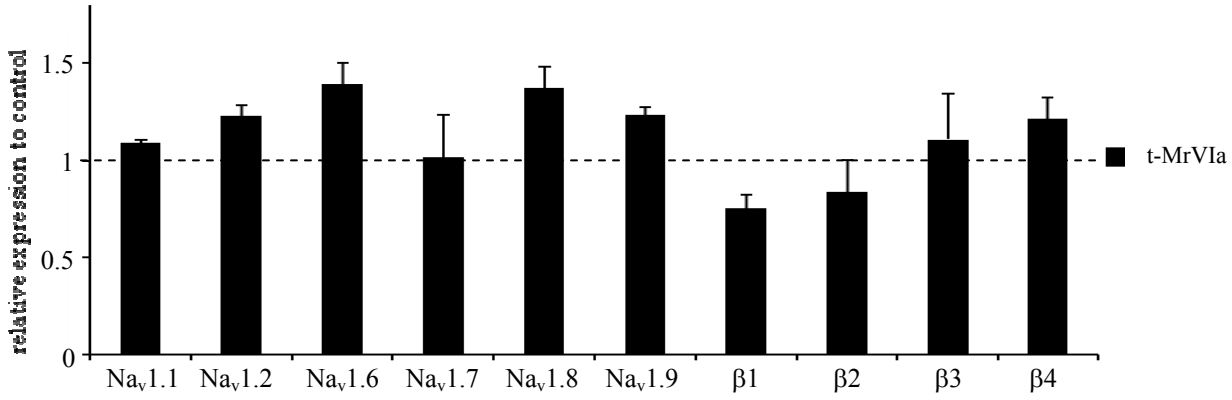

Figure 26: Quantification of VGSC mRNA levels in DRGs of wt and t-MrVIa mice by real-time PCR

Real-time PCR analyses with specific primers for the indicated α and β VGSCsubunits on total RNA prepared from DRGs. Normalized values of the expression levels revealed no significant changes in t-MrVIa mice compared to wt ($p>0.05$, t-test) ($n = 4$ for each subunit). Real-time PCRs of $Na_v1.3$ (embryonic), $Na_v1.4$ (skeletal muscle) and $Na_v1.5$ (heart) are not shown in this analysis.

4.10 T-MrVIa-mediated block of $Na_v1.8$ does not impact cell survival, central target selection or distribution of nociceptive subpopulations

4.10.1 Sensory neuron number is unchanged in t-MrVIa mice

Reduced neuronal activity could have an impact on cell survival. To rule out that the reduced currents in t-MrVIa mice could lead to a difference in sensory neuron number, electron microscopy was performed on sections of the saphenus nerve, which innervates the hind paw. The exact number of non-myelinated (C-fiber nociceptors) and myelinated (Aδ-fiber nociceptors and Aβ-fibers) axons could be determined. Figure 28 shows the quantification of myelinated and non-myelinated fibers of the saphenus nerve which was not altered in t-MrVIa mice compared to wt. Furthermore, no differences in morphology were detected (Figure 27).

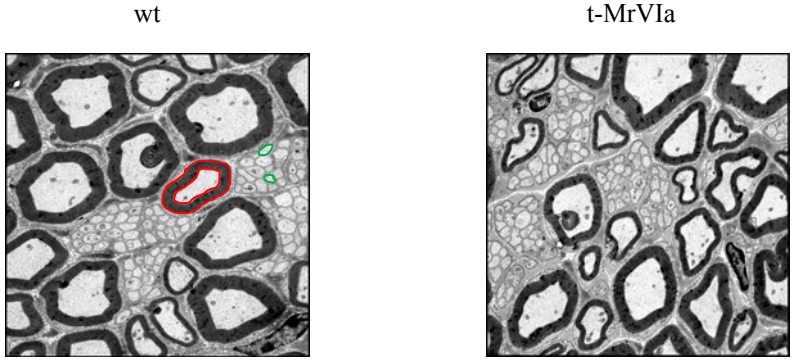

Figure 27: Electron micrographs of sections of the saphenus nerve

No differences in the morphology of myelinated fibers (red) and non-myelinated fibers (green) were detected. Scalebar: 2 µm (pictures were taken by Dr. Bettina Erdmann).

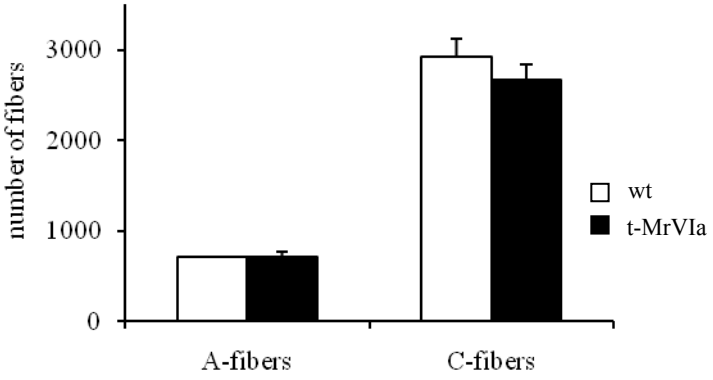

Figure 28: Quantification of the number of axons in the saphenous nerve of wt and t-MrVIa mice

Quantification of myelinated (A-fibers) and unmyelinated (C-fibers) axons of wt and t-MrVIa mice revealed no difference in sensory neuron number (A-fibers: wt: 711.8 ± 3.1, t-MrVIa: 714.8 ± 50.7, C-fibers: wt: 2920.6 ± 197.0, t-MrVIa: 2660.7 ± 173.1) (n = 3 mice) ($p>0.05$ t-test).

4.10.2 Afferent central target selection is unchanged in t-MrVIa mice

The precision in processing sensory information requires coordination between sensory modality and afferent central target selection. To rule out that t-MrVIa expression in nociceptors of t-MrVIa mice impairs the central innervation pattern, immunostainings were done on SC sections using the neurochemical markers IB4 and subP. In both wt and t-MrVIa mice, the central target selection was unchanged. SubP was detected in the lamina $II_{0,}$ whereas IB4 exclusively labeled lamina II_i and the superficial lamina of the dorsal horn (Figure 29).

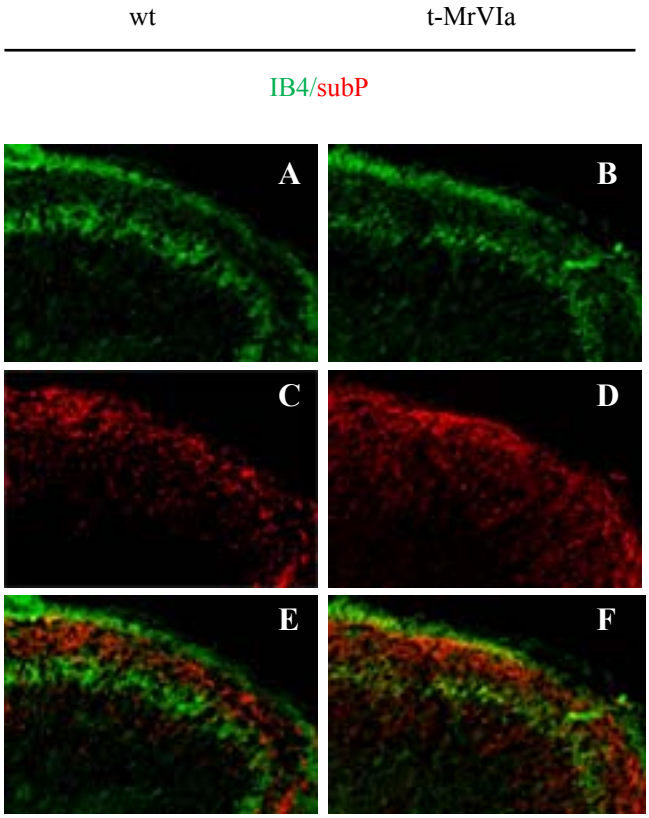

Figure 29: Immunohistochemical expression analysis of subP and IB4 in the dorsal spinal cord from wt and t-MrVIa mice

Doublestaining of IB4 (A, B, E, F) plus subP (C-F) on adult dorsal horn sections from wt and t-MrVIa mice. The afferent central target innervation is unchanged.

4.10.3 Distribution of IB4+ and IB4- subpopulation is unchanged in t-MrVIa mice

To evaluate whether the predominant block of IB4+ nociceptors leads to a redistribution of nociceptive subtypes live labelling of DRG neurons was done with fluorescently labelled IB4. The distribution of the two nociceptive subpopulations were quantified and no differences were detected in t-MrVIa mice compared to wt (Figure 30, 31)

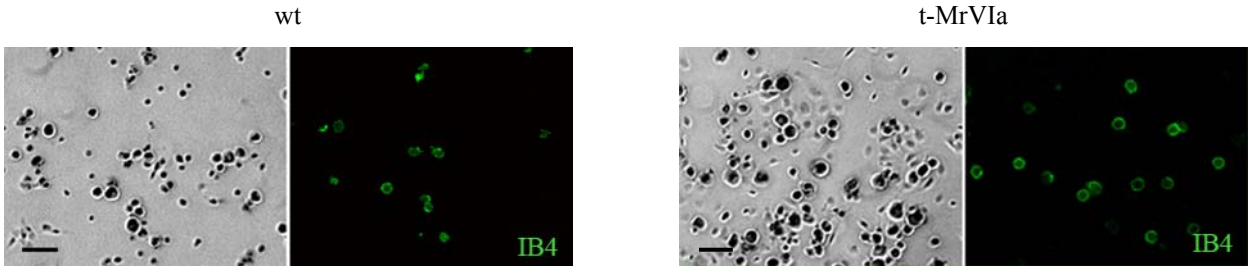

Figure 30: Fluorescent isolectin B4 labeling of DRG neural cultures

Representative pictures of an IB4 labeled DRG culture from wt (left panel) and t-MrVIa mice (right panel). Scalebar: 50 µm

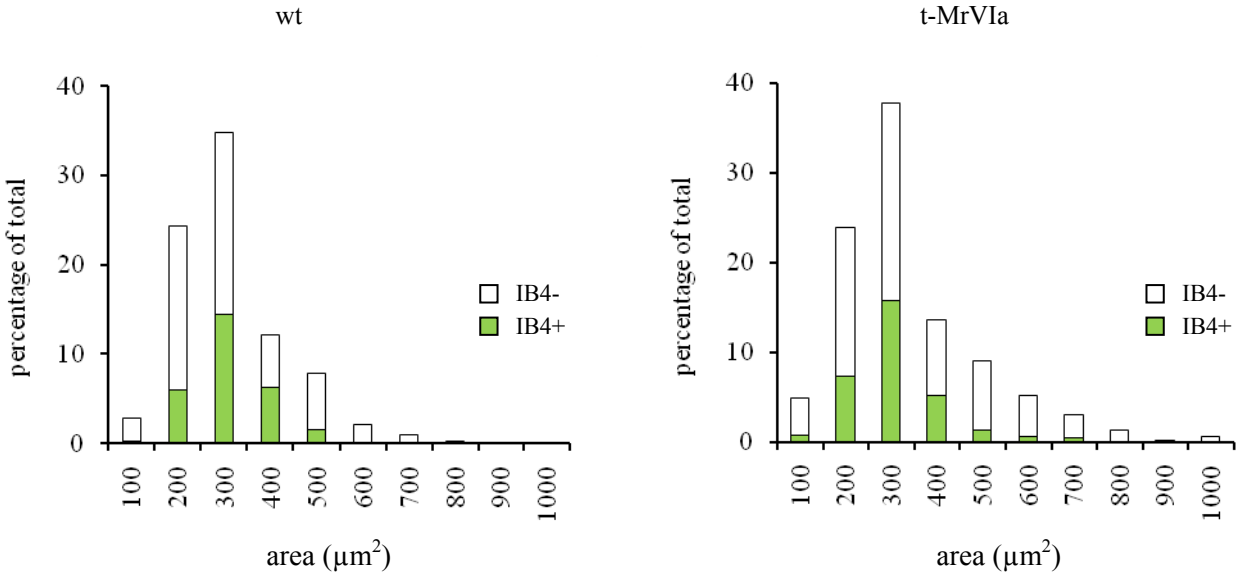

Figure 31: Distribution of IB4+ and IB4- subpopulation in wt and t-MrVIa mice

Quantification of IB4+ cells (green bars) and IB4- cells (white bars) in DRG cultures from wt (left panel) and t-MrVIa mice (right panel) shows no significant differences in number and size distribution (n = 2 mice).

4.11 Behavior analysis of t-MrVIa mice

Animal models of genetically altered rodents have established the importance of VGSC in acute and chronic pain. Therefore, it was postulated that two-fold reduction of TTX-R VGSC currents in t-MrVIa mice might lead to a reduced perception of pain. Behavior tests were carried out with age and sex-matched littermates. Mice were indistinguishable in their body weight, spontaneous behavior and appearance.

4.11.1 Motor coordination is not affected in t-MrVIa mice

$Na_v1.8$ is highly expressed in sensory neurons but no expression in motor neurons has ever been detected. However, to rule out that t-MrVIa mice could have motor deficits, mice were tested using an accelerating rotarod and the time when they fell was scored. No deficits in sensory motor coordination occurred over a period of three days (Figure 32).

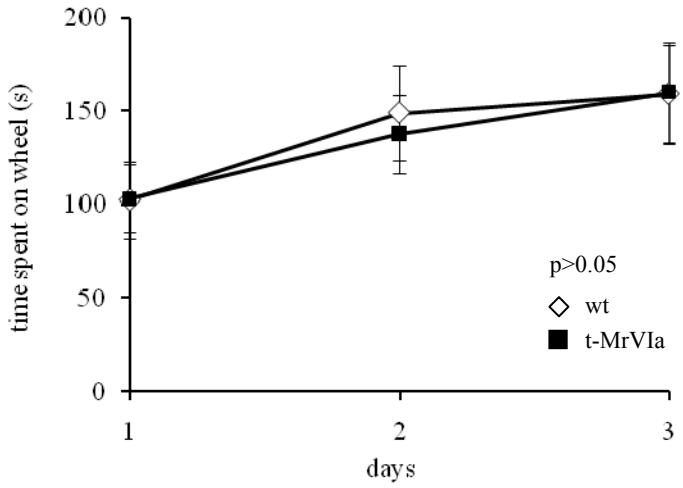

Figure 32: Motor coordination is not impaired in t-MrVIa mice

Mice were placed on an accelerating rotarod. The time until they lost their balance was scored. No differences in motor coordination were detected in t-MrVIa mice compared to wt. Bar graphs show the time averages of 10 mice each ($p>0.05$, two-way-Anova).

4.11.2 T-MrVIa mice show normal responses to acute heat and mechanical stimuli

$Na_v1.8$ is known to be highly expressed in nociceptive neurons. Thus, acute pain behavior tests were performed on t-MrVIa mice. First, the Hargreaves test was done where a radiant heat

source is applied to the hindpaw of the mouse and the latency until paw removal is scored (Hargreaves et al., 1988). No difference in paw withdrawal latency was detected in t-MrVIa mice compared to wt (Figure 33A). To assess the responses of mice to mechanical noxious stimuli a plantar dynamic aesthesiometer was used. This instrument applies force with a blunt probe to the hindpaw of the mouse until paw removal. The force was increased by 1g/s. T-MrVIa mice did not show any altered responses compared to wt mice (Figure 33B).

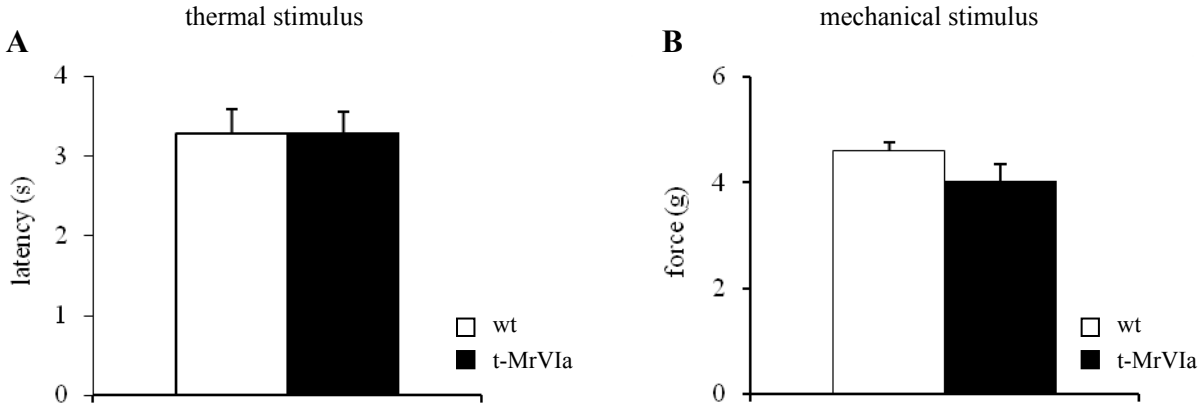

Figure 33: Acute mechanical and thermal nociception develops normally in t-MrVIa mice

A) Responses to noxious thermal stimuli were measured using the Hargreaves apparatus. Bargraphs show the mean latency of paw withdrawal upon exposure to radiant heat. No differences were observed in t-MrVIa mice (n = 8 mice) ($p>0.05$; t-test).

B) Mechanical pain stimuli were applied using a plantar dynamic aesthesiometer and measured as the force applied to the hindpaw of the mouse until withdrawal. No differences were observed in t-MrVIa mice (n = 8 mice) ($p>0.05$, t-test).

4.11.3 Mechanical inflammatory hypoalgesia in t-MrVIa mice

$Na_v1.8$ has also been shown to be involved in tissue inflammation. Thus, the responses of t-MrVIa and wt mice to mechanical noxious stimuli were determined after unilateral injection of carrageenan into the hindpaw of mouse. Over a time period of four hours after injection, wt mice developed a pronounced hyperalgesia, whereas t-MrVIa mice showed a clear delay in the manifestation of hyperalgesia and also a much faster recovery (Figure 34). Thus, t-MrVIa mice were partially protected from mechanically induced hyperalgesia.

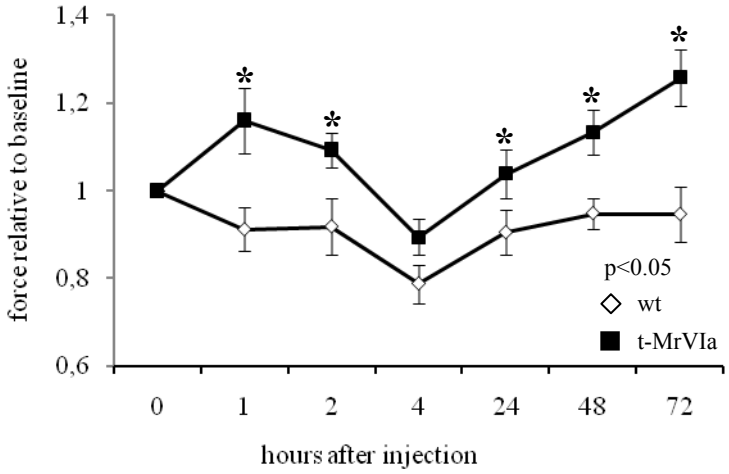

Figure 34: Mechanical inflammatory hypoalgesia in t-MrVIa mice

Intraplantar injection of carrageenan-induced mechanical hyperalgesia in wt mice at 4h. T-MrVIa mice showed delayed responses and faster recovery from mechanical hyperalgesia compared to wt mice ($p<0.05$, two-way-Anova, t-test for single time points: $p<0.05$). However, the maximum level of hyperalgesia was similar in wt and t-MrVIa mice (n = 11).

4.11.4 Thermal inflammatory hyperalgesia developed normally in t-MrVIa mice

The responses to thermal stimuli after carrageenan-induced inflammation were determined using the Hargreaves apparatus. T-MrVIa and wt mice developed the same level of hyperalgesia which was most pronounced at four days after injection (Figure 35) and completely reversed after 72 hours.

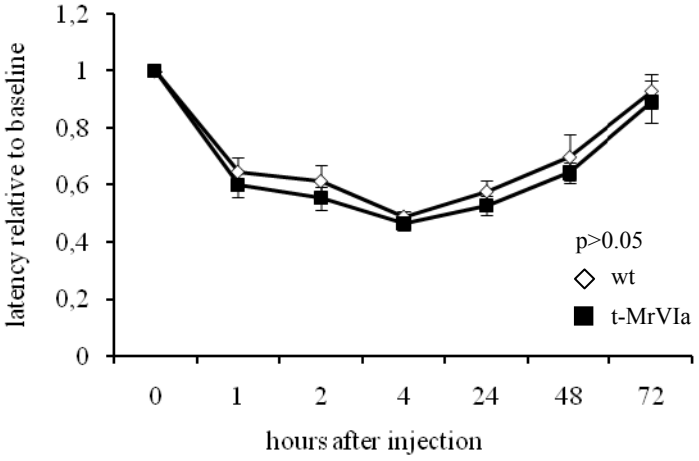

Figure 35: Thermal inflammatory hyperalgesia is unchanged in t-MrVIa mice

Intraplantar injection of carrageenan-induced thermal hyperalgesia in both wt and t-MrVIa mice. No differences were obtained (n = 11 mice) ($p>0.05$, two-way-Anova, t-test for single time points: $p>0.05$).

4.11.5 T-MrVIa mice show negligible responses to noxious cold

It has been recently shown that $Na_v1.8$ is involved in the transduction of noxious cold stimuli (Zimmermann et al., 2007). To test this possibility t-MrVIa mice were tested on a cold plate whose surface was kept at 0 ^{0}C. The number of lickings and jumps was scored over a time period of 90 seconds. As shown in Figure 36A, t-MrVIa mice showed negligible responses to noxious cold compared to wt mice. To rule out a defect in thermoreception a preferential temperature test was carried out where one plate was kept at 30 ^{0}C whereas the other one was cooled to 10 ^{0}C. Mice had free access to both plates and the time they spent on each plate was measured. T-MrVIa mice as well as wt mice favored 30 ^{0}C (Figure 36B)

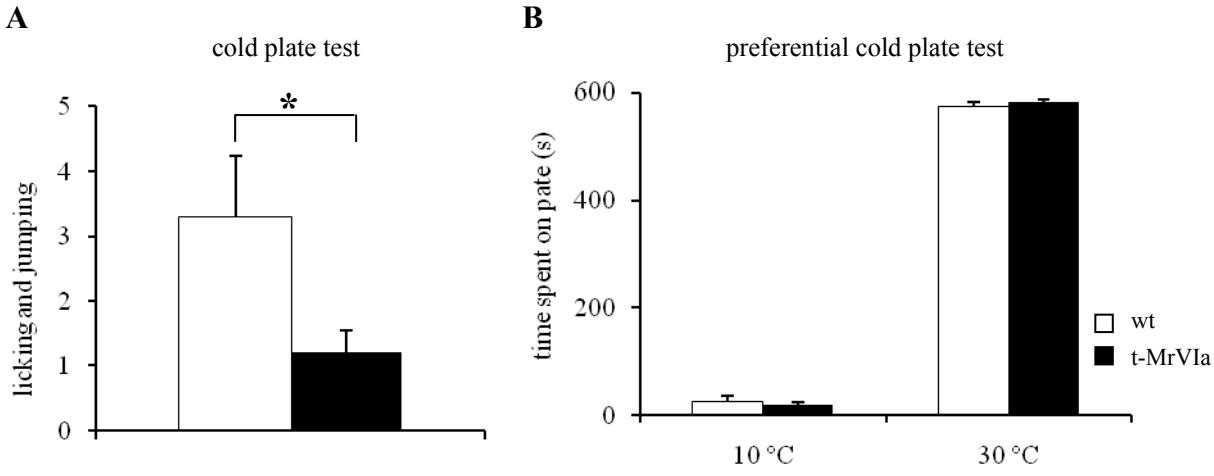

Figure 36: T-MrVIa mice showed reduced sensitivity to noxious cold

A) The response to noxious cold pain was measured by placing the mice on a cooled plate kept at 0 ^{0}C for 90 s. Nocifensive cold responses were scored as the number of paw licking and jumpings. T-MrVIa mice showed negligible responses to noxious cold ($p<0.05$, t-test) (n = 10 mice).

B) The preference of the mice to innocuous cold temperatures was determined using the preferential cold plate test. Temperature detection was assessed by determining the time the mice spent in either of two plates kept at 30 ^{0}C and 10 ^{0}C, respectively (n = 8 mice) ($p>0.05$, t-test) (experiment "B" was carried out by Branka Kampfrath).

4.11.6 Reduced firing rate of cutaneous cold receptive fields in t-MrVIa mice

In vitro skin nerve preparation was used to characterize the stimulus response properties of mouse cutaneous sensory neurons at cold temperatures. This technique allows to record from primary afferents of the saphenous nerve. In these experiments the response properties of cutaneous receptor fields were determined by application of a cold ramp ranging from 30 ^{0}C to 0 ^{0}C (Figure 37A, B). Two types of cold-activated C-fibers were detected: low threshold C-fibers which initiate firing at innocuous cold temperatures (threshold >10 ^{0}C) and high threshold C-fibers firing at noxious cold temperatures (threshold <10 ^{0}C). Whereas no difference in the firing frequency of the C-fibers of t-MrVIa and wt mice was observed in the low threshold population (Figure 37B), C-fibers from t-MrVIa mice fired significantly less in the high threshold population (Figure 37A). The maximal differences were observed at around 0 ^{0}C. The reduced firing frequency of C-fibers in t-MrVIa mice is consistent with their lack of nocifensive behavior at 0 ^{0}C. These results indicate that $Na_v1.8$ is required for the perception of noxious cold temperature *per se*.

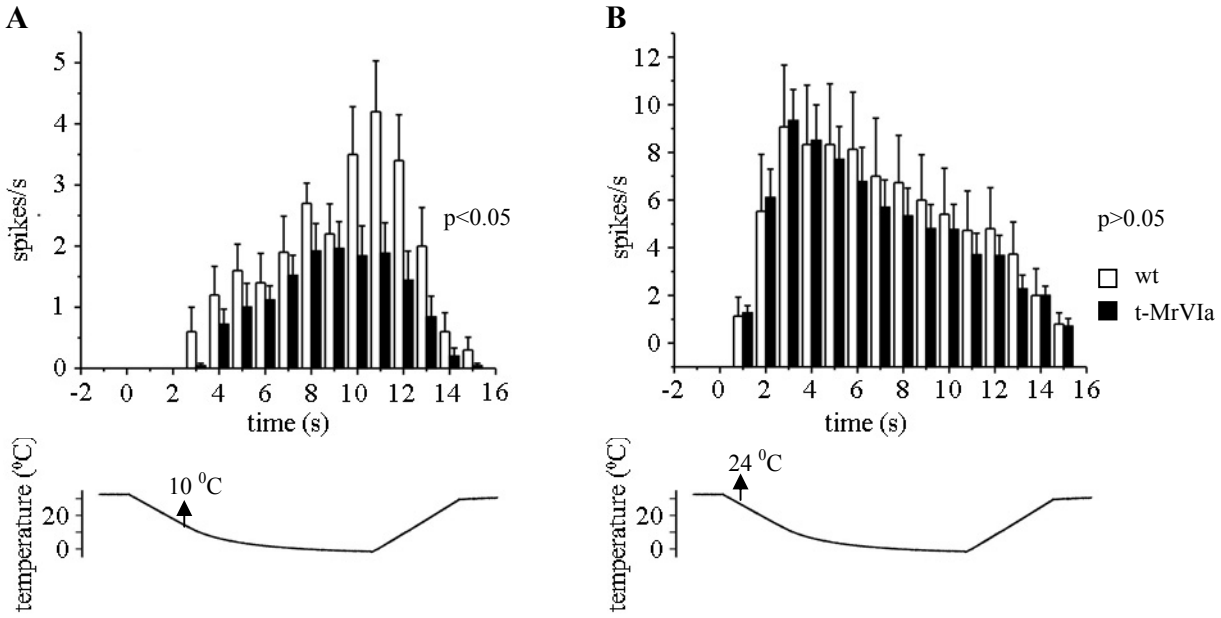

Figure 37: Reduced firing of cutaneous C-fibers in t-MrVIa mice

A) Histogram indicating the firing frequency of cold-sensitive C-fibers with a threshold <10 ^{0}C responding to noxious cold stimuli over a cooling gradient from 30-0 ^{0}C. The firing frequency of cooling units with a threshold below 10 ^{0}C is significantly reduced in t-MrVIa mice (fibers: n = 8) compared to wt mice (fibers: n = 4) ($p<0.05$, two-way-Anova).

B) Histogram indicating the firing frequency of cold-sensitive C-fibers with a threshold >10 ^{0}C over a cooling gradient from 30 to 0 ^{0}C. The firing frequency did not differ between wt (fibers: n = 8) and t-MrVIa mice (fibers: n = 12) ($p>0.05$, two-way-Anova). The lower trace corresponds to the cold ramp stimuli used in both cases (experiment carried out by Dr. Jing Hu).

5 Discussion

VGSC serve as hyperexcitable switches that accompany pain. Many VGSC subunits are coexpressed in nociceptors and it has been difficult so far to assign certain functions to specific sodium channel subtypes by conventional gene deletion studies due to compensatory upregulation of related VGSC (Akopian et al., 1999). This study applies the tethered toxin strategy to determine the contribution of only the $Na_v1.8$ TTX-R VGSC to pain transduction. This approach uses genetic delivery of membrane tethered toxins to inactivate $Na_v1.8$ VGSC in nociceptive neurons in mice. Consistent with the inhibitory action of t-MrVIa on $Na_v1.8$, t-MrVIa, mice showed a two-fold reduction of $Na_v1.8$-mediated currents accompanied by reduced action potential amplitudes in nociceptive neurons. This tethered toxin mediated block was permanent, cell-autonomous and did not result in functional alterations of any related VGSC subunit. T-MrVIa mice showed reduced inflammatory hyperalgesia upon noxious mechanical stimulation and clear pain attenuation in the cold. *In vitro* skin nerve assay revealed the first evidence that $Na_v1.8$ is not only required for mechanical nociception in the cold but that this channel is a cold sensor *per se*. The tethered toxin mediated block of $Na_v1.8$ does not impact on cell survival, nor on the distribution of DRG subpopulation and their central innervations pattern. This study provides the first proof of function of the tethered toxin approach in mice and demonstrates its suitability to dissect specific ion channel functions in certain neuronal circuits when combined to BAC transgenesis.

5.1 Toxin selection

The selection of a potent peptide toxin was a crucial factor to obtain specific blockage of the $Na_v1.8$ TTX-R VGSC. In this study the μO-conotoxin MrVIa was used because it shows a very high affinity for the $Na_v1.8$ VGSC without affecting $Na_v1.9$ and it is 10 times less potent for TTX-S VGSC (Daly et al., 2004). In contrast to μ-conotoxins, MrVIa inhibits sodium conductance independent from the TTX-binding site (McIntosh et al., 1995; Terlau et al., 1996) and therefore facilitates electrophysiological studies of VGSC subtypes. In this study tethered toxins were used to silence the $Na_v1.8$ VGSC in a cell-autonomous manner. The *in vivo* utility of this system has already been shown in zebrafish and chick to target nicotinic receptors (Hruska and Nishi, 2007; Ibanez-Tallon et al., 2004) and in Drosophila to inhibit the inactivation of VGSC (Wu et al., 2008). Since MrVIa is highly hydrophobic, trafficking of tethered MrVIa to

the plasma membrane could be hampered. To optimize plasma membrane expression, several MrVIa constructs with different tethers were tested functionally by two-electrode voltage clamp in X. laevis oocytes. Since this system allows overexpression of the tethered toxin and $Na_v1.8$ cDNA was not available, the effect of those tethers was investigated on $Na_v1.2$ mediated sodium currents. Out of five different tethers, only the GPI-anchored MrVIa (t-MrVIa) was able to significantly reduce $Na_v1.2$ mediated sodium current. TM-MrVIa and TM-AIS MrVIa slightly reduced sodium current but to a much lesser extent than t-MrVIa. Previous studies from our group indicated that TM-MrVIa and TM-AIS-MrVIa fusion proteins are not stably expressed at the plasma membrane anymore when transfected into HEK 293-T cells. This reduced expression at the plasma membrane probably limits their functional use to block VGSC *in vitro* as well as *in vivo*. Tethered MrVIa constructs which were cloned with transmembrane domains derived from the β1 VGSC subunit (β1-MrVIa and Lβ1-MrVIa) increased sodium peak current. This result is in agreement with previous studies showing that the β1-subunit enhances $Na_v1.2$ channel expression at the plasma membrane of both oocytes and mammalian cells (Isom et al., 1992; Isom et al., 1995). Similar effects were described for β1 acting on $Na_v1.8$ VGSC (Vijayaragavan et al., 2004). Thus, combining the β1 transmembrane domain with a μO-conotoxin reverses the natural toxin action. These results, together with the protein expression studies showing correct delivery and insertion into the plasma membrane of the GPI-anchored form of MrVIa made this toxin construct a suitable candidate to be used *in vivo*.

5.2 Targeting the pain pathway in mice using BAC transgenesis

Various pharmaceutical approaches and animal models of genetically modified mice are established tools to study ion channel function. However, $Na_v1.8$ null mutations in mice have led to genetic interference resulting in a dramatic increase of related $Na_v1.7$ VGSC (Akopian et al., 1999). On the other hand, oligodeoxynucleotide mediated silencing or the use of chemical blockers is neither long-lasting nor cell-type specific (Jarvis et al., 2007; Lai et al., 2002). In this study BAC transgenesis was combined with the tethered toxin approach to cell-autonomously block $Na_v1.8$ VGSC in nociceptive neurons without affecting VGSC in the CNS. Many genes are known to be highly expressed in nociceptors (Caterina et al., 1997; Ibanez and Ernfors, 2007; Zhong et al., 2006), however the $Na_v1.8$ BAC was used to drive t-MrVIa expression to ensure toxin expression where the channel is present and to avoid effects on CNS VGSC (Agarwal et al., 2004; Akopian et al., 1996). After the first event of homologous recombination, all clones

were positive by PCR. Such PCR system may produce false positives owing to the low persistence of the free shuttle vectors or unexpected recombination events (Gong et al., 2002). Indeed, only five out of 17 clones were proven positive by southern blot analyses after the induction of the second homologous recombination event. Importantly, the resolved clones all had correct size and did not show any deletion due to uncontrolled recombination. After purification of the resolved clone by $CsCl_2$ gradient ultracentrifugation and injection into fertilized oocytes of BDF/BL6J mice, six transgenic mouse lines were obtained. The offspring of one founder was genotyped negative over three litters probably due to mosaic expression. The remaining lines were analyzed by southern blot and revealed the copy numbers of each founder line. BACs integrate into the genome via tandem repeats which are mostly (80%) just present in one locus (Yang and Gong, 2005). Two founder lines were kept to exclude phenotypes which arise from the integration event into a certain locus. Taken together, the two-step homologous recombination strategy method provides a "clean", powerful and very handy tool to generate BAC transgenic mice to analyze gene expression and function.

5.3 Nociceptor-specific expression of t-MrVIa

Pain signaling initiates at the primary afferents innervating the skin whose somata are located in the DRG. These sensory neurons project to the dorsal horn of the spinal cord. The nociceptive signals are then processed centrally. This study aimed to restrict t-MrVIa expression to sensory neurons using the $Na_v1.8$ gene and avoid affecting other VGSC in the CNS. RT-PCR analyses on different tissues involved in pain signaling revealed coexpression of t-MrVIa and $Na_v1.8$ in DRGs of transgenic mice, but not in skin or the CNS, demonstrating the tissue-specificity of this approach. As no genetic manipulation of endogenous $Na_v1.8$ channel was done, t-MrVIa mice showed an intensity of the $Na_v1.8$ band similar to that in wt mice which lacked the toxin expression.

To gain further insights into the expression level and cell-type specific expression of t-MrVIa in DRGs, *in situ* hybridization was performed. Whereas whole mount *in situ* hybridization showed t-MrVIa expression throughout the whole DRG, DRG sections revealed high expression in small nociceptors and some few medium sized nociceptors, whereas mechanoreceptors did not express t-MrVIa. This result is in agreement with previous studies on the $Na_v1.8$ VGSC which demonstrated its nociceptor-restricted expression pattern (Akopian et al., 1996; Amaya et al., 2000; Waxman et al., 1999). Surprisingly, t-MrVIa RNA was exclusively detected in the nucleus

and not in the cytoplasm of nociceptors. However, *in situ* signals in the nucleus are known from other large genes like G-protein coupled receptors (Chen et al., 2006). Those genes are mainly intronless and therefore often lack a splicing donor sequence which facilitates the transport of mRNA out of the nucleus. Thus, most of the mRNA stays in the nucleus, but small amounts get transferred to the cytoplasm and are sufficient to form functional protein. The t-MrVIa expression cassette contains a very small pA, and no intron was inserted in the $Na_v1.8$ BAC. This might explain the t-MrVIa signal in the nucleus especially because $Na_v1.8$ mRNA was previously shown to be detected in the cytoplasm of DRGs (Waxman et al., 1999). However, whole cell patch clamp recordings on DRG neurons as well as the behavior studies proved that functional protein is expressed at the plasma membrane in t-MrVIa mice.

Transgene expression during embryogenesis could interfere with development. It is known that $Na_v1.8$ expression initiates at E13 and steadily increases until P7 and remains constant into adulthood (Benn et al., 2001). Therefore it was investigated whether t-MrVIa mice show any developmental defects. To investigate the morphology of embryos expressing t-MrVIa and to get an insight into possible expression in the SC, *in situ* hybridization on transversal embryo sections was carried out. Importantly, the embryos strongly expressed t-MrVIa in the DRGs but not in the SC. These data are in agreement with previous studies showing the sensory-neuron specificity of $Na_v1.8$ (Agarwal et al., 2004; Akopian et al., 1996). Taken together, a stable and cell specific expression of t-MrVIa was achieved in the nociceptor population that also expresses $Na_v1.8$.

5.4 Selective reduction of $Na_v1.8$-mediated sodium currents in nociceptors of t-MrVIa mice

$Na_v1.8$ is known to play a key role in the transmission of noxious stimuli and enormous efforts to block this channel have been made using natural toxins (Ekberg et al., 2006), chemical blockers (Jarvis et al., 2007; Kort et al., 2008) or antisense knockdowns (Lai et al., 2002; Mikami and Yang, 2005). However, the effects of these drugs could never be ascribed to a certain cell population. Here the cell-specific promoter of $Na_v1.8$ was used to target expression of a tethered toxin exclusively in nociceptors. Hence, two-fold reduction of VGSC inward current was obtained in nociceptive neurons but not in mechanoreceptors of t-MrVIa mice demonstrating the cell-autonomy of this approach. Since the voltage clamp protocol employed did not allow the detection of $Na_v1.9$-mediated sodium currents, the remaining inward current was produced by $Na_v1.8$ which might be due to the limited amount of toxin expressed *in vivo*. The block of $Na_v1.8$

obtained could be reversed by PI-PLC treatment. This data together with the immunostaining of transfected and PI-PLC-treated DRG neurons suggest that t-MrVIa gets expressed at the plasma membrane and acts from the extracellular site. Thus, the $Na_v1.8$ block can fully be ascribed to the tethered toxin action. The different activation thresholds for whole cell inward currents in nociceptors and mechanoreceptors are based on the diverse expression of VGSC subtypes differing in terms of kinetics and voltage dependence (Catterall et al., 2005). Importantly, t-MrVIa-mediated block did not result in a shift of the current voltage relationship. This finding is in agreement with studies using the soluble toxin (Daly et al., 2004).

The electrical properties of nociceptors are defined by the unique coexpression of two VGSC: TTX-S $Na_v1.7$ and TTX-R $Na_v1.8$. The interplay between these channels defines the firing behavior of these cells upon noxious stimulation. However, it has been difficult to dissect the function of these two channels because they have been shown to interact with each other. For instance, null mutation of $Na_v1.8$ results in drastic overexpression of $Na_v1.7$ (Akopian et al., 1999) and altered inactivation properties of TTX-S current in nociceptors (Matsutomi et al., 2006), while $Na_v1.7$ mutations lead to hyperexcitability or hypoexcitability states dependent on the presence of $Na_v1.8$ (Rush et al., 2006). One possible reason for the apparent upregulation of $Na_v1.7$ in $Na_v1.8$ null mutant mice might be the sharing of common auxiliary subunits. Although the α-subunit alone can form a functional channel, β-subunits are required to define the kinetics and the level of membrane expression *in vivo* (Catterall et al., 2005). Nociceptors express all four β auxiliary subunits but β1 is the most abundant (Lopez-Santiago et al., 2006; Shah et al., 2000). In heterologous expression systems, the β1 subunit dramatically increases $Na_v1.8$ expression and accelerates the inactivation of both $Na_v1.7$ and $Na_v1.8$-mediated sodium currents. (Vijayaragavan et al., 2001; Vijayaragavan et al., 2004). Thus, β1 binding to one or the other α-subunit will change the level of TTX-S or TTX-R VGSC expression in nociceptors. In the central nervous system, β1 also interacts with $Na_v1.1$ and $Na_v1.3$ (Chen et al., 2004). Importantly, β1 knockout mice showed dysregulated expression of $Na_v1.1$ and $Na_v1.3$ VGSC in the hippocampus accompanied by severe seizures and strong ataxia (Chen et al., 2004). No studies have addressed the influence of β1 deletion in the pain pathway yet. Similarly to β1, β3 binding to $Na_v1.8$ increases the current amplitude. Recent evidence indicates that β3 facilitates surface expression of $Na_v1.8$ by masking its endoplasmic reticulum retention motif (Zhang et al., 2008). However, it shifts the inactivation kinetics to more depolarized potentials (Vijayaragavan et al., 2004). Thus, β1 and β3 have opposite effects on channel inactivation kinetics. The modulatory functions of

β1- and β3-subunits together with their competitive binding to α-subunits provide additional levels of regulation and crosstalk which cannot be regulated by traditional knockout strategies.

In this study the tethered toxin approach is used to provide functional block of $Na_v1.8$ at the plasma membrane without interfering with $Na_v1.7$ or any other α- or β-subunit expressed in nociceptors. In cases where the toxin is specific for one ion channel, as MrVIa is for $Na_v1.8$, the electrophysiological changes can be attributed to one channel, whereas broad spectrum venom toxins allow to inactivate multiple receptor combinations at once. This is especially relevant in cases where functional redundancy of receptor families require the impracticality of double or triple conditional knockouts to eliminate all subunits in one cell type. Thus, the tethered toxin approach represents a powerful one step tool to inactivate heteromeric ion channels in specific cells.

DRG neurons are an extensively studied population of sensory neurons whose molecular composition is well defined. Nociceptors can generally be divided into IB4+ and IB4- subpopulations based on the presence or absence of the receptor for plant isolectin (Stucky and Lewin, 1999). Conventional superfusion methods using soluble toxins could not dissect nociceptor function because the effects could not be unequivocally ascribed to a certain subpopulation. In this study the cell-specific promoter $Na_v1.8$ is used to drive the toxin expression. It is known from several reports that $Na_v1.8$ is the main contributor of action potential upstroke and it is highly enriched in the IB4+ subpopulation. Importantly, t-MrVIa reduced the TTX-R currents of both IB4+ and IB4- subpopulations. However, the different contribution of TTX-R current to the whole cell inward current in these two subpopulations is reflected in the decrease of action potential amplitude in the IB4+ subpopulation. This result is in agreement with studies obtained from the $Na_v1.8$ null-mutant mice though no subdivision into IB4+ and IB4- was made (Renganathan et al., 2001). However, the threshold of action potential generation, the action potential half peak duration and the resting membrane potential of nociceptors from t-MrVIa mice were not altered. These parameters have been attributed to $Na_v1.9$ (Fang et al., 2006; Herzog et al., 2001). Thus, these results underline the specificity of t-MrVIa for $Na_v1.8$. Since $Na_v1.8$ is required for action potential generation in nociceptors, blocking this channel could silence neurons. However, there is still a considerable amount of current produced by $Na_v1.7$. Thus, silencing nociceptors will require inactivation of all VGSC. No venom toxin with this characteristic has yet been identified.

5.5 Establishment of mechanical inflammatory hyperalgesia is impaired in t-MrVIa mice

Many studies have shown an important role for $Na_v1.8$ in the transduction of painful stimuli (Akopian et al., 1999; Zimmermann et al., 2007). However, those findings could not be exclusively attributed to $Na_v1.8$ because of functional upregulation of associated ion channels. Here we dissected VGSC by using the membrane-bound conotoxin t-MrVIa directed against $Na_v1.8$. As expected, t-MrVIa mice did not show differences in motor coordination since the conotoxin is exclusively directed to the sensory pathway. Furthermore, t-MrVIa mice did not show any altered responses to acute thermal and mechanical noxious stimuli. For thermal nociception these data are broadly consistent with previous results using soluble blockers and $Na_v1.8$ cell ablation studies (Abrahamsen et al., 2008; Akopian et al., 1999; Jarvis et al., 2007). However, those studies reveal a role for $Na_v1.8$ in the transduction of noxious mechanical stimuli. The difference might result from the partial block of this channel in t-MrVIa mice or the type of behavioral test used.

$Na_v1.8$ is also known to play a role in hyperalgesia associated with tissue inflammation (Abrahamsen et al., 2008; Akopian et al., 1999). Wt and t-MrVIa mice developed similar levels of thermal inflammatory hyperalgesia, whereas mechanical hyperalgesia was impaired in t-MrVIa mice. Importantly, t-MrVIa mice developed the same maximum level of hyperalgesia after 4h of carrageenan injection as wt animals. However, t-MrVIa mice showed a clear delayed onset of mechanical inflammatory hyperalgesia which is consistent with studies on $Na_v1.8$ null-mutant mice (Akopian et al., 1999) and a significantly faster recovery from hyperalgesia. The delayed development of inflammatory hyperalgesia suggests that targets other than $Na_v1.8$ have a later cooperative role in the development of hyperalgesia (Akopian et al., 1999). Taken together, these results underline the assumption that $Na_v1.8$ is not required for the transduction of thermal noxious stimuli but clearly plays a role in the establishment of mechanical inflammatory hyperalgesia.

5.6 Reduced sensitivity to noxious cold in t-MrVIa mice

Identification of ion channels involved in peripheral nociceptor activation is essential in understanding the mechanisms of pain perception. Recently, the two mechano-gated potassium channels TREK-1 and TRAAK have been shown to control heat and cold pain in mice (Noel et al., 2009). Additionally, two major players of cold transduction have been linked to the transient

receptor potential (TRP) family. Whereas TRPM8 is activated by mild environmental cold and does not react to strong noxious stimuli, TRPA1 has been hypothesized to be a main detector of noxious cold (Bautista et al., 2007; McKemy, 2005; Reid, 2005). However, TRPA1 is only expressed in 3.6% of nociceptors and a larger fraction of nociceptive neurons respond to noxious cold (Reid, 2005). Furthermore *in vitro* studies on HEK293-T cells did not show any cold responses when transfected with TRPA1 (Jordt et al., 2004). Thus, the role of TRPA1 in noxious cold sensation is strongly controversial and more unknown cold sensors need to be identified. Importantly, there is recent evidence that $Na_v1.8$-mediated current remains available at noxious cold temperatures when all other VGSC are inactivated (Zimmermann et al., 2007). In agreement with these studies t-MrVIa mice showed negligible responses to noxious cold. To rule out the possibility that there is a global loss of thermoreception in t-MrVIa mice, a temperature preference test was carried out in which the time spent at 10 ^{0}C and 30 ^{0}C was measured. Wt and t-MrVIa mice showed a clear and quantitatively similar preference for surface set to 30 ^{0}C.

Electrophysiological evidence to explain this behavior phenotype was so far missing as cutaneous C-fiber units of $Na_v1.8$ null-mutant mice only revealed an altered firing rate upon mechanical stimulation in the cold but not on direct cooling (Zimmermann et al., 2007). To resemble the situation of the behavior test, a temperature gradient from 30 to 0 ^{0}C was applied to the cutaneous C-fibers of wt and t-MrVIa mice. Two populations of cutaneous C-fibers were identified. Whereas the low threshold C-fiber population responded to innocuous cold (threshold >10 ^{0}C), the second high threshold fiber population started to respond when noxious temperatures were reached. Importantly, high threshold C-fibers (threshold <10 ^{0}C) showed a significantly reduced firing rate compared to wt mice, whereas the firing rate of low threshold fibers was not altered. In the high-threshold fiber population, maximal differences were observed around 0 ^{0}C, but not at 10 ^{0}C, in agreement with the cold behavioral tests. Taken together, these results demonstrate that $Na_v1.8$-mediated currents are not only required for nociception but for the detection of noxious cold temperatures *per se*.

5.7 No altered central innervation, cell death or neurochemical redistribution occurs in t-MrVIa mice

Reduced sensitivity to noxious cold stimuli and mechanical inflammatory hyperalgesia could result from various causes like cell death, altered pattern of innervation in SC or skin. Many studies have already indicated that loss of neuronal activity or reduced firing can lead to

apoptosis. For instance, null-mutations of $Na_v1.2$ in mice lead to apoptosis in brain stem and neocortex and even to postnatal death, whereas deletion of the B subtype cyclic nucleotide-gated (CNG) channel photoreceptor leads to gliosis and apoptotic cell death in retina of $CNGB1^{-/-}$ mice (Huttl et al., 2005; Planells-Cases et al., 2000). In this study it could be ruled out that behavioral effects are triggered by cell death, since electronmicroscopy of the sapheneous nerve did not reveal any differences in the number of myelinated and unmyelinated axons and demonstrated the unaltered morphology of primary afferents. However, the ability of organisms to trigger appropriate behavior upon noxious stimulation not only depends on the number of nociceptors but also requires precise central innervations into the SC. Two parallel pain pathways arise from IB4+ and IB4- nociceptor subpopulations (Braz et al., 2005). Whereas IB4- nociceptors innervate the lamina II_o, IB4+ fibers target to the lamina II_i and the superficial lamina of the dorsal horn from where noxious information is processed centrally. Importantly, both fiber types have distinct central connectivity and thus, altered innervations in mice could dramatically change the behavioral phenotype of transgenic mice. Here we could show by immunostaining using the neurochemical markers subP and IB4 that central targeting of primary afferents is not altered in t-MrVIa mice. It is furthermore possible that interfering with VGSC during development not only leads to reduced neuronal activity, cell death or altered central targeting but also affects the neurochemical diversification of nociceptors. Based on the electrophysiological experiments it could be shown that t-MrVIa preferentially acts on IB4+ nociceptors according to the expression pattern of $Na_v1.8$. Importantly, t-MrVIa mice did not show any redistribution of the IB4+ and IB4- nociceptive subpopulation. Thus, the reduced behavioral responses of t-MrVIa mice upon noxious stimulation are not triggered or influenced by cell death, different central innervations targets, or altered neurochemical composition of nociceptors but can be fully attributed to the block of $Na_v1.8$.

5.8 Outlook

This thesis demonstrates the first proof of function of the tethered toxin approach in mice. Since a selective block of the $Na_v1.8$ VGSC is achieved in t-MrVIa mice this strategy provides a promising future method to study ion channel function i*n vivo*.

Whereas inducible expression of transgenes enables rapid and reversible manipulation of neuronal circuits, long-term inhibition of ion channels could be advantageous in patients

suffering from severe pain. Importantly, some conotoxins are already used as analgesic drugs. For instance, chemically synthesized MVIIA (Prialt, ziconotide), a potent blocker of the N-type voltage-gated calcium channel, has been approved for the treatment of severe neuropathic pain conditions in humans, which are refractory to systemic analgesics and morphine (Thompson et al., 2006; Williams et al., 2008). To avoid affecting voltage-gated calcium channels in the CNS, this therapy requires surgery to implant microfusion pumps close to the spinal cord. However, patients show severe side effects due to uncontrolled diffusion and suffer from repetitive treatments (Thompson et al., 2006). In this direction, systemic injection of adeno-associated virus type 8 has been recently shown to be an effective delivery route to target sensory pathways in chronic pain (Foust et al., 2008). Thus, future developments in improving the safety of gene transfer in humans offers considerable promise for the application of this novel tethered toxin technology to treat such extreme pain in humans.

Electrophysiological recordings of t-MrVIa mice revealed a significant reduction of action potential amplitude in the IB4+ nociceptive subpopulation. It is not clear from this study if this decrease is a direct effect based on the reduction of $Na_v1.8$-mediated current. It should also be taken into account that the current reduction results in altered inactivation curves of other related VGSC and therefore directs the cell into a new electrophysiological state. Such correlations have already been described in hyperpolarization-activated cation channel (HCN2) deficient mice and $Na_v1.8$ null-mutants (Ludwig et al., 2003; Matsutomi et al., 2006). It is also possible that both effects are present in t-MrVIa mice as action potential generation and regulation is mediated by multiple mechanisms that give raise to unique nociceptor function.

Based on the natural toxin action, a $Na_v1.8$-specific block was achieved in nociceptors of t-MrVIa mice. However, the detailed mechanism of tethered toxin action is not fully clear and gives raise to the question if tethered toxins act intra- or extracellularly. Toxins acting from cytosolic site have been described (Olsnes et al., 1993) and the coexpression of t-MrVIa with $Na_v1.8$ under the same gene regulatory elements in principle enables early interaction e.g. in the ER or during protein trafficking which is a highly complex process. However, in this study immunohistochemical investigations on non-permeabilized DRG neurons showed clear removal of tethered toxin construct from plasma membrane after PI-PLC treatment indicating that t-MrVIa gets transferred out of the cell and acts extracellularly. Furthermore electrophysiological

recordings on PI-PLC-treated nociceptors of t-MrVIa mice revealed increased peak current densites which are close to wt levels. For future studies it would be advantageous to generate inducible systems to regulate and control tethered toxin expression.

In this study specific reduction of $Na_v1.8$-mediated current was achieved in mice using a novel genetic toxin-based strategy. Importantly, this method prevents any genetic interference with related ion channels. Extension of this approach to other peptide toxins together with the use of cell-specific genetic methods will allow scientists to specifically intervene in defined neural circuits *in vivo* and potentially treat diseases caused by channelopathies.

Summary

Pain signaling is highly complex and involves a number of cellular and molecular processes that lead to initiation and maintenance of different types of pain. Elucidation of these mechanisms is key to the development of treatments that specifically target underlying causes. Though it is widely known that the detection of painful stimuli in the periphery strongly relies on the activation of the voltage-gated sodium channels (VGSCs) $Na_v1.8$, it has been difficult to assign the function of individual VGSC subtypes. Nine VGSCs are expressed in mammals displaying diverse physiological functions, and gene deletion studies of single subunits lead to functional alterations in other VGSCs whereas antisense treatment is not long-lasting and therefore lacks clinical relevance. Other approaches using naturally occurring peptide toxins derived from venomous animals have been successfully used to study the function of individual ion channels but lack the cell autonomy. Thus, novel therapeutical tools need to be developed.

This thesis demonstrates that permanent and cell-autonomous inactivation of only $Na_v1.8$ channels is possible by transgenic expression of a membrane-tethered conotoxin MrVIa (t-MrVIa). Based on the genetic elements of the $Na_v1.8$ BAC, t-MrVIa expression was exclusively found in nociceptive neurons, whereas adjacent mechanoreceptors were not affected. This expression resulted in a reduction of $Na_v1.8$-mediated currents in t-MrVIa transgenic mice which could be reversed by enzymatic cleavage using PI-PLC, thus providing an additional level of regulation. In contrast to gene deletion studies this block did not result in transcriptional or functional upregulation of other VGSCs. Furthermore, t-MrVIa expression did not alter the cell number of peripheral neurons, the central targeting pattern or the chemical redistribution of nociceptor population. This therefore provides a “clean” genetic method of addressing individual ion channels *in vivo*. Behaviorally, t-MrVIa mice show decreased inflammatory hyperalgesia and insensitivity to noxious cold, accompanied by a reduced firing rate of cutaneous C-fibers at noxious cold temperatures. This study demonstrates that inactivation of $Na_v1.8$ alone is critical for the perception of pain. Thus genetically encoded tethered toxins can be used to unambiguously assign cellular functions to individual ionic currents in the mammalian nervous system.

Zusammenfassung

Die molekularen Mechanismen, die der Schmerzwahrnehmung und -weiterleitung zu Grunde liegen sind äußerst komplex. Die Aufklärung solcher Mechanismen ist von fundamentaler Bedeutung, um die Funktionsweise von Molekülen und Ionenkanälen aufzudecken, um spezielle Arten von Schmerzen klinisch gezielt behandeln zu können. Obwohl es weithin bekannt ist, dass Schmerzreize im peripheren Nervensystem zum großen Teil von dem spannungsabhängigen Ionenkanal $Na_v1.8$ detektiert werden, hat es sich bisher als schwierig herausgestellt die Funktion von einzelnen spannungsabhängigen Natriumkanälen zu analysieren. Neun spannungsabhängigen Natriumkanälen mit unterschiedlichen physiologischen Funktionen werden in Säugern exprimiert. Allerdings haben konventionelle null-Mutationen von $Na_v1.8$ zur kompensatorischen Desregulierung von verwandten spannungsabhängigen Natriumkanälen geführt, während antisense-Versuche keine langanhaltende Runterregulierung zeigte. Andere Studien verwendeten natürlich vorkommende Neurotoxine, welche spezifisch mit $Na_v1.8$ agierten, jedoch nicht zellautonom wirkten. Daher ist es notwendig neue therapeutische Methoden zu entwickeln, welche die Analyse von gezielt einem Ionenkanal ermöglichen.

Diese Doktorarbeit zeigt zum ersten Mal, dass die Expression eines membrangebundenen Toxins MrVIa (t-MrVIa) in Mäusen eine permanente und zellautonome Inaktivierung von $Na_v1.8$ ermöglicht. Anhand der genetischen Elemente von dem verwendeten $Na_v1.8$ BAC wurde die t-MrVIa Expression gezielt auf die Nozizeptoren gelenkt, während benachbarte Mechanorezeptoren das Toxin nicht expremierten. Diese Expression führte zu einer Reduzierung des $Na_v1.8$ Stroms in t-MrVIa Mäusen, welche mittels Spaltung mit dem Enzym PI-PLC rückgängig gemacht werden konnte und so eine zusätzliche Art der Regulierung darstellt. Im Gegensatz zur Nullmutation von $Na_v1.8$ erfolgte keine Desregulierung anderer spannungsabhängiger Natriumkanäle auf RNA Ebene und keine funktionellen Änderungen des Natriumstroms in t-MrVIa Mäusen. Weiterhin änderte die t-MrVIa Expression weder die Anzahl peripherer Neurone, noch die zentrale Innervation ins Rückenmark oder die neurochemische Zusammensetzung nozizeptorischer Subpopulationen. T-MrVIa Mäuse zeigten eine Reduzierung der inflammatorischen Hyperalgesie und waren nicht sensitiv zu noxischer Kälte, was auch durch eine geringeres Auftreten von Aktionspotentialen belegt werden konnte. Diese Ergebnisse demonstrieren, dass die Inaktivierung von $Na_v1.8$ allein entscheidend ist für die Schmerzwahrnehmung. Daher stellen genetisch exprimierte membrangebundene Toxine eine

einmalige Möglichkeit dar, um die zellulär Funktion von einem Ionenkanal im Nervensystem aufzuklären.

Erklärung

„Ich, Annika Stürzebecher, erkläre, dass ich die vorgelegte Dissertationsschrift mit dem Thema: ‚Suppression of pain by nociceptor-specific expression of tethered toxins *in vivo* ' selbst verfasst und keine anderen als die angegebenen Quellen und Hilfsmittel benutzt, ohne die (unzulässige) Hilfe Dritter verfasst und auch in Teilen keine Kopien anderer Arbeiten dargestellt habe."

Ort, Datum

Unterschrift

Literature

Abrahamsen, B., Zhao, J., Asante, C.O., Cendan, C.M., Marsh, S., Martinez-Barbera, J.P., Nassar, M.A., Dickenson, A.H., and Wood, J.N. (2008). The cell and molecular basis of mechanical, cold, and inflammatory pain. Science (New York, N.Y *321*, 702-705.

Agarwal, N., Offermanns, S., and Kuner, R. (2004). Conditional gene deletion in primary nociceptive neurons of trigeminal ganglia and dorsal root ganglia. Genesis *38*, 122-129.

Akopian, A.N., Sivilotti, L., and Wood, J.N. (1996). A tetrodotoxin-resistant voltage-gated sodium channel expressed by sensory neurons. Nature *379*, 257-262.

Akopian, A.N., Souslova, V., England, S., Okuse, K., Ogata, N., Ure, J., Smith, A., Kerr, B.J., McMahon, S.B., Boyce, S., *et al.* (1999). The tetrodotoxin-resistant sodium channel SNS has a specialized function in pain pathways. Nature neuroscience *2*, 541-548.

Amaya, F., Decosterd, I., Samad, T.A., Plumpton, C., Tate, S., Mannion, R.J., Costigan, M., and Woolf, C.J. (2000). Diversity of expression of the sensory neuron-specific TTX-resistant voltage-gated sodium ion channels SNS and SNS2. Molecular and cellular neurosciences *15*, 331-342.

Bautista, D.M., Siemens, J., Glazer, J.M., Tsuruda, P.R., Basbaum, A.I., Stucky, C.L., Jordt, S.E., and Julius, D. (2007). The menthol receptor TRPM8 is the principal detector of environmental cold. Nature *448*, 204-208.

Belmonte, C., and Cervero, F. (1996). Neurobiology of nociceptors (Oxford University Press, USA).

Benn, S.C., Costigan, M., Tate, S., Fitzgerald, M., and Woolf, C.J. (2001). Developmental expression of the TTX-resistant voltage-gated sodium channels Nav1.8 (SNS) and Nav1.9 (SNS2) in primary sensory neurons. J Neurosci *21*, 6077-6085.

Bennett, D.L., Michael, G.J., Ramachandran, N., Munson, J.B., Averill, S., Yan, Q., McMahon, S.B., and Priestley, J.V. (1998). A distinct subgroup of small DRG cells express GDNF receptor components and GDNF is protective for these neurons after nerve injury. J Neurosci *18*, 3059-3072.

Braz, J.M., Nassar, M.A., Wood, J.N., and Basbaum, A.I. (2005). Parallel "pain" pathways arise from subpopulations of primary afferent nociceptor. Neuron *47*, 787-793.

Bulaj, G., and Olivera, B.M. (2008). Folding of conotoxins: formation of the native disulfide bridges during chemical synthesis and biosynthesis of Conus peptides. Antioxidants & redox signaling *10*, 141-155.

Caterina, M.J., Schumacher, M.A., Tominaga, M., Rosen, T.A., Levine, J.D., and Julius, D. (1997). The capsaicin receptor: a heat-activated ion channel in the pain pathway. Nature *389*, 816-824.

Catterall, W.A., Goldin, A.L., and Waxman, S.G. (2005). International Union of Pharmacology. XLVII. Nomenclature and structure-function relationships of voltage-gated sodium channels. Pharmacological reviews *57*, 397-409.

Chahine, M., Ziane, R., Vijayaragavan, K., and Okamura, Y. (2005). Regulation of Na v channels in sensory neurons. Trends in pharmacological sciences *26*, 496-502.

Chen, C., Westenbroek, R.E., Xu, X., Edwards, C.A., Sorenson, D.R., Chen, Y., McEwen, D.P., O'Malley, H.A., Bharucha, V., Meadows, L.S., *et al.* (2004). Mice lacking sodium channel beta1 subunits display defects in neuronal excitability, sodium channel expression, and nodal architecture. J Neurosci *24*, 4030-4042.

Chen, C.L., Broom, D.C., Liu, Y., de Nooij, J.C., Li, Z., Cen, C., Samad, O.A., Jessell, T.M., Woolf, C.J., and Ma, Q. (2006). Runx1 determines nociceptive sensory neuron phenotype and is required for thermal and neuropathic pain. Neuron *49*, 365-377.

Cheng, L.J., Li, J.M., Chen, J., Ge, Y.H., Yu, Z.R., Han, D.S., Zhou, Z.M., and Sha, J.H. (2003). NYD-SP16, a novel gene associated with spermatogenesis of human testis. Biology of reproduction *68*, 190-198.

Cox, J.J., Reimann, F., Nicholas, A.K., Thornton, G., Roberts, E., Springell, K., Karbani, G., Jafri, H., Mannan, J., Raashid, Y., *et al.* (2006). An SCN9A channelopathy causes congenital inability to experience pain. Nature *444*, 894-898.

Cummins, T.R., Dib-Hajj, S.D., Black, J.A., Akopian, A.N., Wood, J.N., Waxman, S.G. (1999). A novel persistent tetrodotoxin-resistant sodium current in SNS-null and wild-type small primary sensory neurons. J Neurosci 19(24), RC43

Daly, N.L., Ekberg, J.A., Thomas, L., Adams, D.J., Lewis, R.J., and Craik, D.J. (2004). Structures of muO-conotoxins from Conus marmoreus. Inhibitors of tetrodotoxin (TTX)-sensitive and TTX-resistant sodium channels in mammalian sensory neurons. The Journal of biological chemistry *279*, 25774-25782.

Dib-Hajj, S.D., Tyrrell, L., Black, J.A., and Waxman, S.G. (1998). NaN, a novel voltage-gated Na channel, is expressed preferentially in peripheral sensory neurons and down-regulated after axotomy. Proceedings of the National Academy of Sciences of the United States of America *95*, 8963-8968.

Drenth, J.P., Te Morsche, R.H., Mansour, S., and Mortimer, P.S. (2008). Primary erythermalgia as a sodium channelopathy: screening for SCN9A mutations: exclusion of a causal role of SCN10A and SCN11A. Archives of dermatology *144*, 320-324.

Ekberg, J., Craik, D.J., and Adams, D.J. (2008). Conotoxin modulation of voltage-gated sodium channels. The international journal of biochemistry & cell biology *40*, 2363-2368.

Ekberg, J., Jayamanne, A., Vaughan, C.W., Aslan, S., Thomas, L., Mould, J., Drinkwater, R., Baker, M.D., Abrahamsen, B., Wood, J.N., *et al.* (2006). muO-conotoxin MrVIB selectively blocks Nav1.8 sensory neuron specific sodium channels and chronic pain behavior without motor deficits. Proceedings of the National Academy of Sciences of the United States of America *103*, 17030-17035.

Fang, X., Djouhri, L., McMullan, S., Berry, C., Waxman, S.G., Okuse, K., and Lawson, S.N. (2006). Intense isolectin-B4 binding in rat dorsal root ganglion neurons distinguishes C-fiber nociceptors with broad action potentials and high Nav1.9 expression. J Neurosci *26*, 7281-7292.

Fertleman, C.R., Baker, M.D., Parker, K.A., Moffatt, S., Elmslie, F.V., Abrahamsen, B., Ostman, J., Klugbauer, N., Wood, J.N., Gardiner, R.M., and Rees, M. (2006). SCN9A mutations in paroxysmal extreme pain disorder: allelic variants underlie distinct channel defects and phenotypes. Neuron *52*, 767-774.

Foust, K.D., Poirier, A., Pacak, C.A., Mandel, R.J., and Flotte, T.R. (2008). Neonatal intraperitoneal or intravenous injections of recombinant adeno-associated virus type 8 transduce dorsal root ganglia and lower motor neurons. Human gene therapy *19*, 61-70.

Garrido, J.J., Giraud, P., Carlier, E., Fernandes, F., Moussif, A., Fache, M.P., Debanne, D., and Dargent, B. (2003). A targeting motif involved in sodium channel clustering at the axonal initial segment. Science (New York, N.Y *300*, 2091-2094.

Gold, M.S., Dastmalchi, S., Levine, J.D. (1996). Co-expression of nociceptor properties in dorsal root ganglion neurons from the adult rat in vitro. Neurosci 71(1), 265-275.

Goldin, A.L., Barchi, R.L., Caldwell, J.H., Hofmann, F., Howe, J.R., Hunter, J.C., Kallen, R.G., Mandel, G., Meisler, M.H., Netter, Y.B., *et al.* (2000). Nomenclature of voltage-gated sodium channels. Neuron *28*, 365-368.

Gong, S., Yang, X.W., Li, C., and Heintz, N. (2002). Highly efficient modification of bacterial artificial chromosomes (BACs) using novel shuttle vectors containing the R6Kgamma origin of replication. Genome research *12*, 1992-1998.

Gong, S., Zheng, C., Doughty, M.L., Losos, K., Didkovsky, N., Schambra, U.B., Nowak, N.J., Joyner, A., Leblanc, G., Hatten, M.E., and Heintz, N. (2003). A gene expression atlas of the central nervous system based on bacterial artificial chromosomes. Nature *425*, 917-925.

Handwerker, H.O., Kilo, S., and Reeh, P.W. (1991). Unresponsive afferent nerve fibres in the sural nerve of the rat. The Journal of physiology *435*, 229-242.

Hargreaves, K., Dubner, R., Brown, F., Flores, C., and Joris, J. (1988). A new and sensitive method for measuring thermal nociception in cutaneous hyperalgesia. Pain *32*, 77-88.

Harper, A.A., and Lawson, S.N. (1985). Conduction velocity is related to morphological cell type in rat dorsal root ganglion neurones. The Journal of physiology *359*, 31-46.

Heinemann, S.H., and Leipold, E. (2007). Conotoxins of the O-superfamily affecting voltage-gated sodium channels. Cell Mol Life Sci *64*, 1329-1340.

Heintz, N. (2001). BAC to the future: the use of bac transgenic mice for neuroscience research. Nature reviews *2*, 861-870.

Herzog, R.I., Cummins, T.R., and Waxman, S.G. (2001). Persistent TTX-resistant Na+ current affects resting potential and response to depolarization in simulated spinal sensory neurons. Journal of neurophysiology *86*, 1351-1364.

Holden, J.E., and Pizzi, J.A. (2003). The challenge of chronic pain. Advanced drug delivery reviews *55*, 935-948.

Hruska, M., and Nishi, R. (2007). Cell-autonomous inhibition of alpha 7-containing nicotinic acetylcholine receptors prevents death of parasympathetic neurons during development. J Neurosci *27*, 11501-11509.

Hunt, S.P., and Mantyh, P.W. (2001). The molecular dynamics of pain control. Nature reviews *2*, 83-91.

Huttl, S., Michalakis, S., Seeliger, M., Luo, D.G., Acar, N., Geiger, H., Hudl, K., Mader, R., Haverkamp, S., Moser, M., *et al.* (2005). Impaired channel targeting and retinal degeneration in mice lacking the cyclic nucleotide-gated channel subunit CNGB1. J Neurosci *25*, 130-138.

Ibanez-Tallon, I., Miwa, J.M., Wang, H.L., Adams, N.C., Crabtree, G.W., Sine, S.M., and Heintz, N. (2002). Novel modulation of neuronal nicotinic acetylcholine receptors by association with the endogenous prototoxin lynx1. Neuron *33*, 893-903.

Ibanez-Tallon, I., Wen, H., Miwa, J.M., Xing, J., Tekinay, A.B., Ono, F., Brehm, P., and Heintz, N. (2004). Tethering naturally occurring peptide toxins for cell-autonomous modulation of ion channels and receptors in vivo. Neuron *43*, 305-311.

Ibanez, C.F., and Ernfors, P. (2007). Hierarchical control of sensory neuron development by neurotrophic factors. Neuron *54*, 673-675.

Inchauspe, C.G., Martini, F.J., Forsythe, I.D., and Uchitel, O.D. (2004). Functional compensation of P/Q by N-type channels blocks short-term plasticity at the calyx of held presynaptic terminal. J Neurosci *24*, 10379-10383.

Isom, L.L. (2001). Sodium channel beta subunits: anything but auxiliary. Neuroscientist *7*, 42-54.

Isom, L.L., De Jongh, K.S., Patton, D.E., Reber, B.F., Offord, J., Charbonneau, H., Walsh, K., Goldin, A.L., and Catterall, W.A. (1992). Primary structure and functional expression of the beta 1 subunit of the rat brain sodium channel. Science (New York, N.Y *256*, 839-842.

Isom, L.L., Scheuer, T., Brownstein, A.B., Ragsdale, D.S., Murphy, B.J., and Catterall, W.A. (1995). Functional co-expression of the beta 1 and type IIA alpha subunits of sodium channels in a mammalian cell line. The Journal of biological chemistry *270*, 3306-3312.

Jarvis, M.F., Honore, P., Shieh, C.C., Chapman, M., Joshi, S., Zhang, X.F., Kort, M., Carroll, W., Marron, B., Atkinson, R., *et al.* (2007). A-803467, a potent and selective Nav1.8 sodium channel blocker, attenuates neuropathic and inflammatory pain in the rat. Proceedings of the National Academy of Sciences of the United States of America *104*, 8520-8525.

Jordt, S.E., Bautista, D.M., Chuang, H.H., McKemy, D.D., Zygmunt, P.M., Hogestatt, E.D., Meng, I.D., and Julius, D. (2004). Mustard oils and cannabinoids excite sensory nerve fibres through the TRP channel ANKTM1. Nature *427*, 260-265.

Julius, D., and Basbaum, A.I. (2001). Molecular mechanisms of nociception. Nature *413*, 203-210.

Kearney, J.A., Plummer, N.W., Smith, M.R., Kapur, J., Cummins, T.R., Waxman, S.G., Goldin, A.L., and Meisler, M.H. (2001). A gain-of-function mutation in the sodium channel gene Scn2a results in seizures and behavioral abnormalities. Neuroscience *102*, 307-317.

Koltzenburg, M., Stucky C.L., Lewin G.R. (1997). Receptive properties of mouse sensory neurons innervating hairy skin. J Neurophysiol 78(4), 1841-1850.

Kort, M.E., Drizin, I., Gregg, R.J., Scanio, M.J., Shi, L., Gross, M.F., Atkinson, R.N., Johnson, M.S., Pacofsky, G.J., Thomas, J.B., *et al.* (2008). Discovery and biological evaluation of 5-aryl-2-furfuramides, potent and selective blockers of the Nav1.8 sodium channel with efficacy in models of neuropathic and inflammatory pain. Journal of medicinal chemistry *51*, 407-416.

Kramer, I., Sigrist, M., de Nooij, J.C., Taniuchi, I., Jessell, T.M., and Arber, S. (2006). A role for Runx transcription factor signaling in dorsal root ganglion sensory neuron diversification. Neuron *49*, 379-393.

Kress, M., Koltzenburg, M., Reeh, P.W., and Handwerker, H.O. (1992). Responsiveness and functional attributes of electrically localized terminals of cutaneous C-fibers in vivo and in vitro. Journal of neurophysiology *68*, 581-595.

Lai, J., Gold, M.S., Kim, C.S., Bian, D., Ossipov, M.H., Hunter, J.C., and Porreca, F. (2002). Inhibition of neuropathic pain by decreased expression of the tetrodotoxin-resistant sodium channel, NaV1.8. Pain *95*, 143-152.

Laird, J.M., Souslova, V., Wood, J.N., and Cervero, F. (2002). Deficits in visceral pain and referred hyperalgesia in Nav1.8 (SNS/PN3)-null mice. J Neurosci *22*, 8352-8356.

Lawson, S.N., and Waddell, P.J. (1991). Soma neurofilament immunoreactivity is related to cell size and fibre conduction velocity in rat primary sensory neurons. The Journal of physiology *435*, 41-63.

Lechner, H.A., Lein, E.S., and Callaway, E.M. (2002). A genetic method for selective and quickly reversible silencing of Mammalian neurons. J Neurosci *22*, 5287-5290.

Leipold, E., DeBie, H., Zorn, S., Borges, A., Olivera, B.M., Terlau, H., and Heinemann, S.H. (2007). muO conotoxins inhibit NaV channels by interfering with their voltage sensors in domain-2. Channels (Austin, Tex *1*, 253-262.

Lerchner, W., Xiao, C., Nashmi, R., Slimko, E.M., van Trigt, L., Lester, H.A., and Anderson, D.J. (2007). Reversible silencing of neuronal excitability in behaving mice by a genetically targeted, ivermectin-gated Cl- channel. Neuron *54*, 35-49.

Lewin, G.R., Lu, Y., and Park, T.J. (2004). A plethora of painful molecules. Current opinion in neurobiology *14*, 443-449.

Lewin, G.R., and Mendell, L.M. (1994). Regulation of cutaneous C-fiber heat nociceptors by nerve growth factor in the developing rat. Journal of neurophysiology *71*, 941-949.

Lewin, G.R., and Moshourab, R. (2004). Mechanosensation and pain. Journal of neurobiology *61*, 30-44.

Lewis, R.J., and Garcia, M.L. (2003). Therapeutic potential of venom peptides. Nat Rev Drug Discov *2*, 790-802.

Lopez-Santiago, L.F., Pertin, M., Morisod, X., Chen, C., Hong, S., Wiley, J., Decosterd, I., and Isom, L.L. (2006). Sodium channel beta2 subunits regulate tetrodotoxin-sensitive sodium channels in small dorsal root ganglion neurons and modulate the response to pain. J Neurosci *26*, 7984-7994.

Ludwig, A., Budde, T., Stieber, J., Moosmang, S., Wahl, C., Holthoff, K., Langebartels, A., Wotjak, C., Munsch, T., Zong, X., *et al.* (2003). Absence epilepsy and sinus dysrhythmia in mice lacking the pacemaker channel HCN2. The EMBO journal *22*, 216-224.

Lumpkin, E.A., and Caterina, M.J. (2007). Mechanisms of sensory transduction in the skin. Nature *445*, 858-865.

Marmigere, F., and Ernfors, P. (2007). Specification and connectivity of neuronal subtypes in the sensory lineage. Nature reviews *8*, 114-127.

Matsutomi, T., Nakamoto, C., Zheng, T., Kakimura, J., and Ogata, N. (2006). Multiple types of Na(+) currents mediate action potential electrogenesis in small neurons of mouse dorsal root ganglia. Pflugers Arch *453*, 83-96.

McCleskey, E.W., and Gold, M.S. (1999). Ion channels of nociception. Annual review of physiology *61*, 835-856.

McIntosh, J.M., Hasson, A., Spira, M.E., Gray, W.R., Li, W., Marsh, M., Hillyard, D.R., and Olivera, B.M. (1995). A new family of conotoxins that blocks voltage-gated sodium channels. The Journal of biological chemistry *270*, 16796-16802.

McKemy, D.D. (2005). How cold is it? TRPM8 and TRPA1 in the molecular logic of cold sensation. Molecular pain *1*, 16.

Meyer, R.A., Davis, K.D., Cohen, R.H., Treede, R.D., and Campbell, J.N. (1991). Mechanically insensitive afferents (MIAs) in cutaneous nerves of monkey. Brain research *561*, 252-261.

Mikami, M., and Yang, J. (2005). Short hairpin RNA-mediated selective knockdown of NaV1.8 tetrodotoxin-resistant voltage-gated sodium channel in dorsal root ganglion neurons. Anesthesiology *103*, 828-836.

Millan, M.J. (1999). The induction of pain: an integrative review. Progress in neurobiology *57*, 1-164.

Miwa, J.M., Ibanez-Tallon, I., Crabtree, G.W., Sanchez, R., Sali, A., Role, L.W., and Heintz, N. (1999). lynx1, an endogenous toxin-like modulator of nicotinic acetylcholine receptors in the mammalian CNS. Neuron *23*, 105-114.

Molliver, D.C., Wright, D.E., Leitner, M.L., Parsadanian, A.S., Doster, K., Wen, D., Yan, Q., and Snider, W.D. (1997). IB4-binding DRG neurons switch from NGF to GDNF dependence in early postnatal life. Neuron *19*, 849-861.

Nassar, M.A., Stirling, L.C., Forlani, G., Baker, M.D., Matthews, E.A., Dickenson, A.H., and Wood, J.N. (2004). Nociceptor-specific gene deletion reveals a major role for Nav1.7 (PN1) in acute and inflammatory pain. Proceedings of the National Academy of Sciences of the United States of America *101*, 12706-12711.

Noel, J., Zimmermann, K., Busserolles, J., Deval, E., Alloui, A., Diochot, S., Guy, N., Borsotto, M., Reeh, P., Eschalier, A., and Lazdunski, M. (2009). The mechano-activated K(+) channels TRAAK and TREK-1 control both warm and cold perception. The EMBO journal.

Olsnes, S., van Deurs, B., and Sandvig, K. (1993). Protein toxins acting on intracellular targets: cellular uptake and translocation to the cytosol. Medical microbiology and immunology *182*, 51-61.

Planells-Cases, R., Caprini, M., Zhang, J., Rockenstein, E.M., Rivera, R.R., Murre, C., Masliah, E., and Montal, M. (2000). Neuronal death and perinatal lethality in voltage-gated sodium channel alpha(II)-deficient mice. Biophysical journal *78*, 2878-2891.

Price, D.D. (2000). Psychological and neural mechanisms of the affective dimension of pain. Science (New York, N.Y *288*, 1769-1772.

Priest, B.T., Murphy, B.A., Lindia, J.A., Diaz, C., Abbadie, C., Ritter, A.M., Liberator, P., Iyer, L.M., Kash, S.F., Kohler, M.G., *et al.* (2005). Contribution of the tetrodotoxin-resistant voltage-gated sodium channel NaV1.9 to sensory transmission and nociceptive behavior. Proceedings of the National Academy of Sciences of the United States of America *102*, 9382-9387.

Raja, S.N., M., R., RA., M., and J.N., C. (1999). Peripheral neural mechanisms of nociception (textbook of pain, 4th edition, Wall PD, Melzack R (Hrsg). Edinburgh: Churchhill Livingstone).

Reid, G. (2005). ThermoTRP channels and cold sensing: what are they really up to? Pflugers Arch *451*, 250-263.

Renganathan, M., Cummins, T.R., and Waxman, S.G. (2001). Contribution of Na(v)1.8 sodium channels to action potential electrogenesis in DRG neurons. Journal of neurophysiology *86*, 629-640.

Rogers, M., Tang, L., Madge, D.J., and Stevens, E.B. (2006). The role of sodium channels in neuropathic pain. Seminars in cell & developmental biology *17*, 571-581.

Rush, A.M., Dib-Hajj, S.D., Liu, S., Cummins, T.R., Black, J.A., and Waxman, S.G. (2006). A single sodium channel mutation produces hyper- or hypoexcitability in different types of neurons. Proceedings of the National Academy of Sciences of the United States of America *103*, 8245-8250.

Scholz, J., and Woolf, C.J. (2002). Can we conquer pain? Nature neuroscience *5 Suppl*, 1062-1067.

Shah, B.S., Stevens, E.B., Gonzalez, M.I., Bramwell, S., Pinnock, R.D., Lee, K., and Dixon, A.K. (2000). beta3, a novel auxiliary subunit for the voltage-gated sodium channel, is expressed preferentially in sensory neurons and is upregulated in the chronic constriction injury model of neuropathic pain. The European journal of neuroscience *12*, 3985-3990.

Sherrington, C.S. (1906). The inegrative action of the nervous system (New York: Scribner).

Silos-Santiago, I., Molliver, D.C., Ozaki, S., Smeyne, R.J., Fagan, A.M., Barbacid, M., and Snider, W.D. (1995). Non-TrkA-expressing small DRG neurons are lost in TrkA deficient mice. J Neurosci *15*, 5929-5942.

Snider, W.D., and McMahon, S.B. (1998). Tackling pain at the source: new ideas about nociceptors. Neuron *20*, 629-632.

Stucky, C.L., and Lewin, G.R. (1999). Isolectin B(4)-positive and -negative nociceptors are functionally distinct. J Neurosci *19*, 6497-6505.

Terlau, H., and Olivera, B.M. (2004). Conus venoms: a rich source of novel ion channel-targeted peptides. Physiological reviews *84*, 41-68.

Terlau, H., Stocker, M., Shon, K.J., McIntosh, J.M., and Olivera, B.M. (1996). MicroO-conotoxin MrVIA inhibits mammalian sodium channels, but not through site I. Journal of neurophysiology *76*, 1423-1429.

Theveniau, M., Durbec, P., Gennarini, G., Wood, J.N., and Rougon, G. (1992). Expression and release of phosphatidylinositol anchored cell surface molecules by a cell line derived from sensory neurons. Journal of cellular biochemistry *48*, 61-72.

Thoenen, H., and Barde, Y.A. (1980). Physiology of nerve growth factor. Physiological reviews *60*, 1284-1335.

Thompson, J.C., Dunbar, E., and Laye, R.R. (2006). Treatment challenges and complications with ziconotide monotherapy in established pump patients. Pain physician *9*, 147-152.

Vijayaragavan, K., O'Leary, M.E., and Chahine, M. (2001). Gating properties of Na(v)1.7 and Na(v)1.8 peripheral nerve sodium channels. J Neurosci *21*, 7909-7918.

Vijayaragavan, K., Powell, A.J., Kinghorn, I.J., and Chahine, M. (2004). Role of auxiliary beta1-, beta2-, and beta3-subunits and their interaction with Na(v)1.8 voltage-gated sodium channel. Biochemical and biophysical research communications *319*, 531-540.

Waxman, S.G. (2000). The neuron as a dynamic electrogenic machine: modulation of sodium-channel expression as a basis for functional plasticity in neurons. Philosophical transactions of the Royal Society of London *355*, 199-213.

Waxman, S.G., Dib-Hajj, S., Cummins, T.R., and Black, J.A. (1999). Sodium channels and pain. Proceedings of the National Academy of Sciences of the United States of America *96*, 7635-7639.

Wetzel, C., Hu, J., Riethmacher, D., Benckendorff, A., Harder, L., Eilers, A., Moshourab, R., Kozlenkov, A., Labuz, D., Caspani, O.*, et al.* (2007). A stomatin-domain protein essential for touch sensation in the mouse. Nature *445*, 206-209.

Williams, J.A., Day, M., and Heavner, J.E. (2008). Ziconotide: an update and review. Expert opinion on pharmacotherapy *9*, 1575-1583.

Wood, J.N. (2004). Recent advances in understanding molecular mechanisms of primary afferent activation. Gut *53 Suppl 2*, ii9-12.

Wood, J.N., Boorman, J.P., Okuse, K., and Baker, M.D. (2004). Voltage-gated sodium channels and pain pathways. Journal of neurobiology *61*, 55-71.

Wu, Y., Cao, G., Pavlicek, B., Luo, X., and Nitabach, M.N. (2008). Phase Coupling of a Circadian Neuropeptide With Rest/Activity Rhythms Detected Using a Membrane-Tethered Spider Toxin. PLoS biology *6*, e273.

Yang, X.W., and Gong, S. (2005). An overview on the generation of BAC transgenic mice for neuroscience research. Current protocols in neuroscience / editorial board, Jacqueline N. Crawley ... [et al *Chapter 5*, Unit 5 20.

Yang, Y., Wang, Y., Li, S., Xu, Z., Li, H., Ma, L., Fan, J., Bu, D., Liu, B., Fan, Z.*, et al.* (2004). Mutations in SCN9A, encoding a sodium channel alpha subunit, in patients with primary erythermalgia. Journal of medical genetics *41*, 171-174.

Yoshimura, N., Seki, S., Novakovic, S.D., Tzoumaka, E., Erickson, V.L., Erickson, K.A., Chancellor, M.B., and de Groat, W.C. (2001). The involvement of the tetrodotoxin-resistant sodium channel Na(v)1.8 (PN3/SNS) in a rat model of visceral pain. J Neurosci *21*, 8690-8696.

Yu, F.H., and Catterall, W.A. (2003). Overview of the voltage-gated sodium channel family. Genome biology *4*, 207.

Zhang, X., and Bao, L. (2006). The development and modulation of nociceptive circuitry. Current opinion in neurobiology *16*, 460-466.

Zhang, Z.N., Li, Q., Liu, C., Wang, H.B., Wang, Q., and Bao, L. (2008). The voltage-gated Na+ channel Nav1.8 contains an ER-retention/retrieval signal antagonized by the beta3 subunit. Journal of cell science *121*, 3243-3252.

Zhong, J., Pevny, L., and Snider, W.D. (2006). "Runx"ing towards sensory differentiation. Neuron *49*, 325-327.

Zimmermann, K., Leffler, A., Babes, A., Cendan, C.M., Carr, R.W., Kobayashi, J., Nau, C., Wood, J.N., and Reeh, P.W. (2007). Sensory neuron sodium channel Nav1.8 is essential for pain at low temperatures. Nature *447*, 855-858.

Zorn, S., Leipold, E., Hansel, A., Bulaj, G., Olivera, B.M., Terlau, H., and Heinemann, S.H. (2006). The muO-conotoxin MrVIA inhibits voltage-gated sodium channels by associating with domain-3. FEBS letters *580*, 1360-1364.

Zylka, M.J. (2005). Nonpeptidergic circuits feel your pain. Neuron *47*, 771-772.

Zylka, M.J., Rice, F.L., and Anderson, D.J. (2005). Topographically distinct epidermal nociceptive circuits revealed by axonal tracers targeted to Mrgprd. Neuron *45*, 17-25.

Publication List

Publications

Annika S. Stürzebecher, Jing Hu, Ewan St. John Smith, Silke Frahm, Julio Santos-Torres, Branka Kampfrath, Sebastian Auer, Gary R. Lewin, Inés Ibañez-Tallon: An *in vivo* tethered toxin approach for the cell-autonomous inactivation of voltage-gated sodium channel currents in nociceptors. Journal of Physiology (2010) *accepted.*

Sebastian Auer*, Annika S. Stürzebecher*, René Jüttner, Julio Santos-Torres, Christina Hanack, Silke Frahm, Beate Liehl, Inés Ibañez-Tallon: Silencing neurotransmission with membrane-tethered toxins. Nature Methods (2010). 7: 229-236.

Oral Presentations

Cold pain attenuation in tethered toxin transgenic mice. Ph.D. retreat of the Max-Delbrück Center for Molecular Medicine (MDC) and the Leibniz-Institut for Molekular Pharmacology (FMP) 2008

Poster

Stürzebecher AS, Hu J, Frahm S, Kampfrath B, Lewin GR, Ibañez-Tallon I: "Reduction of cold pain by nociceptor-specific expression of tethered toxins *in vivo"***.** Workshop: Understanding pain: from transduction to sensation", Baeza, Spain 2008.

Stürzebecher AS, Hu J, Frahm S, Kampfrath B, Lewin GR, Ibañez-Tallon I: "Cold pain attenuation by selective inactivation of sodium channels in transgenic mice expressing a tethered conotoxin". 12^{th} world congress on pain**,** Glasgow, UK, 2008.

Stürzebecher AS, Hu J, Frahm S, Kampfrath B, Lewin GR, Ibañez-Tallon I: "A novel transgenic approach to selectively attain cell-autonomous inactivation of nociceptive ion channels". Development and function of somatosensation and pain, Berlin 2008.

* equal contribuation

Stürzebecher AS, Hanack H, Frahm S, Ibañez-Tallon I: ”Tethered toxin mediated reduction of chronic pain *in vivo*”. Berlin Brain Days, Berlin 2008.

Stürzebecher AS**,** Ibañez-Tallon I: “Genetically targeting of ion channels in the nociceptive pain pathway”. MDC evaluation, Berlin, 2007.

Stürzebecher AS**,** Liehl B, Ibañez-Tallon I: “Optimizing tethered toxins for cell-autonomous inactivation of ion channels”. Berlin Neuroscience Forum (BNF), Bad Liebenwalde, Germany, 2006.

Acknowledgements

Firstly, I would like to thank my lab group leader Dr. Ibañez-Tallon for giving me the opportunity to work on this project, for her advices and supervision throughout the years. I would also send my sincere gratitude to my official supervisor Prof. Dr. Gary R. Lewin for all his support and advices. I thank Dr. Jing Hu for providing data and support with my own experiments as well as inspiring brainstorming. I would also like to thank Dr. Silke Frahm-Barske for providing some experimental data that are included in this thesis for completeness. Additionally I want to thank Dr. Ewan Smith who was always open for discussion and Dr. Bettina Erdmann for help with the EM technique.

I also thank the people I've been working with: Sebastian Auer, Silke Frahm-Barske, Christina Hanack, Mande Holford, Branka Kampfrath, Daniela Kurzhals, Martin Laqua, Beate Liehl, Julio Santos Torres and Marta Slimak who made this lab a wonderful place to work at. They all contributed to the thesis by giving advices or having fruitful discussions. I especially want to thank those colleagues who became friends. I will miss our chats and coffee breaks which were usually accompanied by a lot of laughter. Special thanks to Julio.

Last but not least, I thank my family and friends for their encouragement and support throughout the years.

Curriculum Vitae

Mein Lebenslauf wird aus datenschutzrechtlichen Gründen in der elektronischen Version meiner Arbeit nicht veröffentlicht.